Feather keratin derived sorbents for the removal of trace metals from wastewater produced by energy generation processes

by

Irum Zahara

A thesis submitted in partial fulfillment of the requirements for the degree of

Doctor of Philosophy

in

Land Reclamation and Remediation

Department of Renewable Resources
University of Alberta

Abstract

Water dependency of energy generation systems including renewable energy resources generates polluted water. Efforts are required to purify the energy-related wastewater. Therefore, this thesis emphasizes the development of the keratin-based sorbents from chicken feathers (CFs) that can effectively remove the inorganic contaminants from synthetic water simulating wastewater from energy industry, the evaluation of their adsorption performances under the influence of process parameters (pH, temperature, contact time), the assessment of adsorption mechanisms and the determination of the reproducibility/regeneration of developed sorbents. Thus, this research project is divided into three core themes. **Theme-1** includes the development of eight keratin derived sorbents/biopolymers (KBPs) by chemical modifications. KBP-I (processed CFs), KBP-II (acid modified), KBP-III & KBP-IV (modified with ionic liquids), KBP-V (amine modified), KBP-VI & KBP-VII [polyhedral oligomeric silsesquioxanes (POSS) modified] and KBP-VIII (sodium sulfite modified) were then characterized for their surface morphologies, structural integrities, functional group alterations, crystallinity behaviors, surface areas and pore size distributions using appropriate techniques. Developed biopolymers were then tested against multi-metal synthetic wastewater spiked with a mixture of nine metals including transition and redox sensitive elements (at $100 \ \mu g \ L^{-1}$ each). Among the eight biopolymers, KBP-I removed 87–93% of arsenic (As^{III}) and cadmium (Cd^{2+}), KBP-IV adsorbed 80–91% of copper (Cu^{2+}), vanadium (V^V) and chromium (Cr^{VI}), KBP-V removed 60–90% of cobalt (Co^{2+}), nickel (Ni^{2+}) and zinc (Zn^{2+}), whereas KBP-VI removed 95% of Cr^{VI}. The developed KBPs (KBP-I, KBP-IV, KBP-V and KBP-VII) were also applied for removing the metals from oil sand process affected water (OSPW). The adsorption results demonstrated that KBP-VII removed 87% of barium (Ba^{2+}) and 84% of strontium (Sr^{2+}) from OSPW.

Based on these initial adsorption results, the research was taken to a deeper level in **Theme-2** where the adsorption performances of KBP-I, KBP-IV and KBP-V were further evaluated under a range of environmental factors such as pH, temperature, and contact time to optimize the process parameters. Multi-metal synthetic wastewater was incubated with individual biopolymers at two temperatures (30 °C and 45 °C); KBP-I and KBP-IV showed higher adsorption efficiencies for Co^{2+}, Ni^{2+}, Cd^{2+}, V^{V}, Cr^{VI} and As^{III} at 30 °C, whereas KBP-V revealed higher adsorption for divalent cations at 40 °C. However, the biopolymers tend to achieve maximum adsorption efficiencies within one hour of incubation (contact time). To investigate the effect of pH on adsorption and infer adsorption mechanisms, KBP-IV and KBP-V were selected for the adsorption of oxyanions and divalent cations, respectively, in single-metal synthetic wastewater maintained at pH 5.5 or 8.5. The results revealed that KBP-IV displayed higher adsorption efficiencies for oxyanions (Cr^{VI} and V^{V}) at pH 5.5, and KBP-V showed higher adsorption for divalent cations (Cd^{2+}, Ni^{2+}) at pH 8.5. After this adsorption experiment, the metal loaded KBP-IV and KBP-V were further analyzed for adsorption mechanisms by using XPS technique. The findings revealed that metal ion adsorption by KBP-IV and KBP-V could be considered through electrostatic and/or chemical interactions (chelation or complexation or reduction or ion exchange). The three KBPs (KBP-I for As^{III} and Cd^{2+}, KBP-IV for Cr^{VI}, and KBP-V for Ni^{2+}) were also selected for constructing adsorption isotherms by using single-metal synthetic wastewater. The results indicated that KBPs exhibited adsorption behavior for Ni^{2+}, Cd^{2+}, Cr^{VI} best described by Langmuir, whereas retention of As^{III} was best described by Freundlich model.

Theme-3 examines the reproducibility of KBP-IV and KBP-V by chemically modifying the KBPs in triplicates under the same modifying conditions. The results of surface characterization indicated that all triplicate modifications of KBPs (KBP-IV and KBP-V each)

displayed similar surface physiochemical characteristics. This is further supported by the observations when these triplicate modifications of KBPs yielded similar metals adsorption results, validating the reproducibility of KBPs during chemical modification processes. The KBPs were also regenerated by desorbing the adsorbed metals and the results demonstrated that 2 M HCL (as a desorbing eluent) recovered 84% of Co^{2+}, 85% of Ni^{2+}, 55 % of Cd^{2+} and 67% of V^V from KBP-I, 100% of Ni^{2+} and Cd^{2+}, 82% of V^V, and 39% of Cr^{VI} from KBP-IV, 66% of Ni^{2+}, 58% of Cd^{2+}, 81% of V^V, 50% of Cr^{VI} from KBP-V. At last, the hybrid sorbent (KBP-IX) was developed by mixing the KBP-IV and KBP-V at various ratios to analyze their combined affect for targeting higher removal efficiencies.

Preface

Chapter Two of this thesis has been published as Zahara, I., Arshad, M., Naeth, M. A., Siddique, T., & Ullah, A. (2021). "Feather keratin derived sorbents for the treatment of wastewater produced during energy generation processes". *Chemosphere*, *273*, 128545. I performed all laboratory analyses, data interpretation and writing of the manuscript. Dr. Arshad, contributed to manuscript review. Dr. Ullah and Dr.Siddique contributed to conceptualization, manuscript review and editing.

Chapter Three of this thesis has been prepared as a manuscript for submission to peer-reviewed journal: Zahara, I., Naeth, M. A., Siddique, T., & Ullah, A. "The effect of process parameters (pH, temperature, contact time) on adsorption and metal support interactions (mechanisms) for heavy metals removal from wastewater by keratin derived sorbents." I performed all laboratory analyses, data interpretation and writing of the manuscript. Dr. Ullah and Dr.Siddique contributed to conceptualization, manuscript review, and editing.

Chapter Four of this thesis has been prepared as a manuscript for submission to peer-reviewed journal: Zahara, I., Naeth, M. A., Siddique, T., & Ullah, A. "Reproducibility of feather keratin derived sorbents and their application as hybrid sorbent towards metal ions removal from synthetic wastewater." I performed all laboratory analyses, data interpretation, and writing of the manuscript. Dr. Ullah and Dr.Siddique contributed to conceptualization, manuscript review and editing.

This thesis, and all my life's work, is dedicated to my parents, teachers, and mentors.

"Any river is really the summation of the whole valley. To think of it as nothing but water is to ignore the greater part"

–Hal Borland

Table of Contents

List of Figures

List of Tables

1.0 INTRODUCTION

1.1 Water Pollution from Energy Sector

Water and energy infrastructures are dependent on each other as energy is required for water extraction, desalination, treatment, and transportation. The energy industry also relies on water such as water is needed for resource exploitation (fossil fuels), energy conversion processes (refining), power production, and transportation (Mielke et al., 2010). Every year a large quantity of energy resources [coal, petroleum oil, natural gas, hydrogen fuel, and radioactive minerals (uranium)] is obtained from the earth's crust through mining. Coal and uranium mining consumes water for coal cutting, dust suppression, ore recovery, transportation, and reclamation of mine sites (Scott et al., 2011; Younos et al., 2012). Oil sands deposits contain useful tar like material called bitumen and its surface mining consumes alkaline hot water to extract the bitumen from oil sands. After the extraction of bitumen, the process water is known as oil sand process affected water (OSPW) (Arshad et al., 2016). Water is also used for different purposes within thermoelectric power plants (i) to generate steam, (ii) to cool and condense the turbine exhaust, and (iii) in emissions scrubbing processes. Geothermal power consumes water to produce steam for energy extraction from the natural heat stored beneath the earth's surface. Solar thermoelectric power uses water (as a coolant) for steam generation, and cleaning purposes (Scott et al., 2011).

Therefore, all forms of energy generation systems including clean energy (renewable energy sources) generate contaminated water that contains cobalt (Co), nickel (Ni), copper (Cu), zinc (Zn), cadmium (Cd), arsenic (As), chromium (Cr), lead (Pb), manganese (Mn), fluorine (F), boron (B), and uranium (U) (Zahara et al., 2021). For example, coal and uranium mining activities produce toxic metals such as Pb, Cd, Mn, Cr, U, As, and mercury (Hg) that contaminate surface water resources (Adaikpoh et al., 2006; Suzelei et al., 2012). The OSPW from bitumen extraction is brackish, alkaline in nature and highly toxic to aquatic biota due to the high concentration of naphthenic acids (NAs). Naphthenic acids (NAs) are very complex

and contain linear/cyclic/aromatic acids (with varying molecular masses), other organic compounds (heteroatomic compounds with nitrogen or sulfur atoms) and aromatic hydrocarbons. The OSPW also contains inorganic salts (the ions i.e., Na^+, Mg^{2+}, Ca^{2+}, SO_4^{2-} and HCO_3^-), and trace metals (As, Zn, Co, Ni, Cr, Cu and Pb), which has been identified as aquatic pollutants (Arshad et al., 2016; Qin et al., 2019). The wet deposition of fly ash and disposal of coal combustion waste (CCW) from coal-fired power plants produce Cr, Co, Cu, Pb, Mn, Ni, Zn, Hg, and silver (Ag) to water resources (Igunnu & Chen, 2014). They not only damage the aquatic ecosystems but threaten water quality for irrigation and drinking (Dincer, 2018).

1.2 Wastewater Treatment Technologies/Methodologies

1.2.1 Conventional treatment methods for heavy metals removal from wastewater

From an aqueous environment, heavy metals are separated by conventional (physical, chemical, and biological) methods. Over the past few decades, conventional treatment methods that have been used for the removal of heavy metals from wastewater are chemical precipitation, ion exchange, and membrane filtrations (ultrafiltration UF, and reverse osmosis RO) (Kanamarlapudi et al., 2018).

1.2.1.1 Chemical precipitation

Chemical precipitation is a method that involves the heavy metal removal from aqueous media by its homogenous combination with inorganic ligands that leads to the formation of precipitates (Sarode et al., 2019). The chemical precipitation is better explained by the following chemical reaction:

$$M^{2+} + 2(OH)^- \rightarrow M(OH)_2$$
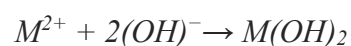
Here, M^{2+} is the dissolved solute (metal) ion, $(OH)^-$ is the precipitant, and $M(OH)_2$ is the insoluble metal hydroxide which is separated later from the solution. This chemical reaction/ precipitation is mainly dependent on the solubility of soluble species and the pH that should be

basic (9-11) during the process. The pH is considered as one of the governing parameters for the chemical precipitation of heavy metals (Barakat, 2011). The precipitants mostly used for precipitating the metals are lime (calcium hydroxide), and potassium/sodium hydroxides. Among the other precipitants, lime is more effective and can target the inorganic effluents with a concentration of metals higher than 1000 mg L^{-1}. Despite being used as an extensive approach for heavy metal removal, this method generates large volumes of sludge with higher metal's concentrations, which is not acceptable. Furthermore, the large volumes of sludge require additional sludge handling facilities (sedimentation and filtration units for effective solid/liquid separation) (Bose et al., 2002).

1.2.1.2 Ion exchange method

Ion exchange is the reversible chemical reaction that involves the replacement of dissolved metal ions with similarly charged ions attached to an ion exchange matrix (Sarode et al., 2019). The ion exchange matrix contains immobile acidic or basic functional group(s) attached to a mobile ion. The functional groups possess an either cationic or anionic character that allows the mobile ions to be exchanged with solute ions which have a stronger affinity towards functional groups. The cationic matrix contains negative immobile ions and exchangeable positive counter ions, whereas the anion matrix contains positive fixed ions and exchangeable negative ions (Rengaraj et al., 2003; Sapari et al., 1996).

The typical cation exchange reaction is: $2NaR + CaCl_{2(aqueous)} \rightleftarrows CaR_2 + 2NaCl_{(aqueous)}$

The typical anion exchange reaction is: $2RCl + Na_2SO_{4(aqueous)} \rightleftarrows R_2SO_4 + 2NaCl_{(aqueous)}$

Where "R" is the structural unit (immobile functional groups) of the ion exchanger and "aqueous" represents the electrolyte in the solution. The fluoride (F$^-$) and sulfate (SO$_4^{2-}$) ions are separated in an anion exchange process and, similarly, the Ca^{2+} and Mg^{2+} are replaced with Na^{2+} and H$^+$ in a cation exchange process. However, the industries often use this method for demineralization, but this technology has several disadvantages such as higher concentrations

of target metals cause fouling on ion exchange matrix in case of impurities (solids and organic matter). Ion exchange technology is highly sensitive to solution pH and demands some additional requirements (Sarode et al., 2019).

1.2.1.3 Membrane filtrations

Membrane filtrations (ultrafiltration UF, and reverse osmosis RO) play a substantial role in removing the heavy metals and other contaminants from wastewater. Membrane filtrations are operated by applying the hydraulic pressure that acts as a driving force for mass transportation. The membranes have specific molecular weight cut-off (MWCO) restrictions that allow and control the required component to pass through a permeate media (Morais et al., 2009). Ultrafiltration (UF) is a well-known pressure-driven membrane that works under low trans-membrane pressure and retains/removes the dissolved and colloidal solutes, whereas water or low molecular weight solutes pass through a membrane. There are two types of UF membranes (i) micellar enhanced ultrafiltration (MEUF) and (ii) polymer enhanced ultrafiltration (PEUF). MEUF is commonly used for the removal of metal ions and organic-colored dyes. The process of contaminant removal includes the addition of anionic, cationic, or non-ionic surfactants to the water that decreases the surface tension and increases the free energy of particles in the bulk of an aqueous solution. To remove the positively charged metal ions, anionic surfactant sodium dodecyl sulfate (SDS) is added in an aqueous solution. The SDS monomers accumulate together, and micelles are formed in the interior of the solution after filling the surface that decreasing the surface tension of the aqueous solution. Metal ions are attracted to (settled on) the oppositely charged surface of micelles by electrostatic or van der Waals forces (Sarode et al., 2019).

Reverse osmosis (RO) as the name mentions, is the reverse of the osmosis process (which describes the natural movement of solvent from a region of low solute concentration to a region of high solute concentration through a permeable membrane without external pressure). But

during the reverse osmosis, external pressure is applied which is higher than osmotic pressure that drives the solvent through a membrane from high concentration to low concentration. The RO operates at pressures between 20 and 80 MPa and retains the contaminants ($\leq$350 Da of sizes) and monovalent ions from the solutions. The mechanisms involved for the mass transfer from RO membranes are solution diffusion, size exclusion, and physical-chemical interactions among all three components (solute, solvent, and the RO membrane) (Malaeb & Ayoub, 2011; Sarode et al., 2019). A wide range of dissolved species are being removed from water by RO and this method has well-known recognition among other wastewater treatment processes. But, the disadvantages of the RO include (i) consumption of high power due to pumping pressure, (ii) high cost, and (iii) difficulty in regeneration/restoration of membranes (Sarode et al., 2019).

1.2.2 Adsorption and recent advances in the production of sorbents

Therefore, in recent years, metal adsorption has attracted attention amongst researchers and environmentalists because of its cost efficiency and the generation of high-quality treated effluents. The adsorption involves the mass transfer that allows metal ions to be transferred from solution to solid surface and then bound by chemical or physical interactions (Raouf & Raheim, 2016). Sorbents may be originated from minerals (activated carbons, natural zeolites, alumina, silica beads), organic (organic polymeric resins), or biological (biological species: bacteria/fungi/algae, plant-derived materials, agricultural wastes: wheat straw, saw-dust, sugar beet pulp, chitin/chitosan, feather/hairs/nails keratins, industrial waste) sources (Crini, 2005). Bio-based sorbents (recognized as biosorbents) are now widely used for the decontamination of heavy metals from wastewater because of their natural abundance, good adsorption performances, cost-effectiveness, and environmental compatibilities (Sarode et al., 2019).

The bio-based sorbents reported in recent literature for the removal of heavy metals are (i) chitosan/calcium alginate/bentonite composite hydrogel for the removal of Pb^{2+}, Cu^{2+} and Cd^{2+} (Lin et al., 2021), (ii) ethylenediaminetetraacetic acid (EDTA) and carboxymethyl (CM)

modified cellulose extracted from pineapple leaf for the removal of Pb^{2+} and Cd^{2+} from wastewater (Daochalermwong et al., 2020), (iii) agro-waste mixed with bacterial biomass for adsorption of Pb^{2+} (Saravanan et al., 2021), (iv) chicken feather derived activated carbon that further magnetized with eggshells for the removal of Pb^{2+}, Cd^{2+}, Cu^{2+}, Zn^{2+}, and Ni^{2+} from wastewater (Rahmani-Sani et al., 2020) and so on.

Bio-based sorbents contain functional groups (amine, amide, imidazole, thioether, sulfonate, carbonyl, sulfhydryl, carboxyl, phosphodiester, phenolic, imine, and phosphate) that play a significant role in the adsorption of metal ions from wastewater (Park et al., 2010). Hence, adsorption using sorbent (which is of biological origin) is a physicochemical process that involves the binding of metal ions (sorbate) onto the functional groups present on sorbent's surface through various interaction mechanisms (i) physical (electrostatic interaction or van der Waal forces), (ii) chemical (displacement of metal cations as ion exchange) binding, (iii) chelation/complexation, (iv) oxidation/reduction, and (v) precipitation (Davis et al., 2003; Mrvčić et al., 2012). Several factors such as sorbent amount, sorbate concentration, pH of an aqueous solution, contact time, and temperature influence the adsorption process (Park et al., 2010).

Adsorption takes place when the sorbent is suspended in the aqueous solution that contains the metal ions (sorbate) and equilibrium is achieved after the incubation for a certain period (Chojnacka, 2010). At equilibrium, the amount of sorbate that disappears from the solution is assumed to be adsorbed by sorbent (Essington, 2005). So, besides other factors, quantitative measurement of contaminant's sorption by sorbents is important in developing the remedial approach for removing the contaminants from wastewaters (Ngah & Fatinathan, 2010).

1.2.2.1 Adsorption Equilibria Models

The adsorption equilibria are explained by the classification of isotherms. The purpose of performing an adsorption isotherm study is to attain the sorbate-specific adsorption parameters that quantitatively describe the adsorption in specific environment (Kocaturk, 2008; Essington, 2005). Adsorption isotherms are constructed and used to analyze the distribution of metal ions in the aqueous phase (wastewater) in equilibrium with the solid phase (sorbent) at the same temperature (therefore, the term is "*isotherm*") (Donner et al., 2019). The classification of adsorption isotherms is important for modeling the adsorption phenomena. The International Union of Pure and Applied Chemistry (IUPAC) has classified six types of isotherms (Kocaturk, 2008) can be seen in Fig 1.1.
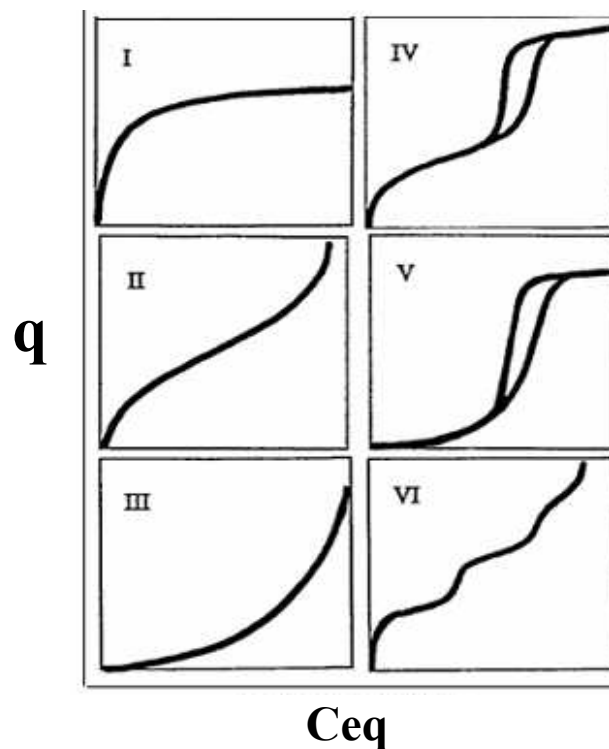
Figure 1.1. Types of adsorption isotherms (Kocaturk, 2008).

Type-I isotherm is usually used to describe the adsorption on microporous sorbents and approaches a "limiting value". This type of isotherm suggests that the sorbate has rather a high affinity for sorbent at low surface coverage. Though, with the increase of surface coverage, the

affinity of the sorbate for the sorbent decreases. Types-II & III isotherms indicate adsorption on macro-porous sorbents with strong and weak sorbate-sorbent interactions, respectively. Types-IV and V describe the mono and multi-layer adsorption. Type-VI represent that adsorption takes place in several steps (Essington, 2005; Kocaturk, 2008).

Various mathematical models have been employed to describe the adsorption isotherms, the most common are Langmuir, and Freundlich models. Originally the Langmuir equation was derived for the gas molecules adsorbed by the solid surface and based on the following assumptions (i) adsorption takes place at specific locations/sites on a surface, (ii) the surface is homogeneous as all adsorption sites are identical, (iii) monolayer of adsorbed molecules on the surface is formed and an adsorption maximum is achieved as the monolayer becomes filled by the sorbate (iv) heat or energy of adsorption is constant over the entire surface, (v) adsorbed species do not interact (vi) volume of the monolayer and the energy of adsorption are independent of temperature, and (vii) equilibrium is attained. However, the Freundlich equation is assumed on the basis of specific distribution of adsorption sites (heterogenous surface) (Essington, 2005).

In a recent study, Daochalermwong and his coworkers constructed the adsorption isotherms (Langmuir and Freundlich) for the removal of Pb^{2+} and Cd^{2+} from wastewater by using the chemically modified cellulose extracted from pineapple leaf. The results indicated that the data was best fitted by the Langmuir model for both metals as R^2 values associated with Langmuir were greater than those associated with Freundlich isotherm, further suggesting that a monolayer of each sorbate formed on the surface of sorbent (Daochalermwong et al., 2020). Donner and his coworkers constructed the adsorption isotherms for the divalent cation (Ni^{2+}) and oxyanions (Cr^{VI}, and V^V) removal from wastewater by using the chemically modified chicken feathers as sorbents. The results suggested that the developed sorbents (for all three metals) revealed adsorption behavior best described by the Langmuir model yielding the higher

R^2 values associated with Langmuir model (Donner et al., 2019). Another research conducted by Giri and his colleagues that includes the construction of adsorption isotherms (Langmuir and Freundlich) for the removal of Cr^{VI} by using the pomegranate peel as low-cost sorbents. The results indicated that the data was best fitted by the Langmuir model for Cr^{VI} adsorption with a higher R^2 value than the R^2 value associated with the Freundlich model (Giri et al., 2021). The present study selects the Langmuir and Freundlich adsorption isotherms to investigate that chemical modification of chicken feathers may expose surfaces that are homogenous in binding sites or may introduce different functional groups with heterogenous energy of binding sites. The maximum adsorption capacities for trace metals by using the bio-based sorbents are presented in Table 1.1.

Sources	Sorbents	Maximum Adsorption Capacities	References
Industrial waste	Chitosan bead (modified with titanium oxide)	V^V = 124.5 mg g^{-1}	Liu & Zhang, 2015
	Chemically modified chicken feathers	V^V = 17 mg g^{-1} Cr^{VI} = 15 mg g^{-1}	Donner et al., 2019
	Chitosan flakes (CF)	V^V = 2.58 mg g^{-1}	Rodriguez et al., 2015
	Glutaraldehyde and epichlorohydrin modified chitosan	Cd = 405 mg g^{-1} Cd = 331 mg g^{-1}	Kyzas et al., 2013
	Pineapple leaves extracted cellulose modified with ethylenediaminetetraacetic acid (EDTA)	Pb^{2+} = 41.2 mg g^{-1} Cd^{2+} = 33.2 mg g^{-1}	Daochalermwong et al., 2020
	Pineapple leaves extracted cellulose modified with carboxymethyl	Pb^{2+} = 63.4 mg g^{-1} Cd^{2+} = 23.0 mg g^{-1}	

Plant-Based	Pomegranate peel	Cr^{VI} = 20.87 mg g^{-1}	Giri et al., 2021
	Iron impregnated biochar from palm waste	Cr^{VI} = 197 mg g^{-1}	Wang et al., 2017
	Leaf derived biochar	Cr^{VI} = 349 mg g^{-1}	Zhang et al., 2017
	Carboxylated cellulose nano crystal-polyethyleneimine composite	Cr^{VI} = 358 mg g^{-1}	Liu et al., 2017
	Ferric oxide hydroxide–activated carbon nanocomposite (Fe–AC)	V^{V} = 119 mg g^{-1}	Shariffard & Soleimani, 2015
Microbial-based	Bacterial biomass	Pb = 480 mg g^{-1} Cd = 267 mg g^{-1} Cu = 210 mg g^{-1}	Luo et al., 2014
	Bacterial biomass	Cd = 46.2 mg g^{-1}	Lu et al., 2006

Table 1.1. The maximum adsorption capacities for inorganic contaminants by using bio-based sorbents.

1.2.3 Chicken feathers as keratin-derived sorbents

1.2.3.1 Structure and composition of keratin proteins

Keratin has originated from the Greek word "*keratos*" meaning "*horn*". The word first appeared in literature in 1850 to represent the hard tissues. Keratins are insoluble proteins, characterized by filamentous structures that are responsible for the development of epithelial and epidermal structures (horns, hooves, hairs, nails, wool, and feathers) (Khosa & Ullah, 2013). Keratin is a high molecular weight natural polymer with large polypeptide chains that are formed by the condensation of amino acids (Fig 1.2.). The polypeptide backbone also contains the R_1 and R_2 groups that signify the side chains of amino acids (Kocaturk, 2008).

Figure 1.2. The condensation reaction of amino acids (Zhang, 2014).

The amino acid is the structural unit of proteins and keratins are heterogenous proteins due to differences in amino acids structures/chemical compositions. There are 20 major amino acids which exist in nature and mainly consist of carbon (C), nitrogen (N), and oxygen (O), except 2 of the 20 amino acids contain sulfur (S) (Whitford, 2005). The amino acid composition of keratin is presented in Table 1.2.

Amino Acids	% Composition	Side Chains
Alanine	3.56 %	neutral, and non-polar
Arginine	5.36%	basic, and polar
Aspartic acid	4.73 %	acidic, and polar
Cysteine	7.63 %	contains thiol -SH group, neutral, and slightly polar
Glutamic Acid	7.65 %	acidic, and polar
Glycine	6.18 %	having no charge, small, neutral, and non-polar side chain
Histidine	0.43 %	Imidazole side chain, basic, and polar
Isoleucine	4.28 %	hydrophobic side chain, neutral, and non-polar
Leucine	7.04 %	hydrophobic side chain, neutral, and non-polar
Lysine	0.53 %	basic, and polar
Methionine	1.3 %	S-containing hydrophobic side chain, neutral and non-polar

Phenylalanine	4.2 %	hydrophobic aromatic side chain, neutral and non-polar
Serine	9.31 %	uncharged side chain, neutral
Threonine	3.5 %	uncharged side chain, neutral
Tyrosine	1.96 %	aromatic side chain, neutral and polar
Valine	6.94 %	hydrophobic side chain, neutral and non-polar

Table 1.2. The amino acid composition of keratin protein.

Besides other amino acid compositions, keratin proteins exhibit a higher cystine content (sulfur-containing diamino acid) (as shown in Fig 1.3) that plays a significant role in the stiffness and stability of the proteins.
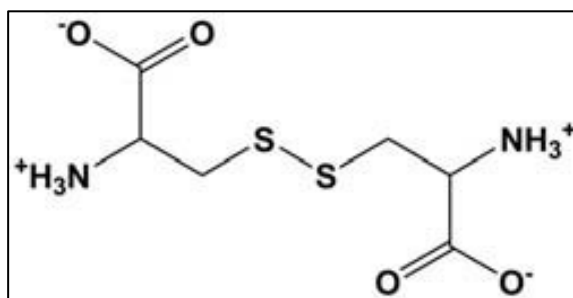
Figure 1.3. The molecular structure of cystine (Johnson, 1997).

Keratins are classified as epithelial (soft) and trichocyte (hard) keratins based on cystine content (Ghosh & Collie, 2014). Soft keratins are found in stratum corneum of the skin and contains the low cystine content (< 3 %) (Meyers et al., 2008; Scheibel, 2005). Hard keratins are found in various bio-fibrous materials such as wool, hair, feathers, nails, and horns of mammals, with the function being to act like structural scaffolding. Hard keratins have a high content of cystine (4-17%) that leads to the high-level protein-protein crosslinking (Khosa & Ullah, 2013).

Amino acids are amphoteric as they contain the acidic and basic functional groups. The carboxyl (acidic) group of an amino acid exhibits a pKa between 1.8 and 2.5, and the amino

(basic) group has a pKa between 8.7 and 10.7. At the physiological pH conditions (pH 6 to 7), the amino group is ionized to $-NH_3^+$ and carboxyl group to $-COO^-$ (Kocaturk, 2008). Therefore, amino acids exist as zwitterions "twin ions" at physiological pH (6-7). The amino acid also exhibits an isoelectric point. The isoelectric point (IEP) is the pH at which the number of positive charges on the molecule is the same as the number of negative charges. Therefore, at the IEP, the molecule remains uncharged, has the lowest ability to interact with water, and possesses the lowest solubility (Buxbaum, 2007).

1.2.3.1.1 Surface charge density: Zeta potential (ζ)

The adsorption is the accumulation of the sorbate at the sorbent-solution interface. This interfacial region resides in the closer proximity to sorbent surface and incorporates the volume of the solution that is under the direct influence of surface (Essington, 2005). Surfaces acquire either (i) partial charge that is due to the polarity (natural or induced) of atoms (in neutral organic functional groups) at a surface or (ii) partial charge that is established through protonation/deprotonation (ionization/dissociation) reactions in inorganic and organic functional groups (Essington, 2005; Sarode et al., 2019). For example, in case of keratin proteins/chitin/chitosan, partial charge is due to dissociation of carboxylic (-COOH) groups that releases the protons or lone pair of electrons present on NH_3/OH groups donated to surrounding metal ions (Kumar, 2000; Rinaudo, 2006). The surface charge is neutralized by counterions/molecules that are present at the sorbent-solution interface (Sarode et al., 2019). The type of chemical bond established at the sorbent-solution interface indicates the mechanism responsible for the adsorption of sorbate. For example, the metal cations that directly bond to sorbent surface atoms, are recognized to be specifically adsorbed, forming the inner-sphere surface complexes. The metal cations that are associated with the formation of inner sphere complexes are transition metals (Co^{2+}, Ni^{2+}, Cu^{2+}, Cd^{2+} and Zn^{2+}) (Essington 2005). Zeta potential (ζ) is the electrical potential difference across the sorbent-solution

interface and can be calculated by measuring the electrophoretic mobility of negatively or positively charged particles/metal ions (as shown in Fig 1.4) in response to an applied constant electric field (Zhou et al., 2012).

Some researchers reported that the calculated zeta potentials resulting from an ionization of the sorbent's (keratin protein's) different functional groups appeared to be dependent on pH and usually change from negative to positive due to the changes in pH values (below the isoelectric point) of the surrounding aqueous media (Capablanca & Watt, 1986). Ghafar et al., 2017 reported the zeta potential of unmodified wool (keratin) fiber as a function of pH:

(i)   At pH below 5.2, zetapotential of unmodified wool is positive due to the sorption of H_3O^+ ions from the aqueous onto the wool surface, as described below:

$$\text{Protein-NH}_2 + H_3O^+ \longleftrightarrow \text{Protein-NH}_3^+ + H_2O$$

(ii)   With increasing the pH value, zeta potential drops down.

(iii)   At pH = 5.2, the corresponding zeta potential is zero (also known as isoelectric point) as there is no excess of negative/positive charges in the shear plane, hence, the numbers of protonated amino groups and deprotonated carboxylic acid groups almost equal (IEP = pH, ζ=0).

(iv)   At pH above than IEP, negative values of zeta potential are observed which is assigned to the preferential adsorption of hydroxide ions from electrolyte solution (Ghafar et al., 2017).
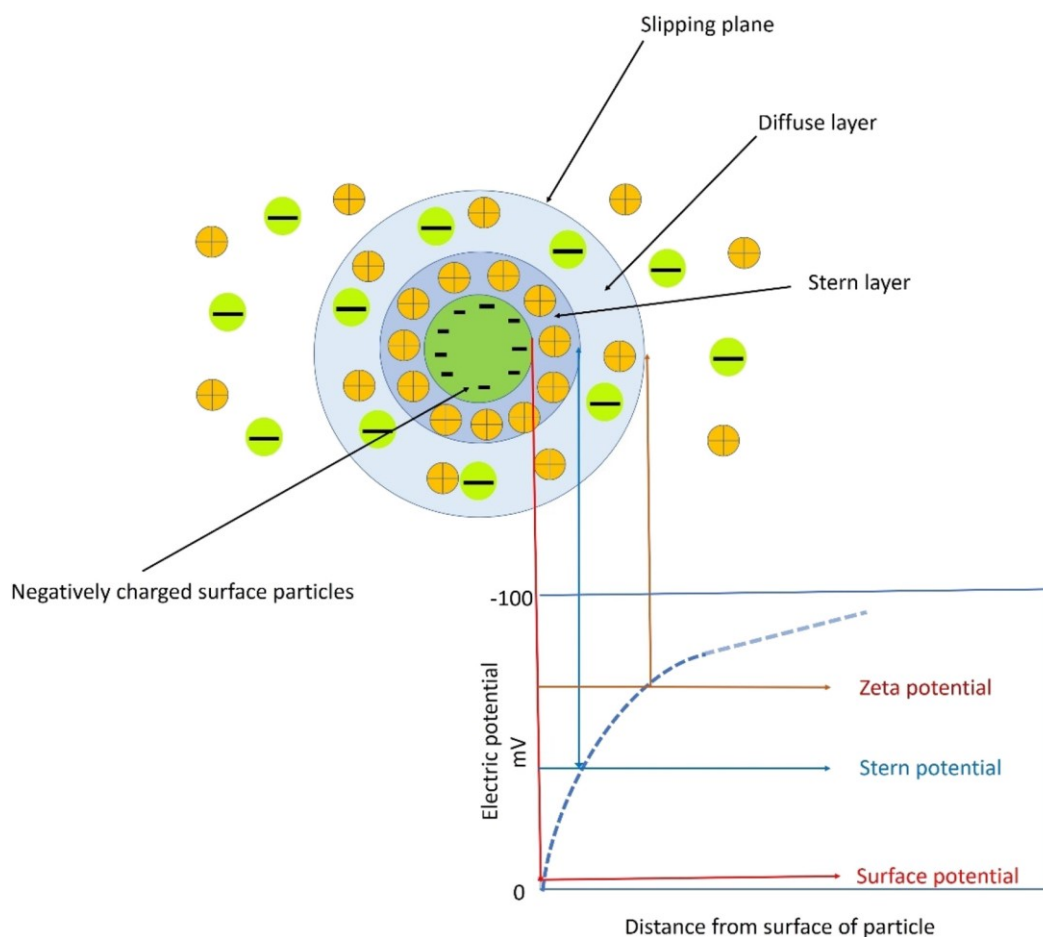
Figure 1.4. Electric double layer and zeta potential (Sarode et al., 2019).

Surface characteristics (chemical composition, charge, wettability) of bio-based sorbents are important aspects to understand the complex sorbent-solution interface that develops when sorbents come into contact with aqueous media. Among them, zeta potential is important for characterizing the sorbents (Ferraris et al., 2018). Here, in this present study several characterization studies have been conducted, in addition to, Fourier transform infrared spectroscopy (FTIR) analysis has been used to determine/investigate the changes in surface functional groups (surface chemistry/chemical composition) of the developed sorbents.

1.2.3.2 Chemical modification of keratin proteins to enhance the metal-binding properties of amino acids

Amino acids act as natural chelators (organic ligands) for many transition metal ions. For example, amino acids (aspartic and glutamic acids) have side chains with carboxyl groups that

give the side chain a negative charge at pH=7. Therefore, aspartic, and glutamic acids are known to be potent chelators for Zn^{2+} and calcium (Ca^{2+}) due to their natural ability to bind with the divalent metal cations. Furthermore, the S of the methionine interacts with heavy metals, particularly Hg and platinum (Pt) by complexation (Whitford, 2005). Due to these distinctive binding properties, wool keratin has been studied since the early 1950s for binding the metal ions, therefore, having a promising role in environmental remediation (Khosa & Ullah, 2013).

Keratin protein is hydrophobic and less reactive, but the presence of several functional groups mainly peptide backbone, disulfide (-S-S), amino (-NH$_2$), and carboxylic acid (–COOH) groups, makes the protein reactive and more soluble under favorable conditions [pH (above or below isoelectric point), high temperature, and reducing agents (Na_2SO_3 or Na_2S)]. Covalent/chemical modification is the method that can be used to modulate the macromolecular functions of keratin. Chemical modification of keratin proteins alters the reactivity of desired functional groups, thus, the resulting molecules exhibit the tailored properties/characteristics for various applications (water purification) (Khosa & Ullah, 2013).

1.2.3.3 Recent Trends and Research Gaps

Although being a waste product from the poultry industry, chicken feathers (CFs) have gained attention to develop into sorbents/biopolymers because of their potential for wastewater treatment. CFs contain about 91% protein (keratin), 1% lipids, and 8% water (Ullah et al., 2011a, Ullah et al., 2011b; Swati et al., 2017). Keratins in feathers are small proteins, having a molecular weight of about 10 kDa, and composed of α-helix and β-sheets conformations (Arai et al.,1983). In CFs, the side chains attached to the polypeptide structure of keratin have specific chemical structures, bonding ability, charge, and reactivity. When treated with different chemicals, these chains can be modified and their contaminant removal efficiencies can be enhanced by exposing more functional groups on the surface (Donner et al., 2019).

17

Therefore, the seven of the keratin biopolymers (KBP-II to KBP-VIII) were developed by chemical modifications of CFs keratin proteins, whereas the KBP-I was the processed CFs without chemical modification. The modifying agents that were used for chemical modifications include (1) citric acid (2) ionic liquids (3) propyl amine (4) polyhedral oligomeric silsesquioxanes (POSS) containing mercaptopropyl isobutyl groups, and (5) mercaptoethanol as reducing agent. The reaction schemes and modification mechanisms for the above-mentioned modifying agents are given below:

1.   Citric acid modification of CFs keratin proteins: The purpose of this modification was the addition of negatively charged carboxyl groups that could enhance the binding of keratin proteins towards positively charged metal ions. The modification includes the hydrolyzation of amino groups of the keratin protein by using sodium hydroxide, then the free amino groups undergone a nucleophilic substitution reaction with carboxyl groups in citric acid to form a new amide bond (Li et al., 2018) as shown in the reaction below:

Citric Acid

Cross-linking by citric acid
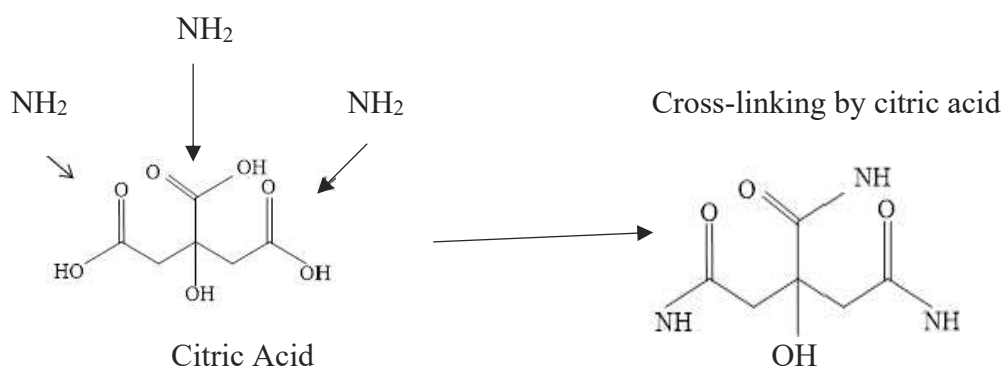
2.   Ionic liquid modification of CFs keratin proteins: The purpose of ionic liquid modification of CFs keratin proteins was to change the hydrophobic character to hydrophilic character by breaking down the hydrogen bonding, that further led to the conversion of hydrophilic amino functional groups to hydrated cationic amino groups which may increase the binding of chemically modified keratins towards oxyanions (Sun et al., 2009). CFs keratin proteins were modified with ionic liquids (1-butyl-3-methyl imidazolium chloride/bromide).

Ionic liquids are molten salts usually contains organic cations and more compact counter ions (halide anions). These ionic liquids are extensively characterized by their hydrogen bonded network as one cation is hydrogen bonded to three anions and one anion is hydrogen bonded to three cations (Dupont, 2004) as shown in Fig 1.5.
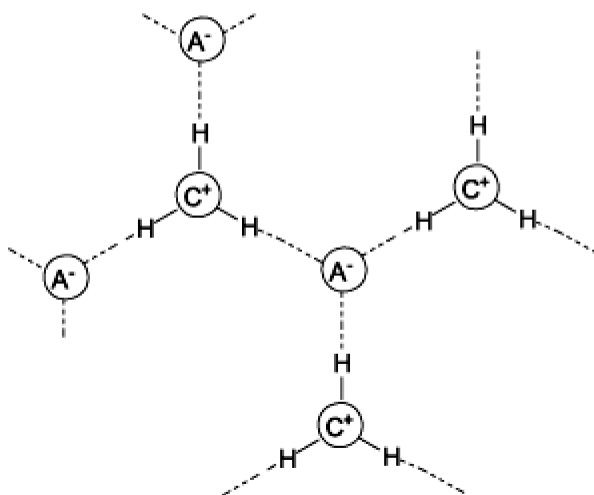
Figure 1.5. Hydrogen bonded network of ionic liquids (Dupont, 2004).

When CFs keratin proteins dissolve in ionic liquids, halide anions (chloride ions) of ionic liquids win the hydrogen bonding competition with the OH groups of proteins against the intra molecular hydrogen bonded network. If this hydrogen bonded network is strong, the hydrophilic chloride anion considers as a mediator between the more hydrophobic imidazolium cation and water, thus, expelling out the cations to some extent as shown in Fig 1.6. This segregation into polar and apolar domains for ionic liquids consequently leads to the accumulation of cations at the apolar domains of the proteins, which affects the activity, solubility of proteins and changes their hydrophobic character to hydrophilic character (Schroder, 2017).
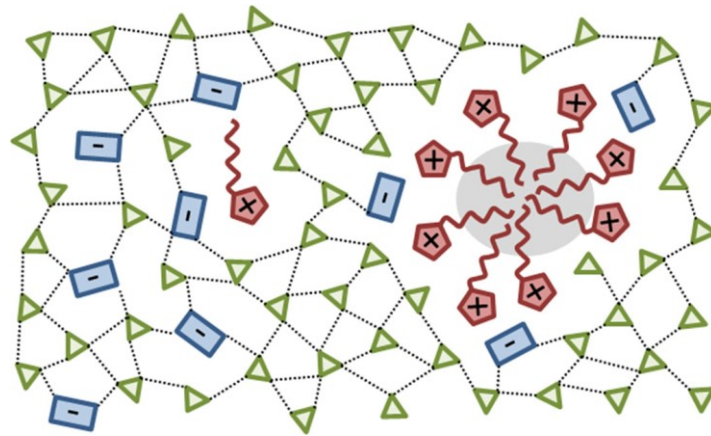
Figure 1.6. Anion water network and cation segregation of ionic liquids (Schroder, 2017).

3.   Propyl amine modification of CFs keratin proteins: The purpose of propyl amine modification was the addition of amino groups (nitrogen atoms containing the lone pair of electrons) towards the CFs keratin proteins to target the divalent metal cations. Propyl amine is used for the amination of carboxyl groups present in the keratin protein structures (can be seen in the chemical reaction below). Amination of carboxyl groups has benefit to convert them to more potent nucleophiles (Wong & Jameson, 2012) that play significant role in adsorbing the contaminants.

$$\text{Protein-C-O}^- + \text{NH}_2\text{-CH}_2\text{-CH}_2\text{-CH}_2\text{-N-CH}_3 \longrightarrow \text{Protein-C-O-NH-CH}_2\text{-CH}_2\text{-N-CH}_3$$
$$\overset{\|}{} \qquad\qquad\qquad\qquad \underset{\text{CH}_3}{|} \qquad\qquad\qquad\qquad \overset{\|}{} \qquad\qquad\qquad \underset{\text{CH}_3}{|}$$
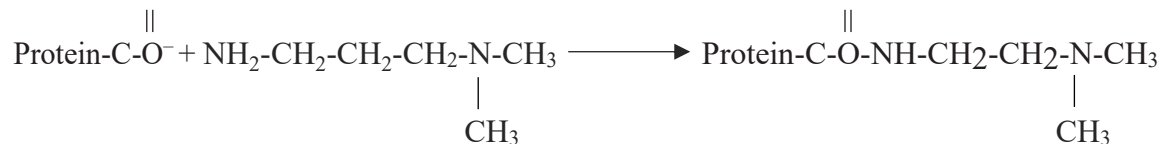
4.   Mercaptopropyl isobutyl POSS modification of CFs keratin protein: The purpose of mercaptopropyl isobutyl POSS modification was to form the disulfide-linked crosslinked network partially retaining the free sulfhydryl groups and to increase the oxide anions that enhances the binding of chemically modified keratin proteins towards positively charged metal ions (Liu et al., 2019). The structure of the mercaptopropyl isobutyl POSS can be seen in Fig 1.7.
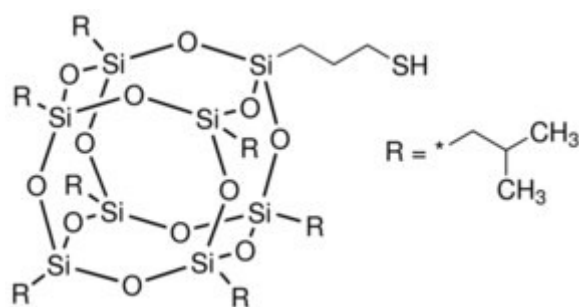
Figure 1.7. Structure of mercaptopropyl isobutyl polyhedral oligomeric silsesquioxanes (POSS) (Liu et al., 2019).

5.   Reducing agent modification of CFs keratin proteins: The purpose of the reducing agent (mercaptoethanol) modification was to break down the disulfide linkages (as shown in Fig 1.8) within the keratin protein structure to expose the thiol contents (Robert et al., 2014) towards the removal of metal ions from wastewater.
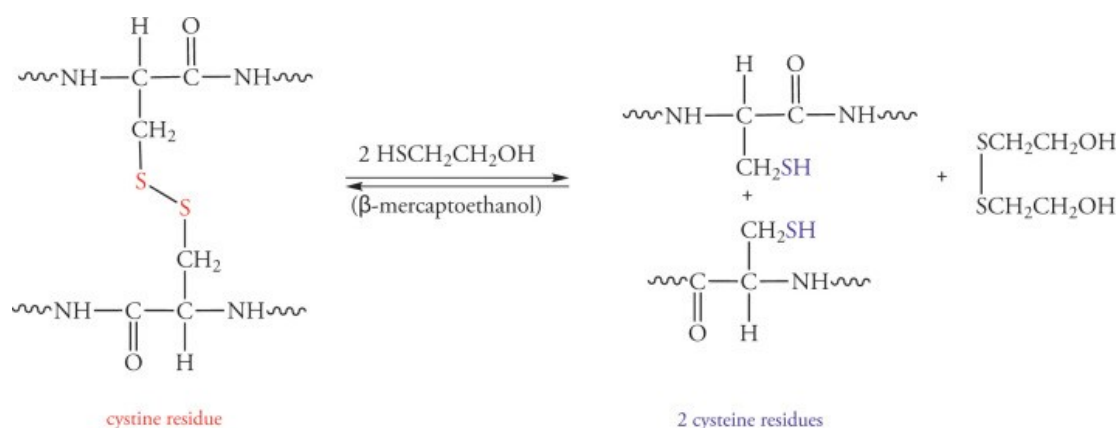
Figure 1.8. Cleavage of disulfide bonds by mercaptoethanol (Robert et al., 2014).

Furthermore, based on the 12 principles of green chemistry, the developed keratin biopolymers (KBPs) possess following criteria for their sustainable applications as sorbents (towards contaminants removal from wastewater) that includes (i) designed less hazardous chemical synthesis, (ii) used safer chemicals/products, (iii) used safer solvents and reaction conditions, (iv) used renewable feedstocks (chicken feathers), (v) analyzed in real time to prevent pollution, and (vi) prevented the waste.

In recent years, Chakraborty and his coworkers modified the CFs by using ethylenediamine and removed the metal ions (Co^{2+}, Cu^{2+}, Fe^{2+}, and Ni^{2+}) from metal-polluted water up to 20 mg L^{-1} concentration. The results showed that the removal efficiencies of Co^{2+}, Cu^{2+}, Fe^{2+}, and Ni^{2+} ions were 98.7%, 98.9%, 98.7%, and 99% respectively (Chakraborty et al., 2020). Donner and coworkers reported two chemically modified keratin biopolymers, having >82% of adsorption efficiencies for divalent cations (Pb^{2+}, Ni^{2+}, Co^{2+}, and Zn^{2+}) and 68–100% for oxyanions (Se^{IV}, $V^{V,}$ and Cr^{VI}) from synthetic wastewater with 50 µg L^{-1} concentrations of each metal (Donner et al., 2019). In another study, CFs were chemically modified using epichlorohydrin and ethylenediamine. The results indicated 90% adsorption efficiency for Cr^{VI} from contaminated water having the initial Cr^{VI} concentration between 10-80 mg L^{-1} (Sun et al., 2009). Another research conducted by Teixeira and Ciminelli, examined a biological route for the adsorption of aqueous arsenic (As^{III}) species by a high fibrous protein (keratin) (Teixeira & Ciminelli, 2005).

To my best knowledge, the adsorption studies (using bio-based sorbents) that have been conducted so far have not provided the clear understanding and detailed enlightenment on the physiochemical characteristic analysis of the developed sorbents and their impacts on adsorption for decontaminating the wastewater. For example, in recent research Daochalermwong et al., 2020 has performed only Fourier transform infrared spectroscopy (FTIR) and scanning electron microscopy (SEM) to investigate the physiochemical characteristics of bio-based sorbent (Daochalermwong et al., 2020).

To fill the knowledge gap, the detailed surface physiochemical characteristics (functional group changes, crystallinity behaviors, thermal degradation/transitions, surface area & pore size distributions, and surface morphologies) of the developed sorbents of the present study were investigated by using the FTIR, X-ray diffraction (XRD) analysis, thermogravimetric analysis (TGA), differential scanning calorimetry (DSC), Brunauer-Emmett-Teller (BET)

analysis, and scanning electron microscopy (SEM), respectively.

Furthermore, there are many keratin-derived sorbents that have a potential role in water remediation, most of them are sorbate specific (metals, dyes, and other organics such as phenols). In case of trace metals, these sorbents have targeted only four-five metals (either the divalent cations or oxyanions) from wastewater with low adsorption rates and low selectivity for different concentrations of heavy metals. In addition, there is no comprehensive study for sorbent's application towards field waters, their regeneration and recycling for sustainable use.

1.3 Research Aim and Objective

1.3.1 Aim of the Study

This study aims to develop an alternative, cost-efficient, and environment-friendly adsorption technology from CFs for the decontamination of wastewaters that will provide a clear understanding of structural characteristics and functional properties of developed sorbents and their role in adsorbing the divalent cations and anions from synthetic water simulating wastewater from the energy industry.

1.3.2 Specific Objectives

1) To develop new sorbents by chemical modifications of CFs keratin protein for the removal of divalent cations and oxyanions from wastewaters.

2) To evaluate the adsorption performances of developed keratin-derived sorbents under the influence of process parameters (pH, temperature, and contact time), with the assessment of binding mechanisms involved in the adsorption process.

3) To reproduce the keratin-derived sorbents by investigating the role of triplicate modifications in adsorption studies and to regenerate the sorbents by desorbing the contaminants with the purpose to restore the original state of sorbents for reusability. Also, to investigate the combined effects of two sorbents (as hybrid sorbent) for enhancing their adsorption affinities towards metal ions removal.

1.3.3 Research Questions and Hypothesis

(i) Does the chemical modification of keratin protein have any subsequent role in sequestering the multi-metal ions (divalent cations and oxyanions) from wastewaters?

Hypothesis (i): It has been hypothesized that the chemical modification of proteins enhances their surface functional groups/active binding sites and makes them more effective for the removal of multi-metals from wastewater.

(ii) Do the process parameters (pH, temperature, and contact time) affect the adsorption performances of keratin-derived sorbents towards the removal of multi-metals from wastewater?

Hypothesis (ii): It has been hypothesized that the pH influences the ionization of sorbate (metal ions) and sorbent's surface sites, hence, affecting the sorbent's binding efficiencies. Furthermore, considering recent literature reports suggesting alterations in the adsorption efficiencies with the increase in temperature.

(iii) Does the multifunctional character of mixed (hybrid) sorbent, make it potentially useful in removing the multi-metal ions from wastewater with higher efficiencies?

Hypothesis (iii): It has been hypothesized that adsorption efficiencies of metal cations and oxyanions increase by the multi-functional character of hybrid sorbent (developed by mixing the two sorbents: KBP-IV and KBP-V).

1.3.4 Research Approach

To answer the research questions, the following analyses were conducted:

a) Assess the surface physiochemical characteristics of developed keratin-derived sorbents after the chemical modifications of CFs, and their potential roles in adsorbing the inorganic contaminants (Co^{2+}, Ni^{2+}, Cu^{2+}, Zn^{2+}, Cd^{2+}, V^V, Cr^{VI}, $As^{III,}$ and Se^{VI}) from synthetic wastewater.

b) Determine the concentrations of inorganic contaminants (Co^{2+}, Ni^{2+}, Cu^{2+}, Zn^{2+}, Cd^{2+}, V^V, Cr^{VI}, $As^{III,}$ and Se^{VI}) in synthetic wastewater, and the concentrations of inorganic contaminants (Ni, V, Ba, and Sr) in oil sand process affected water (OSPW) after the equilibrium with keratin-derived sorbents.

c) Analyze the concentrations of inorganic contaminants (Co^{2+}, Ni^{2+}, Cd^{2+}, V^V, Cr^{VI}, and As^{III}) in synthetic wastewater after the equilibrium with keratin-derived sorbents at pH (5.5 and 8.5), temperature (30 °C and 45 °C), and different incubation times (15, 30, 60, 120, 180 and 360 mins). Also, investigate the adsorption mechanisms involved in the sequestering of inorganic contaminants.

d) Quantify the adsorption of inorganic contaminants (Ni^{2+}, Cd^{2+}, Cr^{VI}, As^{III}) by constructing the adsorption isotherms (Langmuir and Freundlich) models.

e) Determine the concentrations of desorbed inorganic contaminants (Co^{2+}, Ni^{2+}, Cd^{2+}, V^V, Cr^{VI}, As^{III}) after the equilibrium of keratin-derived sorbents with 2 M HCl.

1.3.5 Thesis Outline

This thesis is consisted of five chapters, starting with the introduction (Chapter One) that includes the background information, is followed by three chapters as separate manuscripts (each manuscript deals with the research questions mentioned above) with the final chapter (Chapter Five) that represents the main conclusion. Chapter two elaborates the development of keratin-derived sorbents by chemical modifications and explores their role in removing the inorganic contaminants from synthetic wastewater. Chapter three depicts the influence of process parameters (pH, temperature, and contact time) on the adsorption performances of keratin-derived sorbents with the description of adsorption mechanisms involved in sequestering the heavy metals by keratin derived sorbents. This chapter also includes the application of keratin-derived sorbents towards the removal of metal ions from field waters (OSPW). Chapter four describes the reproducibility of keratin-derived sorbents and their

regeneration by desorbing the metal contaminants from sorbents. This chapter also includes the hybrid sorbent approach (produced by mixing the two sorbents) and discovers its role in the removal of metal ions from synthetic wastewater.

2.0 FEATHER KERATIN DERIVED SORBENTS FOR THE TREATMENT OF WASTEWATER PRODUCED DURING ENERGY GENERATION PROCESSES

2.1 Introduction

Water is required for all forms of energy and has an influential role in energy generation processes (Tripathi et al., 2013). All forms of energy generation systems, including clean energy, are polluting water (Olsson, 2012). For example, coal and uranium mining activities produce toxic metals such as lead (Pb), arsenic (As), mercury (Hg), chromium (Cr), cadmium (Cd), manganese (Mn) and uranium (U) that contaminate surface waters (Adaikpoh et al., 2006; Suzelei et al., 2012). High levels of dissolved minerals due to coal, oil and gas mining processes produce wastewater containing cations and anions ranging from low concentrations to 300,000 mg L^{-1} that affects the conductivity, salinity and pH of water (Dincer, 2018). The resultant water from oil extraction processes is known as produced water, contains heavy metals, hydrocarbons, hydrogen sulfide and organic acids. The wet deposition of fly ash and disposal of coal combustion waste (CCW) from coal fired power plants are the main sources of heavy metal water pollution of water resources by producing chromium (Cr), cobalt (Co), copper (Cu), lead (Pb), manganese (Mn), nickel (Ni), zinc (Zn), mercury (Hg) and silver (Ag) (Igunnu & Chen, 2014). Surface and ground water contamination with heavy metals such as copper (Cu), zinc (Zn), chromium (Cr), tritium oxide (T_2O), carbon-14 (^{14}C), cesium-134 (^{134}Cs), cesium-137 (^{137}Cs) and strontium-90 (^{90}Sr) by nuclear power plants have now become a major environmental concern (Winfield et al., 2006). Geothermal fluids contain heavy metals and other toxic components including cadmium (Cd), mercury (Hg), arsenic (As), manganese (Mn), fluorine (F) and boron (B) due to the interaction of hot fluids with rocks. They not only damage the aquatic ecosystems but threaten water quality for irrigation and drinking purposes. Efforts are being made to control energy-related water pollution (Dincer 1998). Heavy metals are characterized by their persistent behaviors as they are non-degradable and cannot be destroyed (Duruibe et al., 2007). Separation of heavy metals from wastewaters is achieved through physical, chemical, and biological methods. However, these methods have several

drawbacks, such as chemical precipitation producing large volumes of sludge with higher metal concentrations. Ion-exchange technology causes fouling on the ion exchange matrix and is highly sensitive to solution pH, demanding some additional requirements. Biofilm and membrane filtration technologies are not cost efficient and require periodic maintenance (Sarode et al., 2019).

Among the conventional techniques (biological, chemical, electrochemical and oxidation) for removal of heavy metals from wastewaters, adsorption is more effective, economical and ecofriendly, thus recognized as one of the best technologies for decontamination of wastewater (Raouf & Raheim, 2017). Recently, numerous approaches have been studied for development of cheaper and more effective sorbents containing natural polymers (Crini, 2005). Chicken feathers (CFs) being an abundant waste by-product of the poultry industry has gained attention because of its potential for wastewater treatment. Feathers have unique physical and chemical characteristics that enable their chemical modifications to be utilized as a biopolymer for wastewater treatment (Donner et al., 2019). CFs contain about 91% protein (keratin), 1% lipids and 8% water. Keratin consists of peptide bonds of different amino acids containing α-helix and β-sheets conformations (Ullah et al., 2011a, Ullah et al., 2011b; Swati et al., 2017). The structure of amino acid includes central carbon linked to functional groups such as amine (-NH_2), and carboxylic acid (-COOH), the hydrogen atoms and the group R (Kocaturk, 2008). The side chains attached to the polypeptide structure of keratin have specific chemical structure, bonding ability, charge, and reactivity, hence; play a major role in adsorption processes. When treated with different chemicals, these chains can be modified and their contaminant removal efficiencies can be enhanced by exposing more functional groups on the surface (Donner et al., 2019). This study includes (i) modification and detailed structural characterization of developed keratin biopolymers (KBPs) and (ii) their screening for adsorption of targeted multiple metals from energy industry simulated wastewater.

2.2 Materials and methods

2.2.1 Chemicals

The chemicals used for the processing and modification of CFs include: hexane (Sigma Aldrich), sodium hydroxide (Sigma Aldrich ≥97%), citric acid (Fischer Scientific ≥99.5%), 1-butyl-3-methylimidazolium chloride (Sigma Aldrich ≥98%), 1-butyl-3-methylimidazolium bromide (Sigma Aldrich ≥97%), ethanol (Fisher Brand 95%), diethyl ether (Sigma Aldrich ≥99%), sodium sulphite (Sigma Aldrich ≥98%), urea (Fischer Scientific), ethylenediaminetetraacetic acid (Sigma Aldrich ≥99%), tris base (Fischer Scientific 99.8%), 2-mercaptoethanol (Sigma Aldrich ≥99%), 1,4-dioxane (Sigma Aldrich), tetrahydrofuran (Sigma Aldrich), 3-(dimethylamino)-1-propylamine (Sigma Aldrich 99%), polyhedral oligomeric silsesquioxanes (POSS) with mercaptopropyl isobutyl groups on the surface called mercaptopropyl isobutyl-POSS (Hybrid Plastics TH1550), hydrochloric acid (Sigma Aldrich 37%) and methanol (Sigma Aldrich 99.8%).

For the adsorption experiment, individual metal stock solutions were prepared using powder reagents of the following: nickel (Ni) chloride hexahydrate (Fisher Scientific, 99.4%), cobaltous (Co) sulfate heptahydrate (Fisher Scientific, 100%), zinc (Zn) sulfate heptahydrate (Sigma Aldrich, 99%), cupric (Cu) sulfate pentahydrate (Fisher Scientific, ≥98%), cadmium (Cd) chloride (Sigma Aldrich 99.9%), chromium (Cr) oxide (Sigma Aldrich 99.99%), arsenic (As) sodium meta arsenite (Sigma Aldrich ≥99%) and selenium (Se) sodium selenate (Sigma Aldrich 95%). For vanadium V^V, liquid standard solution vanadium [CAS No: HNO_3 7697-37-2, V 7440-62-2 (SpexCertiPrep)] was used.

2.2.2 Source and processing of chicken feathers (KBP–I)

The CFs were procured from the poultry research center at the University of Alberta, Edmonton, Canada, then washed, dried and ground according to the reference (Arshad et al., 2016a; Arshad et al., 2016b). Ground CFs were further washed with 250 mL hexane for 5 h in

Soxhlet apparatus to remove fats and waxes. CFs were dried by evaporating the hexane, and then stored in desiccator at room temperature as KBP-I. Seven KBPs were prepared by chemical modifications of processed CFs to increase functional groups on the surface, hence, to enhance surface reactivity for metals.

2.2.3 Modification of keratin biopolymers with different functional dopants

2.2.3.1 Modification with citric acid (KBP-II)

For production of KBP-II, 1.5 g of processed CFs were stirred in 100 mL of 0.1 M NaOH aqueous solution for an hour. The solution was then filtered and washed twice with 100– 150 mL deionized water and dried in an oven overnight at 105 °C. After drying, 6 g of NaOH processed feathers were blended with 100 mL of 0.6 M citric acid solution at 50 °C over-night, then washed several times with deionized water and dried in an oven at 105 °C for 4.5 h. The dried feathers were washed again with 0.05 M NaOH solution (100 mL), followed by washing with deionized water. The feathers were dried overnight at 105 °C in an oven, then ground and passed through a 40 μm mesh sieve (Kocaturk, 2008).

2.2.3.2 Modification with ionic liquids (ILs) (KBP-III & KBP-IV)

The modification with ionic liquids was carried out using reported method (Sun et al., 2009) with modifications. Briefly, 25 g of ionic liquids [BMIM]Cl and [BMIM]Br were liquified separately in three-necked glass flasks at 100˚ C with continuous stirring under an inert atmosphere of N_2 gas. Then processed CFs (5.75 g) were added to each melted ILs in four fractions with regular time intervals under the same stirring and heating conditions until the CFs were dissolved. After the complete dissolution of feathers in ILs, the CFs were regenerated from a solution by adding 200–350 mL ethanol, or water. The suspended solution was stirred with water for 30 min, then filtered, and rinsed with ethanol several times to remove water. The regenerated feathers were then washed with ether to remove ethanol. Grayish-white particles

were obtained as an end product, which were ground and passed through 40 μm mesh sieve before use as an adsorbent.

2.2.3.3 Modification with methanol and 3-(dimethylamino)-1-propylamine (KBP–V)

The KBP-V was prepared by a method already reported in literature (Khosa et al., 2013; Arshad et al., 2016a; Arshad et al., 2016b) with slight modifications. For preparation of KBP-V, 15 g of processed CFs were placed in a round bottom flask and mixed with 450 mL methanol. Then 15 g Na_2SO_3, 75 g urea, 12 g trisbase, 300 mg EDTA and 5.4 mL of mercapto ethanol were added. The reaction mixture was stirred at 65 °C for 24 h followed by addition of 3-(Dimethylamino)-1-propylamine with continuous heating for 168 h. The mixture was then filtered and thoroughly washed with methanol and water respectively. The modified keratin biopolymers were dried, ground, and passed through a 40 μm mesh sieve.

2.2.3.4 Modification with mercaptopropylisobutyl-POSS under alkaline and acidic conditions (KBP-VI & KBP-VII)

To prepare KBP-VI, 15 g of processed CFs were placed in a 500 mL round bottom flask with 400 mL distilled water. Then, 23.2 g of Na_2SO_3 and 90 g urea were added with continuous stirring at 75 °C for 2 h. Then 1 g of mercaptopropylisobutyl-POSS was dissolved in 30 mL of dioxane and added to the reaction mixture. The pH of the reaction mixture was maintained slightly basic by adding 1 M solution of NaOH. After complete dissolution of feathers, the reaction mixture was cooled to room temperature and pH of the solution was lowered to ≈4.2 to precipitate the dissolved protein. Keratin precipitates were filtered and washed with tetrahydrofuran and water to remove unreacted mercaptopropylisobutyl-POSS and other contents. The obtained precipitates (CF-POSS) were dried at room temperature for few hours and then heated in the oven at 90 °C overnight. The dried contents were ground and sieved. Sieved biopolymer was mixed in distilled water, then treated with 1 M NaOH to make it slightly basic (pH = 7.5–7.7). Maintaining the same pH, the biopolymer was stirred overnight

at room temperature and supernatant was removed after centrifugation of the mixture. The biopolymer was oven dried at 80 °C overnight, then ground and sieved with a 40 μm mesh sieve (KBP-VI) (Arshad et al., 2016a; Arshad et al., 2016b).

The same method was followed to prepare KBP-VII, in which the CF-POSS biopolymer was mixed with distilled water, then treated with 1 M HCl to make it slightly acidic (pH = 6.0–6.25). It was then stirred at room temperature overnight and centrifuged to remove supernatant. The residue was oven dried at 80 °C overnight, then ground and sieved with a 40 μm mesh sieve.

2.2.3.5 Modification with reducing agent (KBP-VIII)

The KBP-VIII was prepared by a method already reported in literature (Arshad et al., 2016a; Arshad et al., 2016b) with modification. Briefly, 15 g of processed CFs were mixed with 500 mL distilled water in a 1 L round bottom flask followed by addition of 24.87 g Na_2SO_3 (reducing agent), 90 g urea, 0.43 g EDTA, 12.1 g trisbase and 4 mL of mercapto ethanol and gently stirred at 70–80 °C for 168 h. To remove salt contents and other dopants, the solution was filtered and dialysed against water for 48 h using dialysis tubing of molecular weight cut-off (MWCO) of 6000–8000 Da. The semi liquid keratin biopolymer was first dried at room temperature and then in an oven at 70 °C for 24 h. The dried KBP was ground, sieved with a 40 μm mesh sieve and stored at room temperature.

2.2.4 Surface characterization of keratin biopolymers

The surface functional groups of all KBPs were examined using a fourier transform infrared spectrometer (FTIR; Bruker Vertex 70, Billerica,MA, USA) equipped with Hyperion 2000 FTIR microscope spectrometer having a germanium attenuated total reflection (ATR) microscope objective with mercury cadmium telluride (MCT) detector. The spectra were obtained within the frequency range 4000–500 cm^{-1} as the same background conditions. All sample spectra were obtained at 64 scans and 4 cm^{-1} resolution, and spectra of

two replicate measurements for each sample were averaged. The infrared spectra were acquired using Bruker OPUS software (version 5.5) and analyzed by using Thermo Scientific OMNIC software package (version 7.1).

To determine the structural crystallinity of all KBPs, X-ray powder diffraction patterns (XRD) were obtained using Rigaku Ultima IV diffractometer operating at 38 kV (voltage) and 38 mA (current) equipped with cobalt tube and the D/Tex ultra-high-speed position sensitive system containing Kβ filter.

Thermogravimetric analysis (TGA) and differential scanning calorimetry (DSC) were attained under a continuous nitrogen purge to analyze thermal degradation and phase transitions of KBPs as a function of temperature. For TGA, Q50 thermogravimetric analyzer was used and ~10 mg of the sample was heated at 10 °C min^{-1} from 25 to 600 °C. The DSC analysis was conducted by using calorimetric apparatus (Modulated DSC 2920) where ~5 mg of samples was inserted and scanned at a rate of 5 °C min^{-1} within a temperature range of 25–260 °C.

Surface areas and pore size distributions of KBPs were analyzed by Brunauer-Emmett-Teller (BET) analyser. The BET surface area was determined using nitrogen adsorption/desorption isotherms obtained by liquid nitrogen temperature at 77 K. Prior to analysis, appropriate weight of the samples was degassed at 100 °C for 8 h under a vacuum with a nitrogen gas flow to ensure absence of moisture in the sample. The adsorption-desorption isotherms were also used to determine pore size distribution of the samples based on Density Functional Theory (DFT).

To observe changes in the surface morphologies of KBP-I and modified KBPs, scanning electron microscopy (SEM) images were taken with Zeiss Sigma 300 VP-FESEM operating at 15 kV and 10 nm resolution, equipped with the Bruker energy dispersive X-ray spectroscopy (EDS) system having dual silicon drift detectors each with an area of 60 mm^2 and a resolution of 123 eV. Prior to analysis, the samples were prepared by dispersing powder samples on to

adhesive surface of stubs, then coated with conductive gold or carbon using a Leica EM SCD005 evaporative carbon coater.

2.2.5 Application of keratin biopolymers for the removal of contaminants from synthetic wastewater

Synthetic wastewater was prepared by using nano-pure water (18.2 MΩ cm; Barnstead, Thermo Scientific™). The ionic strength of nano-pure water was raised to I = 0.05 by addition of 0.02 M NaCl and 0.01 M CaCl$_2$. The synthetic water was then spiked with 9 different metals (up to 100 µg L^{-1} each) and pH was adjusted to 7.5 using 0.1 N NaOH. Trace metals chosen for experiment were: Ni, Co, Zn, Cu, Cd, V^V, Cr^{VI}, As^{III}, and Se^{VI}. KBP-I, and each modified KBP were weighed (0.1 g) in triplicates to 15 mL centrifuge tubes, then 10 mL of metal-spiked synthetic wastewater was added to each tube. The tubes were placed on reciprocating shaker for 24 hours at ambient temperature and then centrifuged at 5000 rpm for fifteen minutes. After centrifugation, 0.5 mL of supernatant was removed, diluted, and analyzed using inductively coupled plasma mass spectrometer (ICP-MS; iCapQThermo Scientific) under kinetic energy discrimination mode (KED; He gas). The metal loaded KBPs residue will be regenerated by desorbing the metals from KBPs surfaces and will be recycled in our next studies.

2.3 Results and discussion

2.3.1 Surface and structural characterizations of keratin biopolymers

2.3.1.1 Fourier transform infrared spectroscopy (FTIR)

The existence of amide functionalities in all KBP samples (before and after modifications) is examined by FTIR spectra. FTIR spectra of all eight KBPs are described in Fig 2.1a, identifying three distinct amide vibrational transitions as amide A (N–H stretching at 3300 cm^{-1}), amide I (C=O, with a minor contribution from N–H bending at 1600–1700 cm^{-1}), amide II and amide III (N–H bending and C–N stretching, at around 1540 and 1240 cm^{-1}) (Sun et al., 2009). An absorption band of all KBP samples appearing at 3268 cm^{-1} (Fig 2.1a) is

assigned to N–H stretching that corresponds to hydrogen bonding required to develop a link between peptide N–H groups and C═O groups in secondary structure of protein. Noticeable band shifting or variation in KBP-I, KBP-II, KBP-III, KBP-IV and VII at 2921 cm^{-1} is attributed to stretching vibration of C–H in methylene (Arshad et al., 2016a; Arshad et al., 2016b). The presence of additional peaks at 1162 cm^{-1} and 619 cm^{-1} in modified KBP-III and KBP-IV, indicates the asymmetric and symmetric S–O stretching vibrations of Bunte salt residues (Sun et al., 2009). The spectra of KBP-VI and KBP-VII (modified with POSS) represent additional absorption peaks at 1061 cm^{-1}, which are assigned to Si–O–Si stretching vibrations of POSS molecules (Ullah et al., 2011a; Ullah et al., 2011b) grafted or trapped in the keratin chains (Arshad et al., 2016a; Arshad et al., 2016b). These results are also evidenced by XRD analysis.
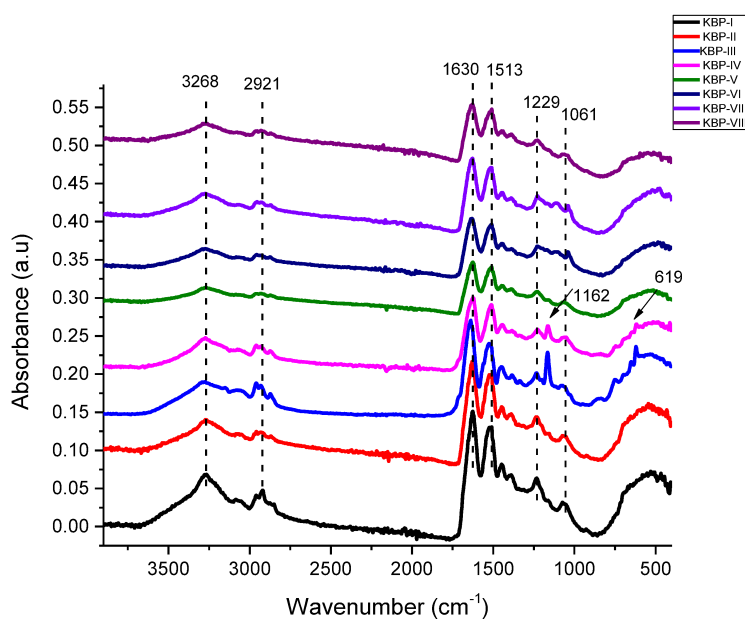
Figure 2.1 a. FTIR spectra of KBP-I and modified KBPs.

Among all the amide bands, the most intense and most widely used band is amide I of the backbone peptide groups in the proteins. Predominantly, this band appears in the region between 1700 and 1600 cm^{-1} and begins from the C═O stretching vibration of the amide carbonyl group weakly coupled with the in-plane N–H bending and the C–N stretching

36

vibration (Ullah & Wu, 2013). In the second derivative region, the amide I band is directly separated into its components and positions of individual amide I bands are identified. The main component bands are evident at 1633, 1651, 1659 and 1667 cm^{-1} in all KBPs and correspond to β-sheets, α-helices, and 3_{10}-helices, respectively. The peaks at 1681 cm^{-1} can be assigned to antiparallel β-sheets/aggregated strands (Jackson & Manstsch, 1995). Second derivative FTIR spectra (1600-1700 cm^{-1}) of all samples is represented by Fig 2.1b. Significant differences can be observed between KBP-I and modified KBPs. The KBP-IV, KBP-V, KBP-VI, KBP-VII and KBP-VIII decrease in peak intensities at 1651 and 1659 cm^{-1} compared to KBP-I, suggesting that chemical modifications of KBPs promote the formation of β-sheet structures at the expense of α-helices. New peaks at 1622 and 1628 cm^{-1} in KBP-III and KBP-IV indicates the presence of stronger intermolecular hydrogen bonds between keratin molecules (Sun et al., 2009).
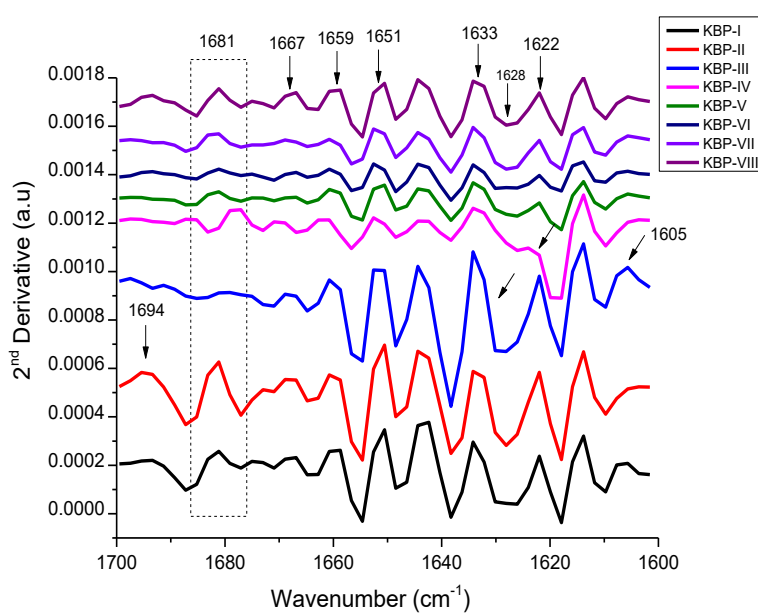
Figure 2.1 b. Amide I region, second derivative spectra of KBP-I and modified KBPs.

2.3.1.2 X-ray powder diffraction (XRD)

The protein consists of semi-crystalline structures, their conformation of chains and crystallinity are susceptible to surface interactions (Zubair et al., 2019). The crystalline structures of KBP-I and modified KBPs were determined by XRD analysis. In general, keratin feathers show a typical XRD pattern that includes one prominent 2θ degree peak at 9.9° corresponding to the *α*-helix configuration; the other more intense band at 19° belongs to *β*-sheets (Arshad et al., 2016a; Arshad et al., 2016b). XRD measurements plotted in Fig 2.2 revealed that KBP-I has only one characteristic crystallinity peak at 9.4°, while the second 2θ peak at 19° has not appeared, indicating the deformed *β*-sheet network (Khosa et al., 2013). KBP-II, KBP-V and KBP-VIII (modified with citric acid, amine and reducing agent) have more obvious 2θ peaks at 9.9° and more intense bands at 22.07°. This mild increase in value of 22.07° seems to reflect the enhancement of crystalline character of biomasses with more d-spacing (Nuutinen, 2017). The KBP-II, KBP-V and KBP-VIII show slight increase of 2θ values confirms the decrease of the *β*-sheet content and partial cleavage of *α*-helix network (Rakesh & Antony, 2017). However, in case of KBP-III, both crystallinity peaks were significantly reduced indicating the disruption of *α*-helices and *β*-sheets network of KBP after modification (Khosa et al., 2013), while KBP-IV (KBP-III and KBP-IV modified with ionic liquids) has more obvious 2θ peak at 9.9°. The first 2θ peaks of KBP-VI and KBP-VII shifted toward lower angle value of 9.2°, indicating the entrapped POSS particles in keratin chains which have interacted chemically with CFs during modifications. This small quantity of entrapped POSS makes aggregates and may cause transition of signal in XRD pattern. These results suggest that the network of *α*-helices and *β*-sheets in modified KBPs had been altered during modifications exposing more active surfaces/functional groups for metal adsorption (Arshad et al., 2016a; Arshad et al., 2016b). The heterogeneous structures of

modified KBPs are also prominent from the differences in their degradation behavior and crystalline melting temperature mentioned by TGA and DSC results.
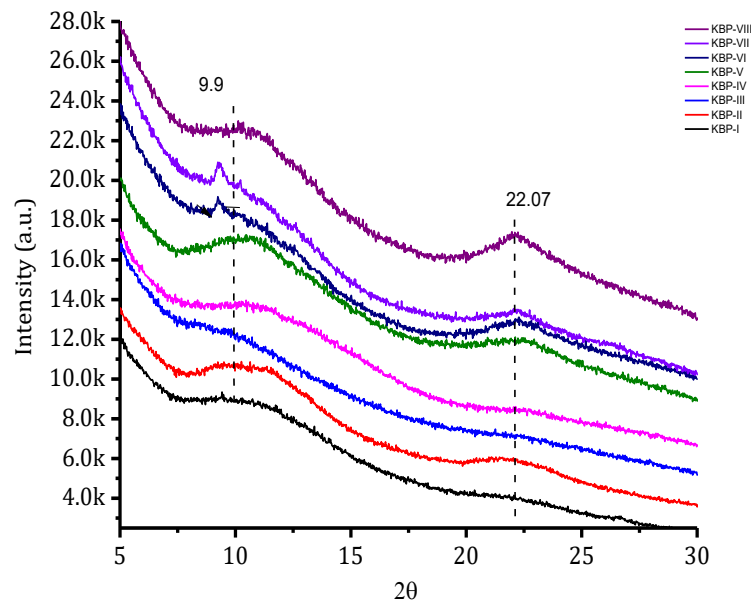
Figure 2.2. XRD pattern of KBP-I and modified KBPs.

2.3.1.3 Thermogravimetric analysis (TGA)

Thermal stability of KBP-I and modified KBPs was determined by TGA. Keratin biopolymers generally exhibit three steps of degradation. The first weight loss at ≤ 100 °C can be attributed to loss of entrapped moisture. The second weight loss after 200 °C, represents that KBPs undergo degradation. In step three KBPs starts to decompose from 350 °C and so on (Arshad et al., 2016a; Arshad et al., 2016b). As shown in Fig 2.3 the similar pattern of first slight weight loss (prior to 100 °C) is observed by all keratin biopolymers. Afterwards, all biopolymer samples show stability until at 200 °C as no weight loss is observed. For the second weight loss, a steep decline as a function of temperature within a range of 250 °C can be seen by all KBPs that corresponds to degradation of KBPs. This second step weight loss of KBPs can be assigned to destruction of internal hydrogen bonding, denaturation of di-sulfide linkages in protein and decomposition of salt bridges (between positive and negative side chains) of the secondary network of KBPs (Sun et al., 2009). There is an additional associated decomposition to some volatile compounds such as HCN, H_2S, CO_2 and H_2O (Swati et al., 2017). For the third

weight loss, the complete decomposition of KBPs can be seen at 380 °C. However, the differences in their weight loss are obvious from Fig 2.3 as KBP-I and KBP-II have shown maximum degradation at 338 °C, while other biopolymers (KBP-III to KBP-VIII) showed maximum weight loss at temperatures between 309 and 322 °C. These results are also evidenced by SEM images showing that KBP-I and KBP-II have more intact surface morphology as they require higher temperature to degrade than the other modified biopolymers. As indicated by Fig 2.3 the modifications of keratin proteins did not affect their thermal stability to a greater extent.
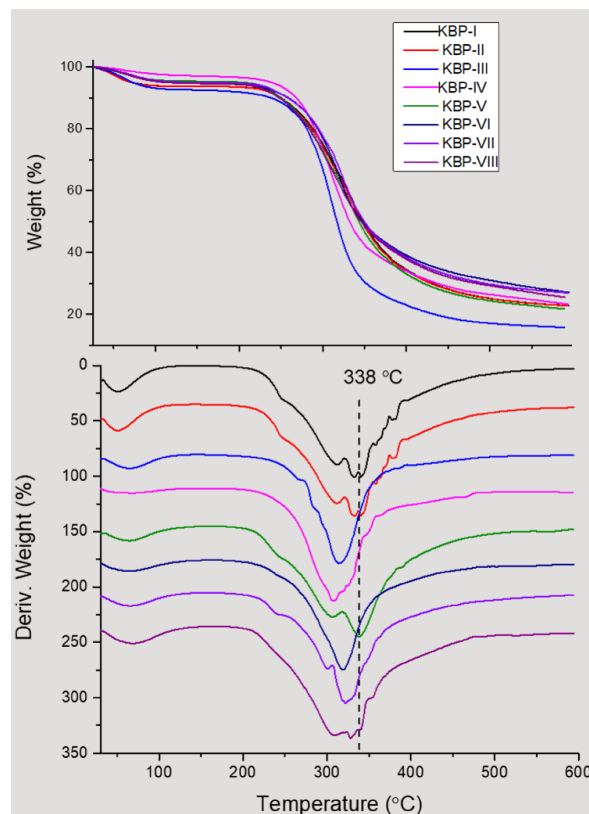
Figure 2.3. Thermogravimetric weight (%) loss and derivative curves of all keratin biopolymers.

2.3.1.4 Differential scanning calorimetry (DSC)

DSC analysis of all KBP samples was carried out to investigate their phase transitions. Fig 2.4 represents DSC curves for KBP-I and modified KBPs indicating the two-phase transitions within 25–250 °C. A low temperature phase transition around 100 °C describes the evaporation of residual moisture/denaturation of the protein (Khosa et al., 2013). A significant change in denaturation curves can be observed in all samples. As shown in Fig 2.4, KBP-I and KBP-IV shows smooth heat flow variation covering a wide range of temperature increase. The KBP-III and KBP-VI shows broader transition with lower peak intensity indicating heterogeneous interactions of dopant with keratin molecules. For keratin biopolymers (KBP-II, KBP-V, KBP-VII and KBP-VIII), heating curves drop distinctly and de-moisturizes rapidly, indicating a dip in the graph along the temperature axis (Sun et al., 2009). The melting curve of all samples can be observed by DSC analysis showing an exothermic peak at $\geq$ 230 °C, which is designated to α-helix disorganization and destruction (Khosa et al., 2013). Many factors; for instance, biomaterial molecular masses, hydrophobic property, chemical bonding of added dopant and denaturation or decomposition of α-helix and β-sheets producing heterogeneous surface during and after the chemical modifications, play an important role for the development of DSC transitional plot (Arshad et al., 2016a; Arshad et al., 2016b). Aluigi and his cowrokers reported the DSC thermogram of wool keratin regenerated with water and formic acid, and similar transitional plot was observed explaining that the first endotherm peaks <100 °C was due to water/moisture loss, followed by the peaks within the 200–250 °C temperature range, related to the α-helix denaturation (Aluigi et al. 2007).
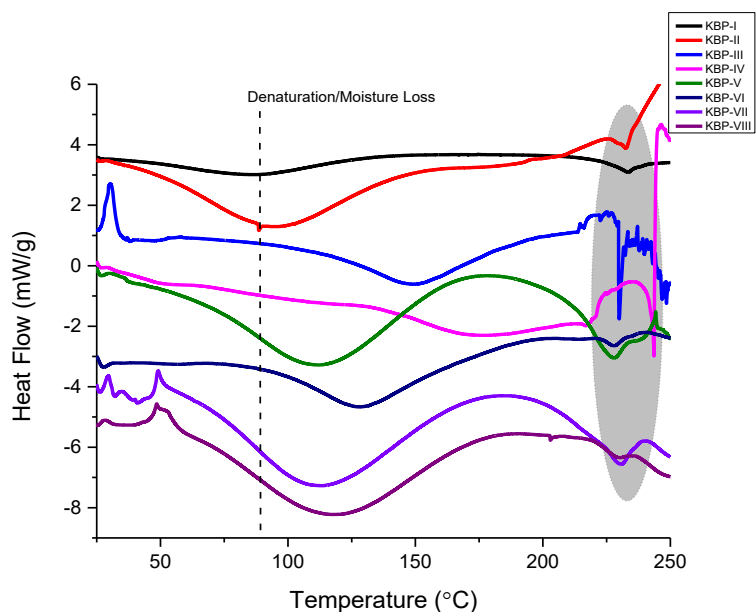
Figure 2.4. DSC heat flow signals of KBP-I and modified KBPs.

2.3.1.5 BET analysis

One important parameter for characterization of porous materials is their specific surface area.

BET surface area (S_{BET}) of the sample is determined according to the proposed criteria of

multilayer formation within the relative pressure range of 0.01<p/po < 0.08 (Weber et al.,

2010). The BET specific surface area for KBP-1 is recorded as 0.006 m^2/g, KBP-II is

6.606 m^2/g, KBP-III is 0.559 m^2/g, KBP-IV is 2.293 m^2/g, KBP-V is 0.550 m^2/g, KBP-VI is

1.094 m^2/g, KBP-VII is 0.987 m^2/g and KBP-VIII is 0.902 m^2/g (Appendix- AI: Table A1).

The pore volume and pore diameter also contribute to the surface area (Sathivika et al., 2018).

In addition to surface area, pore size distribution can also be obtained from gas sorption

isotherms. The data are evaluated by different methods with an application of microscopic

models such as density functional theory (DFT) or grand canonical Monte Carlo (GCMC)

(Weber et al., 2010). DFT describes the adsorbed phase at molecular level and is considered as

superior because it provides more reliable approach to pore size analysis. IUPAC (International

Union of Pure and Applied Chemistry), has classified pores according to their size, (i) Pores

with widths greater than 50 nm are called macropores, (ii) Pores having widths between 2 nm

and 50 nm are called mesopores, (iii) Pores with widths less than 2 nm are called micropores (Thommes et al., 2015).

According to the criteria, Fig 2.5a represents pore size distribution of KBP-I between 80 and 180 nm, concluding that the sample fractions were macro-porous material (Tefsaye et al., 2017). For the KBP-II, the pore size distribution in Fig 2.5b shows a primary maximum at pore size of 15.72 nm and secondary maximum at pore size of 24.29–80 nm, suggesting that KBP-II has higher meso to macro pore size distribution. For the other KBPs (KBP-III, KBP-V, KBP-VI, KBP-VII and KBP-VIII) the pore size distribution shows a primary maximum at a pore size between 10 and 20 nm, and secondary minimum at a pore size of 144 nm, explaining that there is higher pore size distribution in mesoporous region and lower pore size distribution in the macro-porous region. For the KBP-IV, primary maximum pore size between 10 and 20 nm and secondary maximum pore size distribution at 144 nm indicates that KBP-IV has higher mesopore and macropore distributions (Thommes et al., 2015).

The KBP-I sample has lowest value for BET specific surface area (0.006 m^2/g) and the KBP-II has the highest one (6.606 m^2/g). The clear differences in the specific surface area values among developed KBP samples suggest that these values depend on the modifications and ratio of precursors used to prepare the final products. The pore sizes of KBP-III, KBP-V, KBP-VII and KBP-VIII decrease gradually reaching to a value of 10–20 nm, while KBP-I, KBP-II and KBP-IV has shown reverse pore size behavior. The differences in the pore size distributions and changes in the characteristic of KBPs from macro-porous to mesoporous material also depend on the modifications and quantities of precursors used (Klapiszewski et al., 2013; Weber et al., 2010).

As observed from adsorption results, KBP-I, KBP-IV, KBP-V and KBP-VI displayed good adsorption capacities for different metal uptakes having smaller surface areas. This indicates that apart from surface area other factors such as availability of more functional groups on the

surface aid in enhancing the metal uptake (Tefsaye et al., 2017). FTIR analysis of this study also confirms that the surface of biopolymers has amine and carbonyl/esters which tend to participate in the metal uptake, hence, increasing the adsorption phenomena for heavy metals.
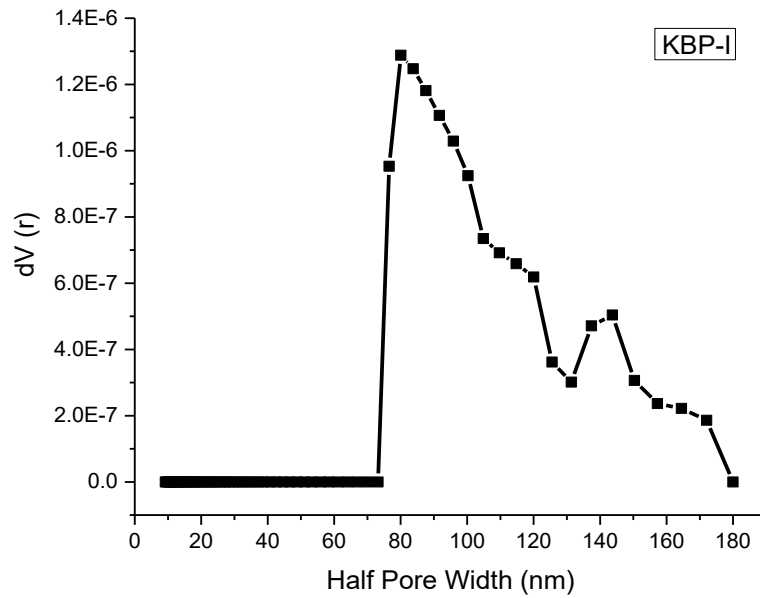
Figure 2.5 a. Pore size distribution obtained from DFT method for KBP-I.
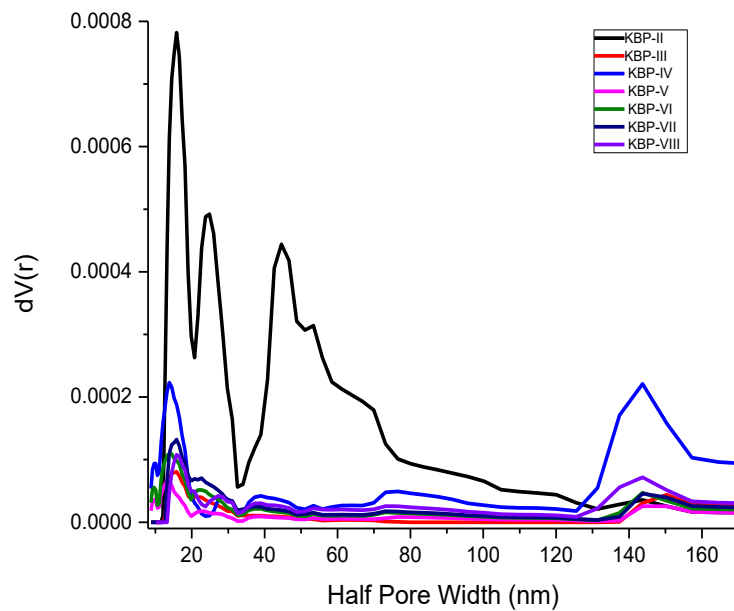
Figure 2.5 b. Pore size distribution obtained from DFT method for modified KBPs (KBP-II, KBP-III, KBP-IV, KBP-V, KBP-VI, KBP-VII and KBP-VIII).

2.3.1.6 Scanning electron microscopy (SEM)

The shape and size of sorbents play an important role in adsorption of contaminants (Khosa et al., 2013). Chemical modification of keratin protein affects its morphology by exposing more functional groups on the surface increasing the adsorption phenomena (Arshad et al., 2016a; Arshad et al., 2016b). SEM images of the samples in Fig 2.6 confirmed that chemical modifications of KBPs have noticeable impacts on the overall morphology of materials. The KBP-I seems to have a fibrous structure with smooth surface (Khosa et al., 2013). In comparison, KBP-II modified with citric acid has a rough surface indicating the outer layer (cuticle) of keratin fibers opened up, exposing active functional groups on the surface (Kocaturk, 2008). The keratin biopolymers modified with ionic liquids show significantly different surface morphologies. KBP-III indicates surface roughness with deep micro-cracks and dark patches (Arshad et al., 2016a; Arshad et al., 2016b), while the native structural integrity of KBP-IV has been entirely lost with great surface roughness and more divulged structure showing the higher level of modification (Khosa et al., 2013). For the KBP-V modified with methanol and 3-(dimethylamino)-1-propylamine has a smooth and less damaged surface with no adhered particles (Khosa et al., 2013). KBP VI modified with POSS under alkaline conditions shows the loss of an original smooth surface (Sim et al., 2016). The keratin biopolymers KBP-VII (modified with POSS under acidic conditions) and KBP-VIII (modified with reducing agent) display prominent structural changes with the dark patches and adhered particles on the surfaces increasing the surface roughness. As illustrated from SEM images in Fig 2.6, the dissolution/regeneration and in-situ modifications of KBPs have changed their surface morphologies (encircled and represented by arrows). This indicates to the denaturation of helix structure and destruction of peptide chain linkages signifying the increased surface functionality for adsorption of contaminants. (Donner et al., 2019). The chemical changes on the surface of KBP-I and modified KBPs are consistent with our metal uptake investigations

as discussed in this adsorption study. These structural changes are also evidenced by FTIR, XRD and BET analysis. The differences in surface elemental composition between processed and modified KBPs can be observed by Energy Dispersive X-Ray Spectroscopy (EDX) and X-ray Photoelectron Spectroscopy (XPS) results (Appendices-AII, AIII: Fig A1-A2).

Figure 2.6. Dissimilarity in surface morphologies of keratin biopolymers was observed using scanning electron microscopy. SEM images were taken within the scale bar range of 100 nm-200 nm.

2.3.2 Adsorption capacities of keratin biopolymers towards the removal of metals from synthetic wastewater

The adsorption capacities of KBPs are evidently influenced by the sorbent's modifications (Martinez et al., 2018). Here, the keratin derived biopolymers were examined for simultaneous removal of trace metals from synthetic wastewater. With trace metal cations in Fig 2.7, KBP-I revealed adsorption results removing 17% of Co, $\geq$ 51% of Ni, $\geq$ 73% of Cu and $\geq$93% of Cd. KBP-II adsorbed 16% of Co, $\geq$ 23% of Ni and $\geq$51% of Cd. KBP-III removed $\geq$58% of Cu. KBP-IV adsorbed $\geq$16% of Ni and $\geq$79% of Cu. KBP-V demonstrated good adsorption results removing $\geq$70% of Co, $\geq$ 94% of Ni, 53% of Cu, $\geq$ 62% of Zn and $\geq$92% of Cd. KBP-VI removed $\geq$10% of Co, $\geq$ 32% of Ni, $\geq$ 30% of Cu and 61% of Cd. KBP-VII removed $\geq$20% of Cu and $\geq$44% of Cd. KBP-VIII removed 70% of Ni and $\geq$47% of Cu (concentration values with standard deviation are given in Appendix-AIV: Table A2). Although Cu and Zn recovery by KBPs from synthetic wastewater is impaired by the additional contribution of Cu and Zn from the biopolymers themselves, indicated by the control treatment (KBPs plus ultrapure water; Appendix-AV: Fig A3), denoting that KBPs served as a source of Cu and Zn to the equilibrating solution.

Heavy metal ions have different physical and chemical properties, hence, possessing different affinities for oxygen, nitrogen- and sulfur-containing ligands. The adsorption of the heavy metal ions depends on their complexation with active sites of the keratin proteins in CFs. The interactions of metal cations with active sites of keratins can be elucidated with their Lewis acid and base principles. Lewis acid accepts the electron pair, while a Lewis base donates an electron pair. The metal cations are classified into hard and soft "Lewis" acids. Cd^{2+}, Cu^{2+}, Ni^{2+}, and many other ions are classified as intermediate class, with Ni^{2+} shifting to hard class and Cd^{2+} to soft class. Oxygen and aliphatic nitrogen sites of the keratin molecules are recognized as hard, aromatic nitrogen as intermediate, and sulfur as soft Lewis bases explaining

that Ni^{2+} would bind to aromatic nitrogen, and Cd^{2+} to SH-groups (Kocaturk, 2008). KBP-V has demonstrated good adsorption for divalent metal cations (Co, Ni, Cu, Zn and Cd) due to structural changes (evidenced by XRD results) incorporated in CFs when modified with 3-(dimethylamino)-1-propylamine.

For redox sensitive oxy-anionic elements in Fig 2.7, KBP-I removed $\geq$67% of V^V, $\geq$ 90% of Cr^{VI} and $\geq$87% of As^{III}. KBP-II removed $\geq$32% of V^V and $\geq$58% of Cr^{VI}. KBP-III retained 81% of V^V and Cr^{VI}. KBP-IV removed $\geq$85% of V^V and $\geq$91% Cr^{VI}. KBP-V removed $\geq$35% V^V and $\geq$19% Cr^{VI}. KBP-VI removed 24% V^V and $\geq$95% Cr^{VI}. KBP-VII removed 44% of V^V and $\geq$92% of Cr^{VI}. KBP-VIII removed $\geq$35% of V^V, $\geq$91% of Cr^{VI} and $\geq$12% of As^{III} (concentration values with standard deviation are given in Appendix-AIV: Table A3).

The chemical reduction of Cr^{VI} and V^V as oxyanionic species (CrO_4^{2-}, $H_2VO_4^-/HVO_4^{2-}$ at neutral pH) from synthetic wastewater by KBPs through exposed thiol/sulfhydryl (-SH) and amine (-NH$_2$) functional groups appears to be a significant process (Nuutinen, 2017). Removal of Cr^{VI} from an aqueous phase by natural/bio-based sorbents include direct and indirect reduction mechanisms. In direct reduction mechanism, Cr^{VI} is directly reduced to Cr^{III} by contact with the electron-donor groups of the bio-based sorbents. The reduced Cr^{III} then forms complexes with bio-based sorbents or remains in the aqueous phase. However, indirect mechanism involves three steps, anionic Cr^{VI} first make bonds with positively charged functional groups on the bio-based sorbent surface then the Cr^{VI} is reduced to Cr^{III} by adjacent electron-donor groups and at last the Cr^{III} make complexes with adjacent functional groups. Amino and carboxyl groups of bio-based sorbents may involve in indirect reduction mechanism (Park et al., 2007).

All keratin derived biopolymers did not show affinity for removal of As^{III} and Se^{VI} except the KBP-I and KBP-III. KBP-I demonstrates good adsorption results for As^{III}. The adsorption of arsenic by KBP-I involves an ion-exchange process in which arsenic oxyanions tend to

approach positively charged active sites of the bio-based sorbent (Khosa et al., 2013). KBP-III indicating very little affinity for Se^{VI} removing 12% of Se^{VI} from synthetic wastewater. This low affinity trend of biopolymers towards arsenic and selenium uptake is elaborated by surface complexation theory. This theory explains that lowering pH increases the positive charge of the surface, thus increasing adsorption of the negative species $HSeO_3^{-}$(IV), SeO_3^{2-}(IV), and SeO_4^{2-}(VI), below and above the acidic pH, uptake by polymer is declined greatly (Ishikawa et al., 2004).
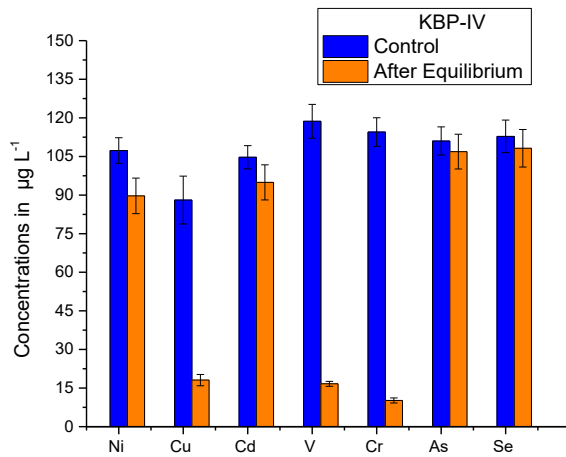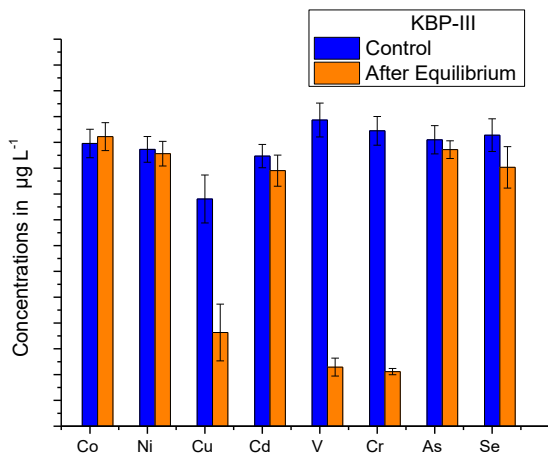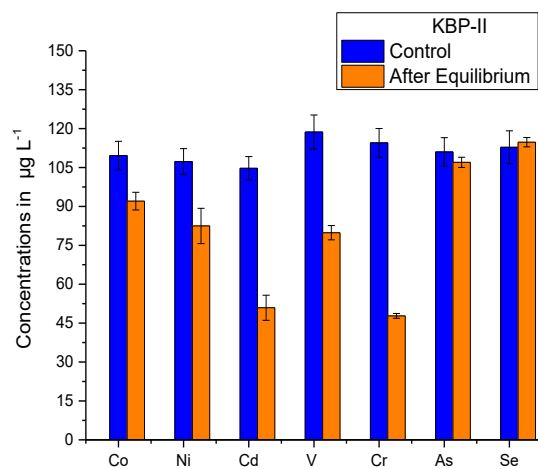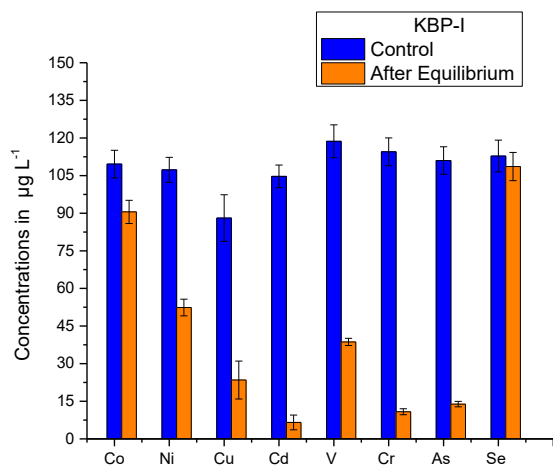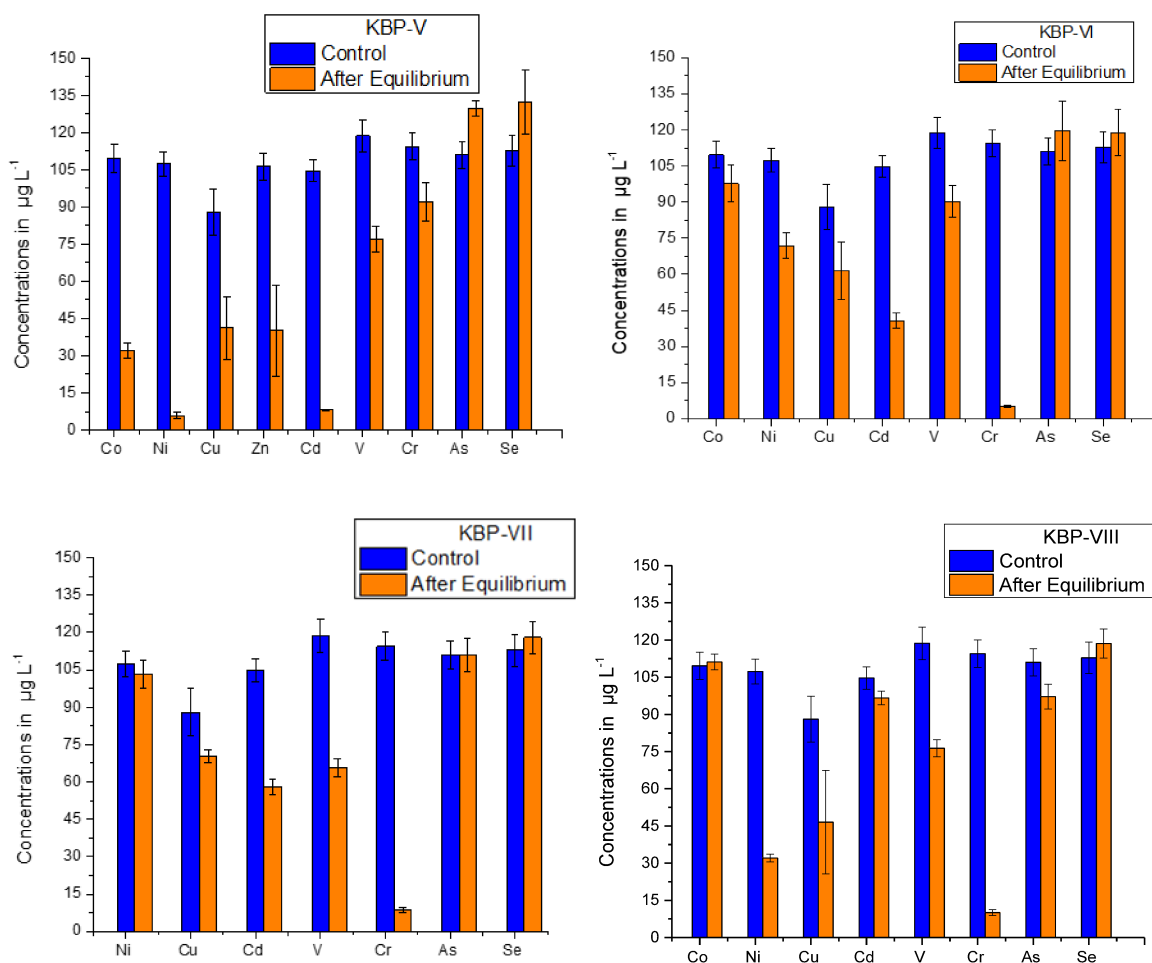
Figure 2.7. Removal of transition metals (Co, Ni, Cu, Zn and Cd) and oxyanions of redox sensitive trace metals (V^V, Cr^{VI}, Se^{VI} and As^{III}) in synthetic wastewater by KBP-I and modified KBPs (KBP-II to KBP-VIII). Concentrations are an average of triplicate samples measured after 24 h of incubation. Control values represent the analyte in the ultrapure water without biopolymer addition.

2.4 Conclusion

This work highlights the role of keratin derived biopolymers as an emerging area towards remediation of heavy metal water pollution. The proposed methodology has illustrated the ability of keratin feathers (before and after modifications) as effective sorbents to sequester the transition and redox sensitive heavy metals from energy simulated wastewater. The characterization studies of keratin derived biopolymers provide an additional insight about surface functionality that also reflect the adsorption analysis. Based on initial screening, all KBPs performed well where KBP-I removed 87–93% of As and Cd, KBP-IV showed adsorption capacity of 80–85% for Cu and V^V and 91% for Cr^{VI}, KBP-V represented 60–90%

efficiency for the removal of Co, Ni and Zn and KBP-VI demonstrated removal efficiency of 95% for Cr^{VI} metal. All of the developed biopolymers have shown better metal adsorption capabilities owing to their larger accessibility of functional groups present on surface. On an optimistic approach, keratin derived biopolymers open diverse possibilities in detoxifying pollutants from energy related wastewaters and also make them potential candidate for the scale-up treatment of multi-metal contaminated industrial wastewaters. The utilization of these keratin biopolymers provides multiple benefits, including economical and eco-friendly filtration system for wastewater treatment and diversion of feather waste generated by poultry processing plants leading to social, economic, and environmental benefits.

2.5 Acknowledgements

3.0 THE EFFECT OF PROCESS PARAMETERS (PH, TEMPERATURE, CONTACT TIME) ON ADSORPTION AND METAL SUPPORT INTERACTIONS (MECHANISMS) FOR HEAVY METALS REMOVAL FROM WASTEWATER BY KERATIN DERIVED SORBENTS

3.1 Introduction

Due to growing urbanization, the water resources have now become perilously scarce and befouled, therefore, the most crucial challenge of the time is to access safe water (Werber et al., 2016). The consumption of raw materials and industrial goods has pushed mining and manufacturing industries to release the aberrant levels of divalent cations and oxyanions to soil and water streams (Donner et al., 2019; Melnyk et al., 2018; Sun et al., 2020; Zubair et al., 2020). Although active participation in physiological functions of living organisms, divalent cations are toxic and have harmful effects on living organisms, for example, nickel (Ni) and cobalt (Co) are known for their potentially hazardous nature. Furthermore, oxyanions such as arsenic (As) and chromium (Cr) (in its hexavalent form) are known to be carcinogens (Melnyk et al., 2018).

In a comparison of physicochemical processes, biological systems have been discovered as natural alternatives to remediate wastewater. Sorption using low-cost natural sorbents (agricultural waste and seafood processing wastes) with their implications towards wastewater treatment (even at very low concentrations of contaminants) is one of the promising substitutes (Ngah & Fatinathan, 2010). Bio-based sorbents, despite being environmentally compatible, are appraised based on their adsorption characteristics due to the abundance of nitrogen (N) and oxygen (O) containing functional groups that increase the sorbent's affinities for metal ions removal (Manzoor et al., 2019; Matouq et al., 2015).

The adsorption is affected by the pH of the solution, temperature, and the contact time (Yu & He, 2018). The pH of the aqueous media is the most important parameter governing metal adsorption by sorbent's surface (Anastopoulos et al., 2019). The pH of the solution influences the ionization of solute metal ions and sorbent's surface sites, hence, affects the adsorption efficiencies (Chen et al., 2010). The effect of temperature on adsorption phenomena cannot be neglected, considering recent literature reports suggesting alterations in the adsorption

efficiencies with the increase in temperature. The kinetics performance of test sorbent is also an important aspect to be considered, thus, determining the minimum time to reach adsorption equilibrium. (Anastopoulos et al., 2019). Furthermore, the adsorption mechanisms provide additional insights into the performances of sorbents. Also, the fundamental step in the development of wastewater remedial system for metal ion's removal is to quantify the adsorption by constructing the adsorption isotherms at constant temperature (~20 °C) that assess the distribution of metal ions in the aqueous phase (wastewater) in equilibrium with solid phase (sorbent) that deduces the maximum adsorption capacities of sorbents (Donner et al., 2019).

Chicken/keratin feathers (CFs) is a waste product generated from poultry industry in large quantities and is burnt or landfilled. Therefore, has gained attention as a natural bio-based sorbent for its abundance and potential to be used in wastewater treatment. The CFs are composed of 91 % keratin, a strong fibrous protein that possesses different chemical functionalities based on their amino acid's compositions (each with identifying side chains) (Ullah et al., 2011). By applying different chemical treatments, the structure of CFs can be modified, and these side chains reveal different functionalities for removing contaminants from wastewater. Hence, these side chains have an influential role in adsorption processes (Donner et al., 2019; Zahara et al., 2021).

Previously (first data chapter), the eight keratin derived biopolymers (KBPs) were developed by modifying the CFs with different chemical agents, and their effectiveness were tested for divalent cations and oxyanions removal from multi-metal synthetic wastewater (Zahara et al., 2021). Herein, among the eight KBPs, three KBPs (KBP-I, KBP-IV, KBP-V) have been selected (based on their initial adsorption screening) to expand the research towards optimizing the adsorption process. The objectives of this study are to (i) evaluate the adsorption performances of KBPs (KBP-I, KBP-IV, KBP-V) towards metal ions removal from synthetic

wastewater under the influence of process parameters (pH of the solution, temperature, and contact time), (ii) investigate the adsorption mechanisms involved in the oxyanions removal by KBP-IV and divalent cations removal by KBP-V from synthetic wastewater, (iii) quantify the adsorption by constructing the adsorption isotherms, data analyzing and fitting by Langmuir and Freundlich isotherm models, and (iv) imply the use of KBPs (KBP-I, KBP-IV, KBP-V, and KBP-VII) towards the removal of vanadium (V), nickel (Ni), barium (Ba), and strontium (Sr) from oil sand process affected water (OSPW).

3.2 Materials and methods

3.2.1 Chemicals

The chemicals used for the processing and modification of chicken feathers include: hexane (Sigma Aldrich), sodium hydroxide (Sigma Aldrich ≥97%), 1-butyl-3-methylimidazolium bromide (Sigma Aldrich ≥97%), ethanol (Fisher Brand 95%), diethyl ether (Sigma Aldrich ≥99%), sodium sulphite (Sigma Aldrich ≥98%), urea (Fischer Scientific), ethylenediaminetetraacetic acid (Sigma Aldrich ≥99%), tris base (Fischer Scientific 99.8%), 2-mercaptoethanol (Sigma Aldrich ≥99%), 1,4-dioxane (Sigma Aldrich), tetrahydrofuran (Sigma Aldrich), 3-(dimethylamino)-1-propylamine (Sigma Aldrich 99%), polyhedral oligomeric silsesquioxanes (POSS) with mercaptopropylisobutyl groups on the surface called mercaptopropylisobutyl-POSS (Hybrid Plastics TH1550), hydrochloric acid (Sigma Aldrich 37%) and methanol (Sigma Aldrich 99.8%).

For the adsorption experiment, individual metal stock solutions were prepared using powder reagents of the following: nickel (Ni) chloride hexahydrate (Fisher Scientific, 99.4%), cobaltous (Co) sulfate heptahydrate (Fisher Scientific, 100%), cadmium (Cd) chloride (Sigma Aldrich 99.9%), chromium (Cr^{VI}) oxide (Sigma Aldrich 99.99%) and arsenic (As^{III}) sodium meta arsenite (Sigma Aldrich ≥99%). For vanadium V^V, liquid standard solution vanadium [CAS No: HNO_3 7697-37-2, V 7440-62-2 (SpexCertiPrep)] was used.

3.2.2 Processing of chicken/keratin feathers (KBP–I) and preparation of KBP-IV, KBP-V, and KBP-VII

The chicken/keratin feathers (CFs) were collected from the Sofina Foods, Edmonton, Canada, then washed, dried, and ground according to the reference (Arshad et al., 2016; Zahara et al., 2021). After grinding, the CFs were Soxhlet extracted, dried, and ground according to the reference (Zahara et al., 2021). These processed and washed CFs were stored in a desiccator at room temperature as KBP-I. The KBP-IV was prepared by the chemical modification of processed CFs using the ionic liquid [1-butyl-3-methylimidazolium bromide (BMIM)Br] according to reference (Sun et al., 2009; Zahara et al., 2021). As reported in literature, the purpose of this modification was to change the surface hydrophobic character of CFs to a hydrophilic character by breaking the hydrogen bonding of keratin proteins with the exposure of buried functional groups towards surfaces (Sun et al., 2009; Zahara et al., 2021). The KBP-V was prepared from processed CFs by a method already reported in the literature (Zahara et al., 2021). The purpose of this modification was the amination of the carboxyl groups (present in the CFs keratin proteins) that enhances the keratin's adsorption affinity towards metal cations from wastewater (Guibal, 2004; Randall et al., 1979; Wong & Jameson, 2011). The KBP-VII was modified by using the mercaptopropylisobutyl- polyhedral oligomeric silsesquioxanes (POSS) according to reference (Arshad et al., 2016; Zahara et al., 2021).

3.2.3 Removal of metal ions under the influence of process parameters (pH of the aqueous solution, temperature, and contact time) by developed KBPs from synthetic wastewater

The synthetic wastewater was prepared by following a method already reported in the literature (Zahara et al., 2021). Synthetic wastewater was prepared by using nano-pure water (18.2 MU cm; Barnstead, Thermo Scientific™). The ionic strength of nano-pure water was raised to I = 0.05 by adding the 0.02 M NaCl and 0.01 M $CaCl_2$. The synthetic water was then spiked with

six metals (Ni^{2+}, Co^{2+}, Cd^{2+}, V^V, Cr^{VI}, and As^{III}) up to 100 µg L^{-1} concentrations of each (designated as multi-metal synthetic wastewater).

To determine the effect of pH on adsorption, the multi-metal synthetic wastewater was divided into two sections, and the pH of each section was adjusted to 5.5 and 8.5 individually. Then, the triplicates of 15 mL centrifuge tubes containing 0.1 g of KBPs (KBP-I, KBP-IV, or KBP-V separately) and 10 mL of multi-metal synthetic wastewaters (prepared either with pH 5.5 or 8.5), were placed on a reciprocating shaker for 24 hours at ambient temperature.

To investigate the effect of temperature on adsorption, the batch equilibrium experiment was conducted by placing the triplicates of 15 mL centrifuge tubes each containing 0.1 g of either KBP-I or modified KBPs (KBP-IV and KBP-V) with 10 mL of multi-metal synthetic wastewater (prepared as prescribed above with pH=7.5) on reciprocating shaker for incubation time (24 hours) at two temperature ranges (30 °C and 45 °C) separately.

To analyze the effect of contact time on adsorption, 0.1 g of KBP-I or modified KBPs (KBP-IV and KBP-V) each with 10 mL of multi-metal synthetic wastewater (prepared as prescribed above with pH=7.5) were taken in 15 mL centrifuge tubes and incubated on a reciprocating shaker for (15, 30, 60, 120, 180 and 360 mins) at same temperature (24 °C).

After their incubation times (for each batch experiment), the samples were removed, filtered, diluted, and metal concentrations were analyzed by inductively coupled plasma mass spectrometer (ICP-MS; iCapQThermo Scientific) under kinetic energy discrimination mode (KED; He gas).

3.2.4 Investigating the adsorption mechanisms involved in the removal of divalent cations and oxyanions from synthetic wastewater by KBP-IV and KBP-V

To investigate the adsorption mechanisms, synthetic wastewaters were prepared (as prescribed above) with the two pH ranges (5.5 and 8.5 individually) and had no spiked metal concentrations. Afterwards, 0.1 g of each KBP (either KBP-IV or KBP-V) was weighed in

triplicates in 15 mL centrifuge tubes, and then the 10 mL synthetic wastewaters with two initial pH ranges (5.5 and 8.5) were added to the tubes. The centrifuge tubes were then placed on the reciprocating shaker, meanwhile, measuring and maintaining the pH after every 3-4 hours. Once the pH (5.5 and 8.5) was maintained, aqueous metals concentrations of either Cd^{2+}, Ni^{2+}, $V^{V,}$ or Cr^{VI} from stocks were added individually to 10 mL synthetic water (designated as single-metal synthetic wastewater) in centrifuge tubes. The final concentration of metals in centrifuge tubes was 4 µmol L^{-1}. Then, the samples with specified metal concentrations were further incubated for 24 hours on a shaker for adsorption results. After 24 hours, the samples were removed, filtered, diluted, and metals concentrations were analyzed by ICP-MS. After the adsorption experiment, the metal-loaded KBPs (KBP-IV and KBP-V) were characterized by using the X-ray Photoelectron Spectroscopy (XPS) analytical technique for investigating the adsorption mechanisms.

3.2.5 Construction of adsorption isotherms for modified KBPs

Based on the adsorption potential of KBP-I for arsenic (As^{III}) and cadmium (Cd^{2+}), KBP-IV for chromium (Cr^{VI}), and KBP-V for nickel (Ni^{2+}), these KBPs were chosen for constructing the adsorption isotherms. The synthetic water was prepared as prescribed above (Section: *3.2.3*). The synthetic water was then spiked with either Cd^{2+} (0.2, 0.4, 0.8, 10, 50 or 100 mg L^{-1}) or Ni^{2+} (0.2, 0.4, 0.8, 10 or 50 mg L^{-1}) or Cr^{VI} (0.2, 0.4, 0.8, 10, 50, 100 or 200 mg L^{-1}) or As^{III} (0.2, 0.4, 0.8 and 10 mg L^{-1}) individually, pH was adjusted to 7.5, and then treated with KBPs (0.1 g) in centrifuge tubes as described in the preceding section (Section: *3.2.3*). All samples were created in triplicates. The samples were filtered, diluted after their incubation time/batch adsorption experiment, and metal concentrations were analyzed by ICP-MS.

Once the system reached an equilibrium state, adsorption isotherms can be used for determining the distribution of adsorbate molecules between the aqueous phase (synthetic wastewater) and the solid phase (KBPs) (Donner et al., 2019). The adsorption was quantified

(Eq 1) and the results were analyzed and fitted according to the Langmuir and Freundlich isotherm models. The Langmuir model (Eq 2) is based on the assumptions that adsorption occurs at specific homogenous sites in the monolayer formation of atoms whereas the Freundlich model (Eq 3) presumes adsorption in heterogeneous systems.

$$q = \frac{V_i (C_{in} - C_{eq})}{m_s} \qquad (1)$$

$$q = \frac{q_{max} K_L C_{eq}}{1 + K_L C_{eq}} \qquad (2)$$

$$q = K_F C_{eq}^N \qquad (3)$$

where q is the equilibrium mass of adsorbed metal ion per unit mass of adsorbent (KBPs) (mg kg^{-1}), V_i is the volume of equilibrating solution containing metals, m_s is the mass of biopolymer (kg), C_{in} is the initial concentrations of metal ions (mg L^{-1}) before adsorption, C_{eq} is the equilibrium concentration of metal in solution (mg L^{-1}) after adsorption by KBPs, q_{max} is adsorption maximum having the units of q, K_L is the adsorption constant related to Langmuir model and K_F is the adsorption constant for Freundlich model with N is heterogeneity factor confined between 0 and 1.

3.2.6 Application of keratin biopolymers towards metal ions removal from field-collected wastewater (OSPW)

To determine the KBPs applicability towards the removal of the inorganic contaminants form field-collected wastewater, another batch adsorption experiment was conducted using the oil sand process affected water (OSPW). The OSPW was diluted, and the metal concentrations in OSPW were analyzed using an ICP-MS (iCapQThermo Scientific) under kinetic energy discrimination mode (KED; He gas). For adsorption of inorganics from OSPW, the same batch equilibrium experimental procedure was followed (as described above for synthetic wastewater, section: *3.2.3*) using 0.1 g of KBPs (KBP-I, KBP-IV, KBP-V, and KBP-VII) with

10 mL of OSPW incubated on a reciprocating shaker for 24 hours at ambient temperature. After 24 hours, the samples were filtered, diluted, and aqueous metal concentrations were analyzed using the ICP-MS.

3.3 Results and discussion

3.3.1 Effect of solution pH on adsorption

The solution pH is the most dominant factor for the adsorption of metals (Wang & Chen, 2006). The effect of initial solution pH on multi-metal (divalent cations and oxyanions) removal by KBP-I, KBP-IV, and KBP-V can be observed (Fig 3.1) after 24 hours of incubation/equilibrium. At pH= 5.5, KBP-I adsorbed 9 μg L^{-1} of Co^{2+}, 44 μg L^{-1} of Ni^{2+}, 83 μg L^{-1} of Cd^{2+}, 71 μg L^{-1} of V^{V}, 78 μg L^{-1} of Cr^{VI} and 56 μg L^{-1} of As^{III}, KBP-IV adsorbed 4 μg L^{-1} of Co^{2+}, 9 μg L^{-1} of Ni^{2+}, 28 μg L^{-1} of Cd^{2+}, 96 μg L^{-1} of V^{V}, 85 μg L^{-1} of Cr^{VI} and 83 μg L^{-1} of As^{III}, and KBP-V removed 73 μg L^{-1} of Co^{2+}, 95 μg L^{-1} of Ni^{2+}, 86 μg L^{-1} of Cd^{2+}, 48 μg L^{-1} of V^{V}, and 21 μg L^{-1} of Cr^{VI} from multi-metal synthetic water.

At pH= 8.5, KBP-I removed 6 μg L^{-1} of Co^{2+}, 52 μg L^{-1} of Ni^{2+}, 106 μg L^{-1} of Cd^{2+}, 72 μg L^{-1} of V^{V}, 93 μg L^{-1} of Cr^{VI} and 61 μg L^{-1} of As^{III}, KBP-IV adsorbed 5 μg L^{-1} of Co^{2+}, 15 μg L^{-1} of Ni^{2+}, 46 μg L^{-1} of Cd^{2+}, 99 μg L^{-1} of V^{V}, 96 μg L^{-1} of Cr^{VI} and 88 μg L^{-1} of As^{III}, and KBP-V adsorbed 79 μg L^{-1} of Co^{2+}, 95 μg L^{-1} of Ni^{2+}, 105 μg L^{-1} of Cd^{2+}, 53 μg L^{-1} of V^{V}, and 26 μg L^{-1} of Cr^{VI} from multi-metal synthetic wastewater.
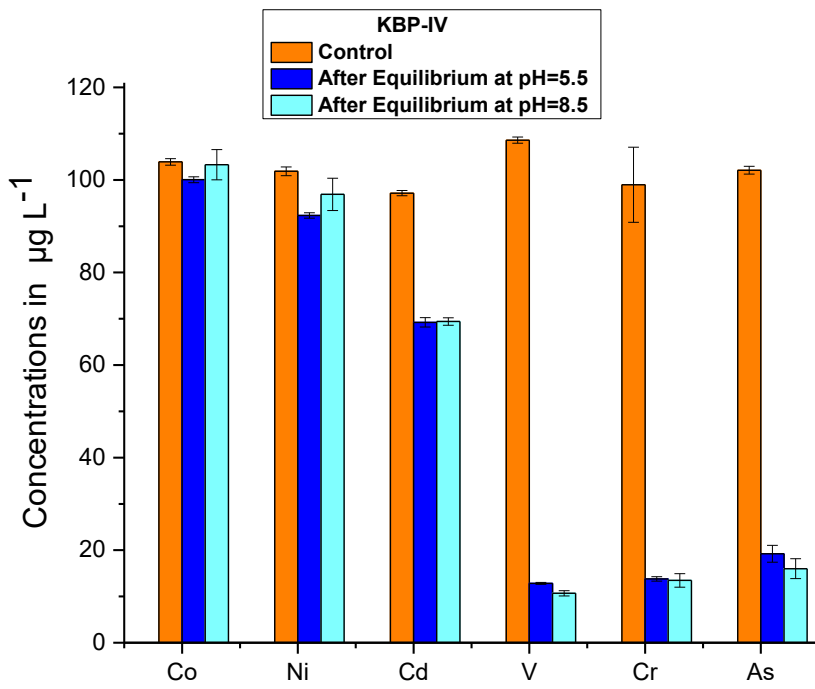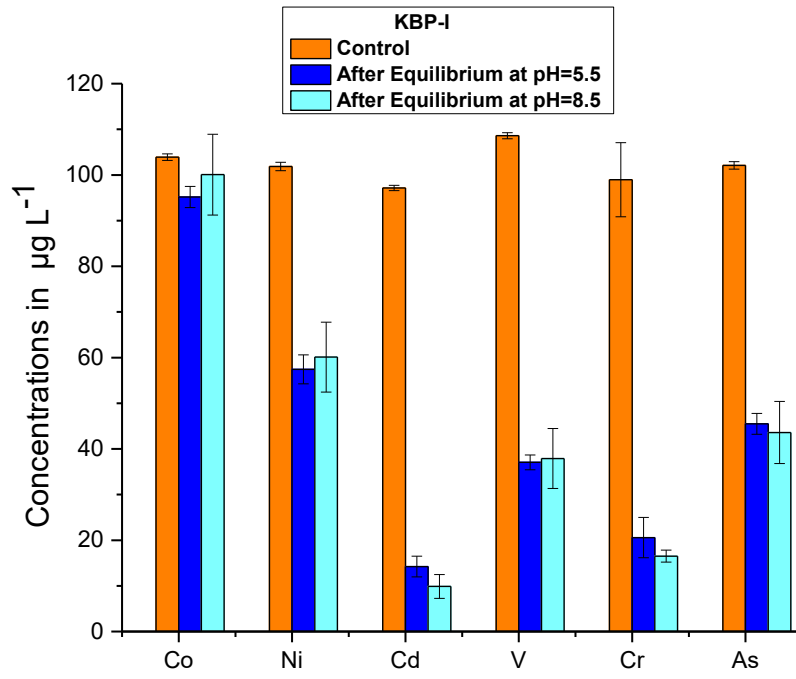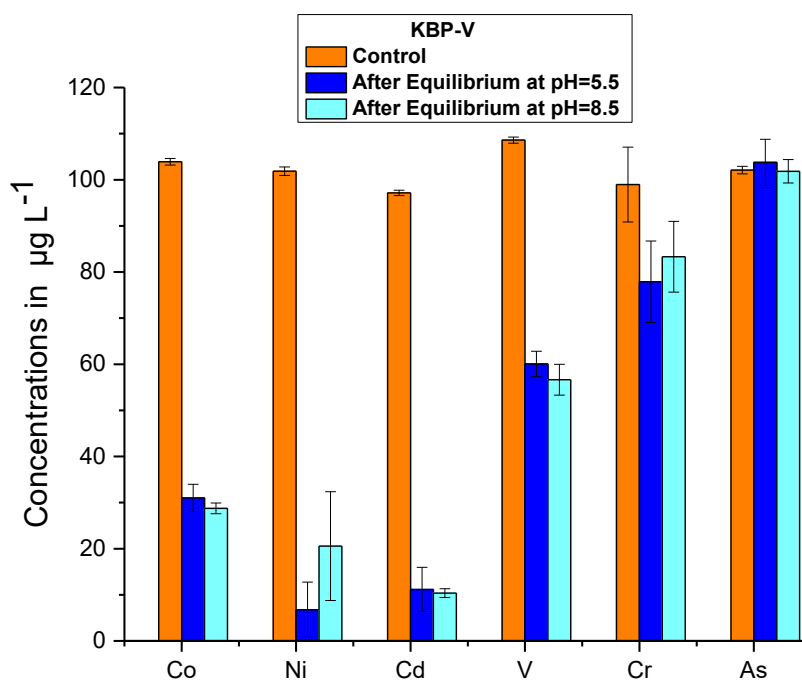
Figure 3.1. The effect of solution initial pH (5.5 and 8.5) on adsorption of (Co^{2+}, Ni^{2+}, Cd^{2+}, V^V, Cr^{VI} and As^{III}) by KBPs (KBP-I, KBP-IV, and KBP-V) from multi-metal synthetic wastewater. Control values represent the analyte in the nano-pure water without KBPs addition. Concentrations are an average of triplicate samples measured after their mentioned incubation times.

As seen from Fig 3.1, there are no significant differences observed in adsorption results obtained by KBP-I, KBP-IV, and KBP-V for removing the divalent cations and oxyanions from multi-metal synthetic wastewaters at two pH (5.5 & 8.5) ranges. Consequently, the pH of the multi-metal synthetic wastewater was measured again after the 24 hours of incubation/equilibrium, and the results (Appendix-VI, Table A4) elaborated that the KBPs were buffering the pH of the synthetic wastewater. The KBP-I buffered both pH values (5.5 and 8.5) to 6.5, KBP-IV buffered the pH values (5.5 and 8.5) to 4.5, and KBP-V buffered the pH values (5.5 and 8.5) to 8.0, therefore no differences are observed in the adsorption results of metals at both pH ranges. The KBP-V adsorbed divalent cations, whereas KBP-IV removed oxyanions at both pH ranges (5.5 and 8.5) due to their buffering capacities. The keratins used in the present study consist of carboxyl and amine groups and the FTIR/ XRD results *(sections: 2.3.1.1 & 2.3.1.2)* confirmed that the chemical modifications of keratin (development of sorbents) changed the chemical structure of keratins and had exposed the functional groups

towards the surfaces. Therefore, the pH of the solution was influenced by such functional groups (due to the protonation or deprotonation of amine and carboxyl groups) and affected the chemical bonding with metal ions (Chakraborty et al., 2020; Khosa et al., 2013). Therefore to minimize the buffering capacities of KBPs and to investigate the adsorption mechanisms involved in the metal ions removal at certain pH, another batch experiment was performed while maintaining/stabilizing the pH of single-metal syntehtic wastewater (as prescibed above section: Section *3.2.4*) during the adsorption process.

As seen from Fig 3.2, the KBP-V displayed high adsorption effeiciencies (2.2 µmol L^{-1} of Cd^{2+}, and 2.6 µmol L^{-1} of Ni^{2+}) at pH 8.5 and low adsorption efficiencies at pH= 5.5 for divalent cations. The high adsorption efficiencies of KBP-V for divalent cations (Cd^{2+} and Ni^{2+}) at pH = 8.5 and could be attributed to speciation of metal ions present in aqueous media. At solution pH range between 6.0 and 8.0, the dominating chemical states of cadmium are Cd^{2+} (minor) and Cd $(OH)^+$ (major). However, the nickel is present in the solution in the form of Ni^{2+} ions (major) up to pH 8.5, whereas $Ni(OH)_2$ (minor) starts to precipitate at pH 8.5. The positively charged $Ni(OH)^+$ also emerges in the pH range of 8-11 (Lei et al., 2019; Ma et al., 2018; Pivarciova et al., 2014). The KBP-V was modified with propylamine with the purpose of amination towards carboxyl groups of the keratin proteins (converting the carboxyl groups to more potent nucleophiles). At neutral or slightly alkaline pH range, the amino groups exist as NH_2 (or =NH) and nitrogen acts as a binding site (due to presence of lone pairs of electrons) for divalent cations (Wong & Jameson, 2012; Zubair et al., 2020). Furthermore, the higher pH deprotonated the functional groups (carboxyl) and increased the surface negatively charged binding sites that led to the increased ionic/electrostatic attractions between negatively charged binding sites and positively charged divalent cations [Cd^{2+}, Cd $(OH)^+$ and Ni^{2+}, $Ni(OH)^+$] (Lei et al., 2019; Ma et al., 2018; Pivarciova et al., 2014). Hence, complexation/chelation or electrostatic attraction mechamisms could be involved in the adsorption of divalent cations.

At low (acidic) pH range, the amino groups in the KBP exist as NH_3^+ (or NH_2^+). The low adsorption efficiencies for divalent cations by KBP-V at pH = 5.5 indicated that the protonotaed amino groups prevented the divalent cations from approaching the surface of KBP-V.Therefore, less divalent metal cations were adsorbed because of the electrostatic repulsion between protons on the KBP-V surface and the metal cations (Hammaini et al., 2007; Zhang et al., 2016).

As seen from Fig 3.2, the KBP-IV removed 3.9 $\mu mol\ L^{-1}$ of Cr^{VI} and 3.3 $\mu mol\ L^{-1}$ of V^V, displaying high adsorption efficiencies for oxyanions at pH 5.5 from single metal synthetic wastewaters. At slightly acidic pH range, the predominant species of Cr^{VI} are Cr_2O7^{2-}, $HCrO_4^-$, CrO_4^{2-} and predominant species of V^V are $H_2VO_4^-/HVO_4^{2-}$ (Gao et al., 2014; Rodriguez et al., 2015). When the KBP-IV was modified with ionic liquid [BMIM]Br, the hydrophobic character of the modified KBP changed to the hydrophilic character. During the regeneration step (when the CFs/KBPs were regenerated with water after their dissolution in ionic liquid), the hydrophilic groups (amino and carboxyl groups) of CFs had a tendency to self-assemble themselves towards the aqueous phase. The interaction of hydrophilic amino groups with water, converted them to cationic amino groups that leads to the adsorption of oxyanions through electrostatic attraction between the protonated surface functional groups and oxyanionic species (Cr_2O7^{2-}, $HCrO_4^-$, CrO_4^{2-}, and $H_2VO_4^-/HVO_4^{2-}$) (Sun et al., 2009; Zahara et al., 2021). Moreover, the adsorption of oxyanions at high pH decreased due to the electrostatic repulsion between negatively charged surfaces of KBP and oxyanionic species of Cr^{VI} and V^V (Ahalya et al., 2010; Zahara et al., 2021).
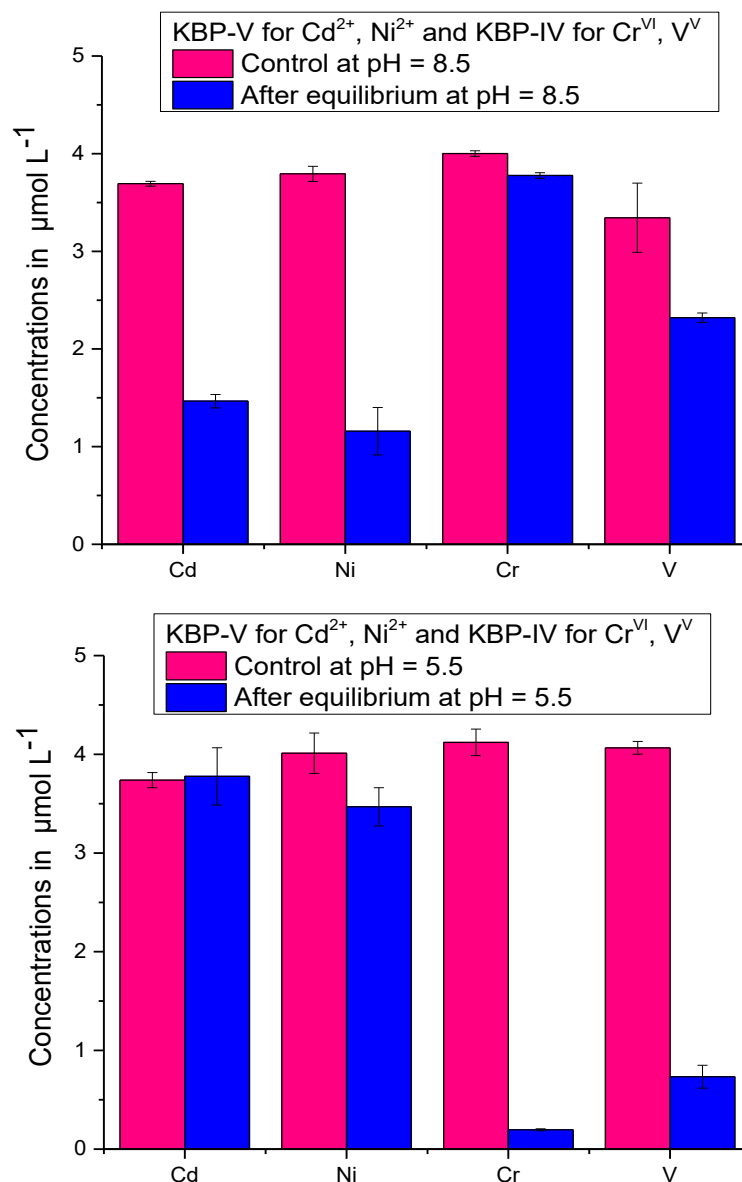
Figure 3.2. The effect of maintaining the solution pH (8.5 and 5.5) on adsorption of Cd^{2+}, Ni^{2+}, Cr^{VI}, and V^V by KBPs (KBP-IV and KBP-V) from single-metal synthetic wastewater. Control values represent the analyte in the nano-pure water without KBPs addition. Concentrations are an average of triplicate samples measured after the 24 hours of incubation times.

3.3.1.1 Adsorption mechanisms

The adsorption mechanisms cannot be directly investigated by simple kinetic equilibrium experiments or models fittings. Instead, the characterization analytical techniques (XPS analysis) are used to characterize the surface functionalities of sorbents that could be involved in the interaction mechanisms for the removal of inorganic contaminants from wastewaters.

The XPS C 1s, N 1s, and O 1s high-resolution spectra of KBP-IV (A; neat KBP before adsorption, B; after adsorption for Cr^{VI}, C; after adsorption for V^V) and KBP-V (A; neat KBP before adsorption, B; after adsorption for Cd^{2+}, C; after adsorption for Ni^{2+}) are presented in Fig 3.3, Fig 3.4, and Fig 3.5 respectively. The XPS survey spectrum of KBP-IV and KBP-V (Appendix-III; Fig A2) mainly contains C, N, O with binding energies 283, 398, and 530 eV might correspond to C 1s, N1s, and O1s.

The XPS spectrum of C 1s for neat KBP-IV (before adsorption) was deconvoluted into three peaks (Fig 3.3) at binding energies 288, 286, and 285. The peaks at binding energies 288 (288, 287.9) correspond to C=O/ O−C−O. The peaks at binding energies 286 (286.2, 286.3, 286.4) correspond to C−N, C=N, C−O/O−C−O. The peaks at binding energies 285 (284.9/284.8, 285.7) correspond to C−C and C=O, respectively (Kaur et al., 2018; Vieira et al., 2011; Sitko et al, 2013). After the adsorption of Cr^{VI} by KBP-IV, an increase in the intensity of peak (which was at 288.3 eV) and the slight shift of peak at 286.2 eV towards lower 284.9 eV binding energy were observed, assigned to C-N or C=N bonds, suggesting that chromium adsorption can take place either on imino or on hydroxyls and non-reacted amino groups (Vieira et al., 2011). After the adsorption of V^V, Cd^{2+}, and Ni^{2+} by KBP-IV and KBP-V, there are no differences are observed in XPS C 1s peak values at binding energies 286.2 eV and 285 eV.

Figure 3.3. High resolution C 1s spectra of KBP-IV (A; before adsorption, B; after adsorption for Cr^{VI}, C; after adsorption for V^{V}) and KBP-V (A; before adsorption, B; after adsorption for Cd^{2+}, C; after adsorption for Ni^{2+}).

The XPS spectrum of N 1s for neat KBP-IV and KBP-V (before adsorption) was deconvoluted into two peaks (Fig 3.4) at binding energies 401 eV and 400 eV, respectively. The peak at 401 eV is assigned to high oxidation of N atoms with positive charges (NH^{3+} groups) and the peak at 400 eV can be attributed to N atoms in the forms of $-NH_2$ and -NH groups of KBPs. After

the adsorption of Cd^{2+}, the N 1s two peaks shifted to 400.5 eV and 399.9 eV. Yang & Jiang, 2014 conducted the XPS analysis for biochar after the adsorption of copper and explained that these peaks shift to lower binding energies could be attributed to the nitrogen atoms sharing electrons with copper, hence, reducing the electron cloud of the nitrogen atoms (Yang & Jiang, 2014). The adsorption mechanism for divalent cation (Cd^{2+}) could also be suggested by another XPS study conducted by (Jiang et al, 2014), which elaborated the adsorption mechanism of Cu by chitosan. They explained that these changes in N 1s two peaks were attributed due to the formation of R-NH-Cu or $R-NH_2.Cu^{2+}$. It indicated that the complexation/chelation was being involved between surface functional groups of chitosan andCu , in which the lone pair electrons were donated to Cu by N atoms (Jiang et al., 2014). After the adsorption of $V^{V,}$ the shift of binding energies from 401 eV to 399.99 eV and 399.99 eV to 400.5 eV (assigned to $C-NH_2$ and C=NOH) were observed indicating that V mainly not only interacted with C=NOH but also with $C-NH_2$ (Zheng et al., 2021).

Figure 3.4. High resolution N 1s spectra of KBP-IV (A; before adsorption, B; after adsorption for Cr^{VI}, C; after adsorption for V^{V}) and KBP-V (A; before adsorption, B; after adsorption for Cd^{2+}, C; after adsorption for Ni^{2+}).

The XPS peak of O 1s for neat KBP-IV (before adsorption) was observed (Fig 3.5) at binding energy 532 eV. After the adsorption of Cr^{VI}, some additional peaks were observed at 532.7 eV and 531.8 eV assigned to C=O, and Cr(III)-OH groups. The appearance/enhancement of the peak assigned to C=O was due to the oxidation of -OH groups, indicating that the hydroxyl groups played a significant role as electron donor in reducing the Cr^{VI} to Cr^{III} (Jiang et al., 2013). After the adsorption of Cd^{2+}, some additional XPS O 1s peaks are observed at binding energies 532.5 eV [attributed to organic O (O–C, –COH, O–C = O)] and the peaks at binding energies 531.7 eV/531.5 eV associated with inorganic O, suggesting that oxygen-containing functional groups on the surface of KBP involved in adsorption of divalent metal cations (Sitko et al., 2013; Guo et al., 2019).
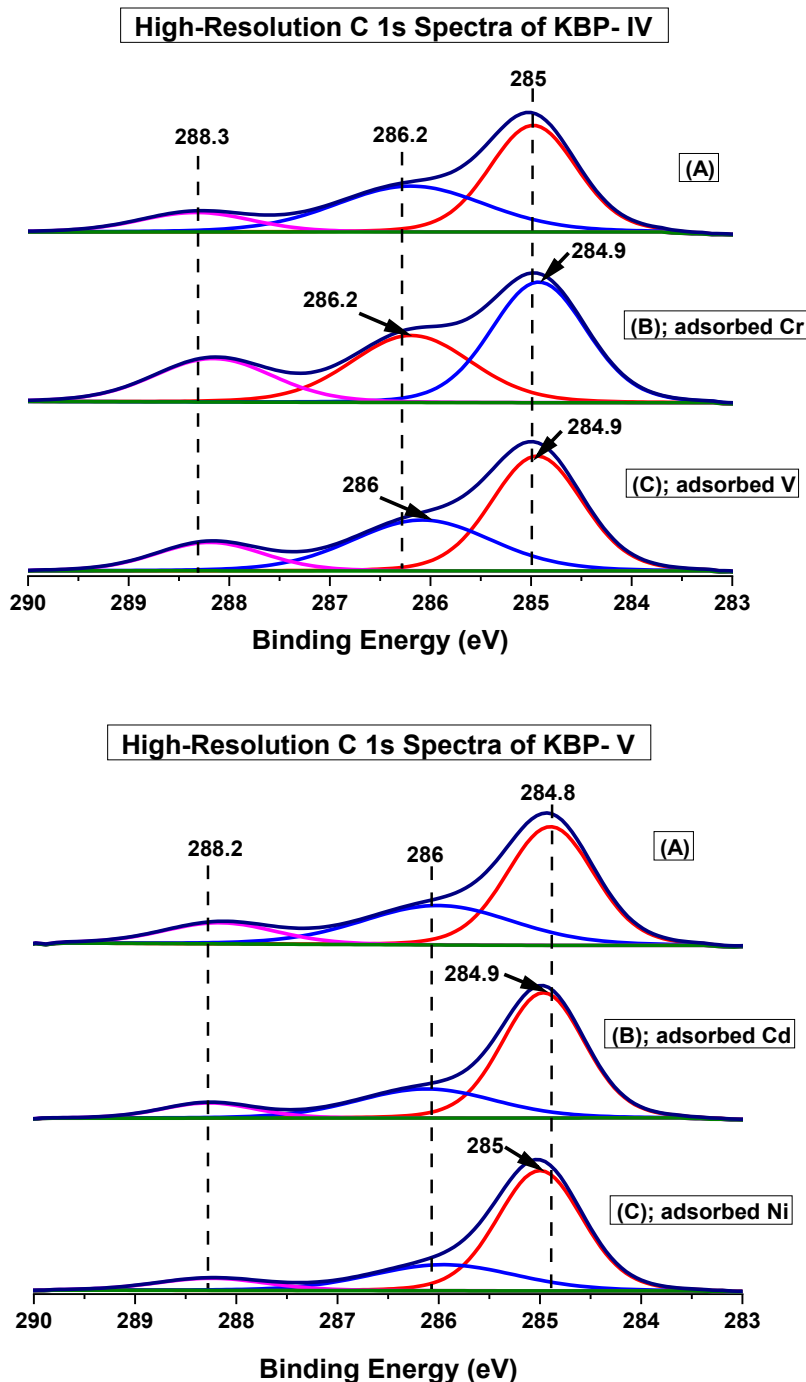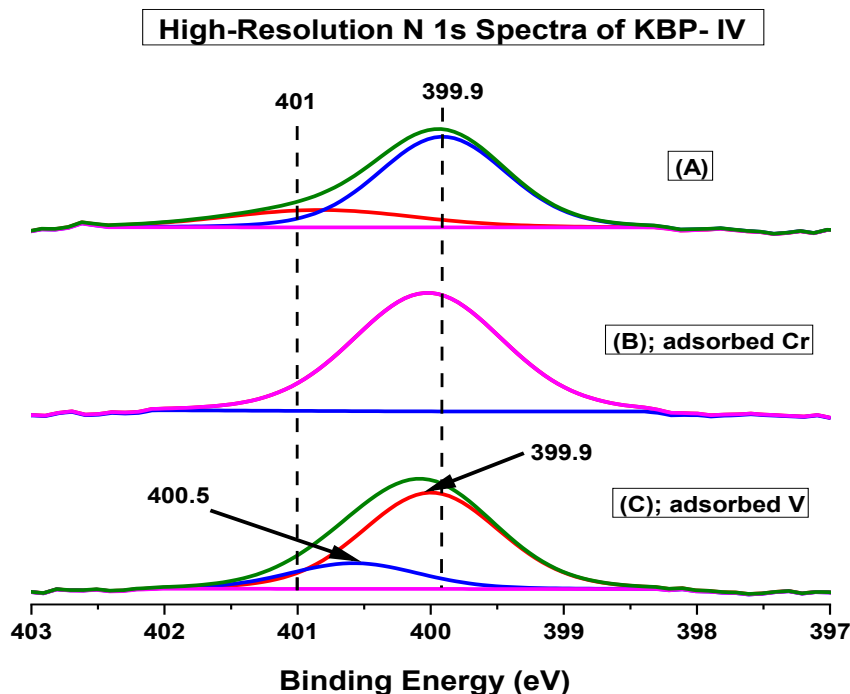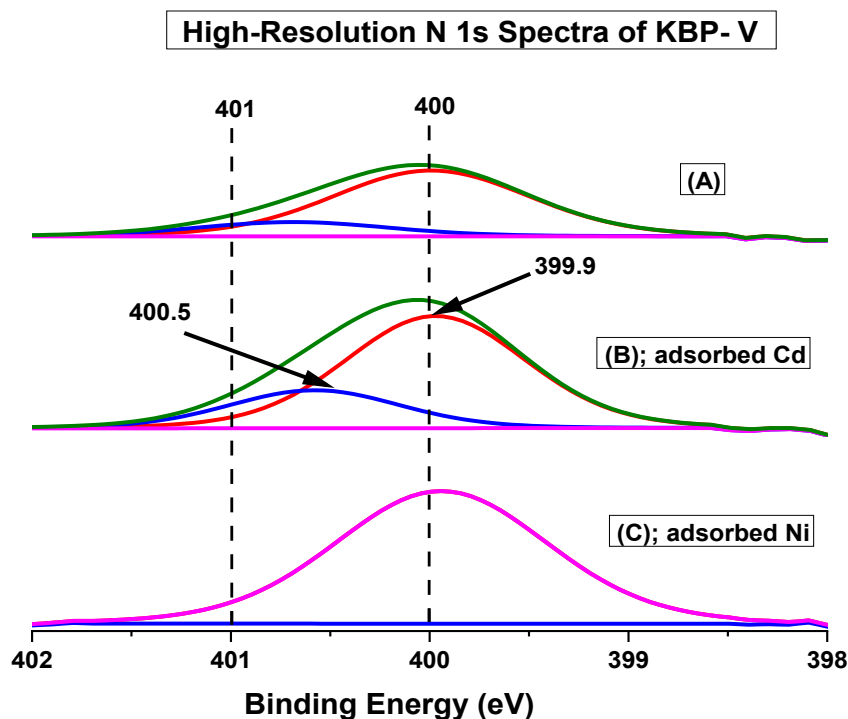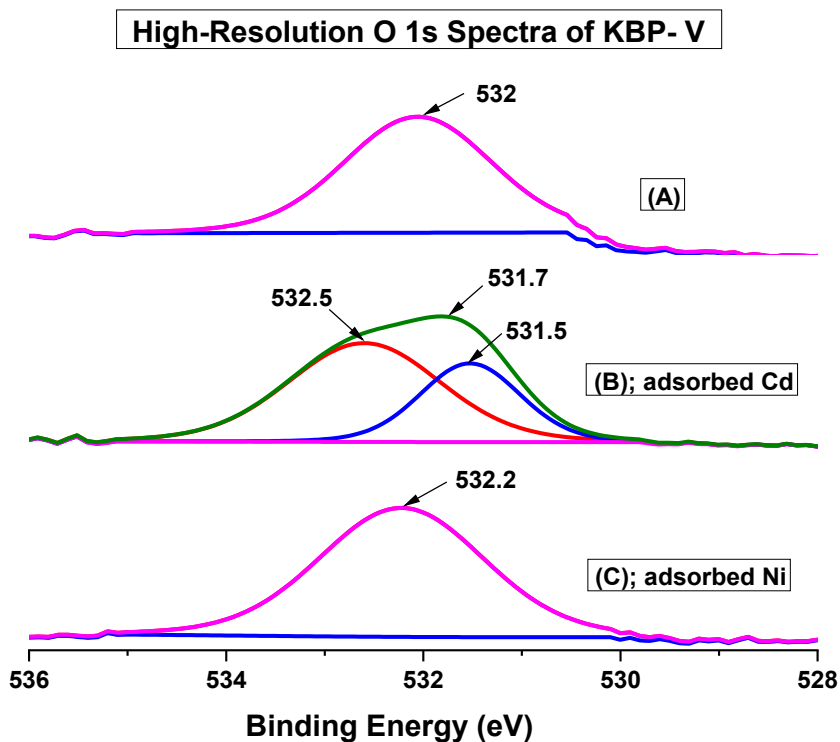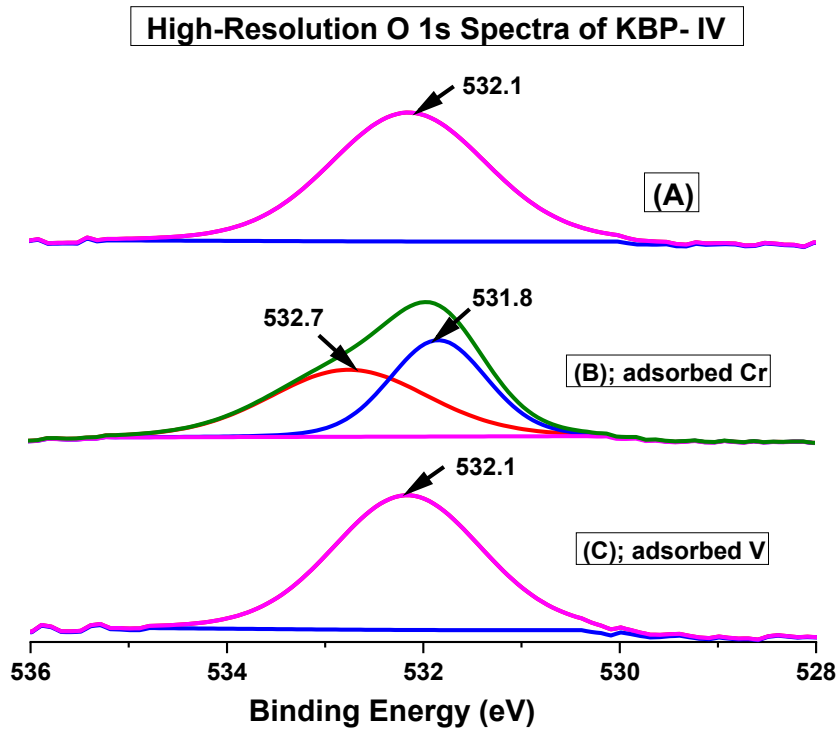
Figure 3.5. High resolution O 1s spectra of KBP-IV (A; before adsorption, B; after adsorption for Cr^{VI}, C; after adsorption for V^V) and KBP-V (A; before adsorption, B; after adsorption for Cd^{2+}, C; after adsorption for Ni^{2+}).

3.3.2 Effect of temperature on adsorption

The temperature of the metal ion's solution influences sorbent-sorbate interfaces and the metal ion's mobility towards sorbent surfaces, suggested whether the temperature is favorable or unfavorable for the adsorption process (Zhang et al., 2016). The effect of temperature at two ranges (30 °C and 45°C) on adsorption efficiencies of KBP-I, KBP-IV, and KBP-V for (Co^{2+}, Ni^{2+}, Cd^{2+}, V^V, Cr^{VI}, and As^{III}) were studied at pH 7.5 for 24 hours of incubation. For divalent cations, the adsorption results (Fig 3.6) of KBP-I towards Co^{2+}, Ni^{2+}, and Cd^{2+} removal were consistent with increasing the temperature from 30 °C to 45°C.

The removal of Co^{2+}, Ni^{2+}, and Cd^{2+} by KBP-IV from synthetic wastewater was increased (20 $\mu g\ L^{-1}$, 42 $\mu g\ L^{-1}$ and 28 $\mu g\ L^{-1}$) by decreasing temperature (30 °C), and decreased by increasing temperature (45 °C), suggested that at further increase in temperature, the thermal vibration of metal ions became much faster than the adsorbent-adsorbate interactions that induced the desorption of metals from KBP-IV (Manzoor et al., 2019; Zhang et al., 2016). Therefore, its adsorption efficiencies were minimum at 45 °C. The KBP-V adsorbed 85 $\mu g\ L^{-1}$ of Co^{2+} , 93 $\mu g\ L^{-1}$ of Ni^{2+} and 94 $\mu g\ L^{-1}$ of Cd^{2+} (yeilded higher adsorption results) at high temperature (45 °C), indicated that when the temperature raised initially, it increased the thermal energy of the metal ions, thus, increased the probability of interaction between sorbent's sites and the metal ions (Manzoor et al., 2019). The high temperature (45 °C) reduced the mass transfer resistance of adsorbate in the boundary layer that decreased the boundary layer thickness. Hence, the active sites became available on the sorbent surface. (Anastopoulos et al., 2019).

For oxyanions (Fig 3.6), the adsorption of V^V and Cr^{VI} by KBP-I somehow increased at 30 °C. The adsorption of V^V and Cr^{VI} by KBP-IV was independent of the change in temperature from 30 °C to 45 °C.
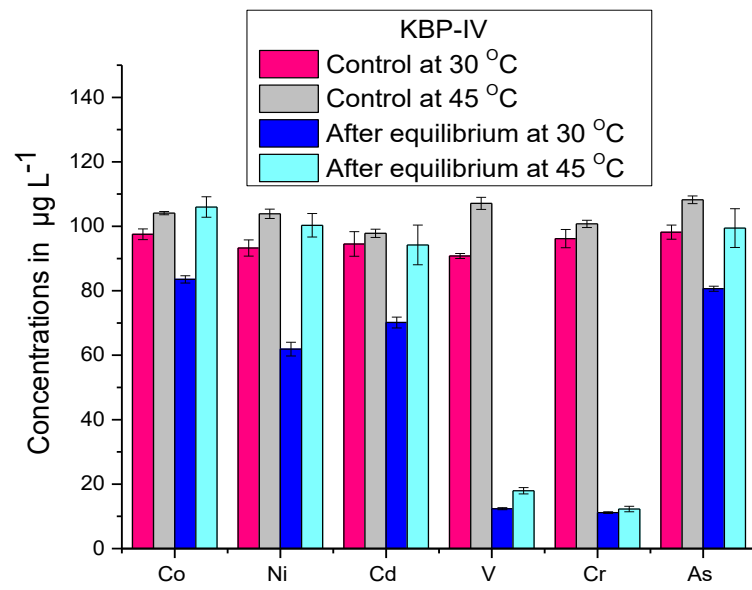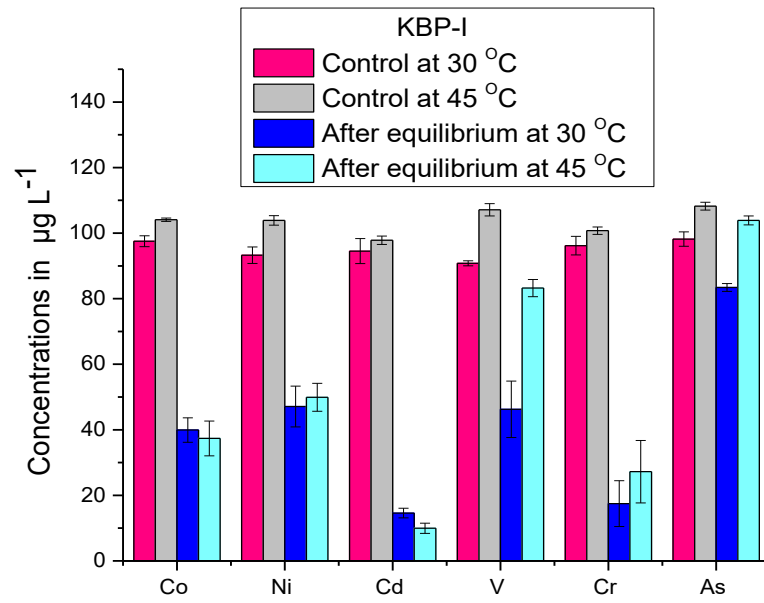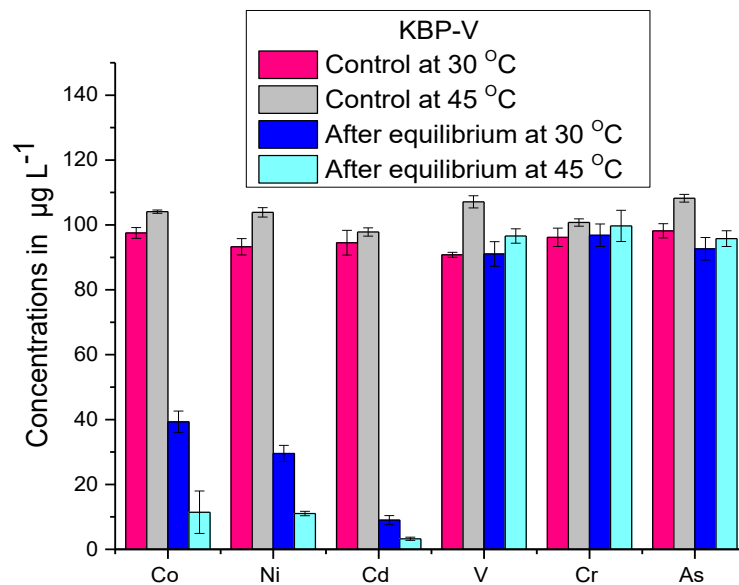
Figure 3.6. The effect of temperature (30 °C and 45 °C) on adsorption of (Co^{2+}, Ni^{2+}, Cd^{2+}, V^V, Cr^{VI} and As^{III}) by KBPs (KBP-I, KBP-IV and KBP-V) from multi-metal synthetic wastewater. Control values represent the analyte in the nano-pure water without KBPs addition. Concentrations are an average of triplicate samples measured after their mentioned incubation times.

3.3.3 Effect of contact time on adsorption

Predicting the equilibrium time of sorbate at the solid-solution interface is the major contribution towards developing the wastewater remedial system, as the contact time between sorbate molecules and sorbent surface determines the adsorption capacity of sorbents (Anastopoulos et al., 2019; Manzoor et al., 2019). As can be seen from Fig 3.7 for divalent cations, the fast adsorption for Ni^{2+} and Cd^{2+} by KBP-I was observed, achieving equilibrium within 15 mins of incubation. However, the equilibrium times for Co^{2+}, $Ni^{2+,}$ and Cd^{2+} by KBP-IV and KBP-V were achieved within 60 mins. In the case of oxyanions (Fig. 3.7), the adsorption process for V^V by KBP-I, KBP-IV, and KBP-V proceeded fast at a shorter period (60 mins) of equilibrium times. Whereas, according to the 1st data chapter (Zahara et al., 2021) the equilibrium times are longer for Cr^{VI} and As^{III} by KBP-I, which were achieved within 1440 mins of incubation. The adsorption of Cr^{VI} by KBP-IV was very fast as equilibrium was

attained within 15 mins. However, the adsorption of As^{III} by KBP-IV increased over time and reached equilibrium at 360 mins.

These minimum equilibrium times could be explained by initial vacant adsorbent sites that were rapidly occupied by sorbate molecules as soon as they came in contact with sorbent sites. (Badawi et al., 2017; Manzoor et al., 2019). Afterward, no further increase in adsorption was observed, suggested that all vacant adsorption sites were occupied, and dynamic equilibrium was achieved in which the number of adsorbed molecules is equal to the number of desorbed molecules (Manzoor et al., 2019).
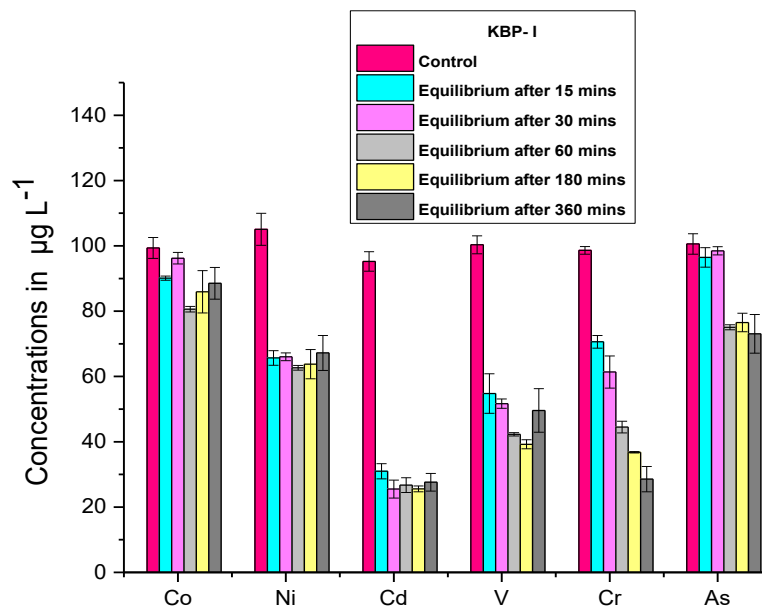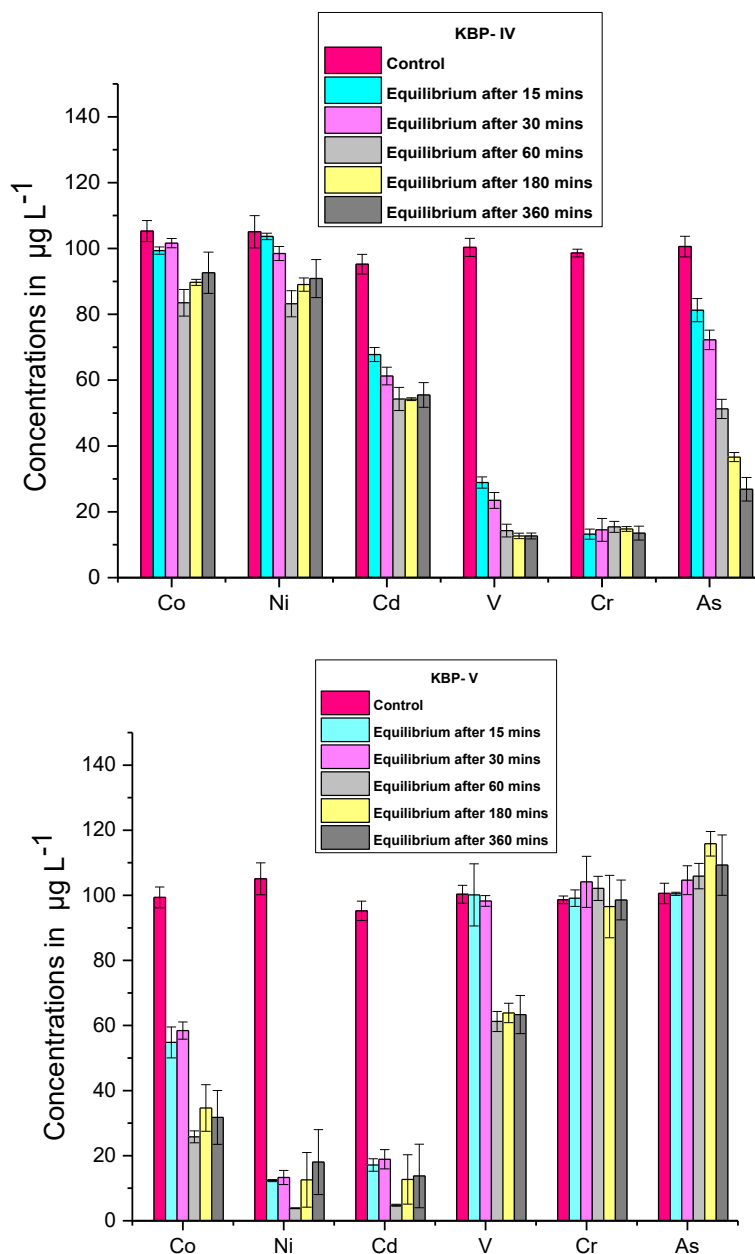
Figure 3.7. The effect of contact time (15, 30, 60, 180, 380 mins) on adsorption of (Co^{2+}, Ni^{2+}, Cd^{2+}, V^V, Cr^{VI} and As^{III}) by KBPs (KBP-I, KBP-IV and KBP-V) from multi-metal synthetic wastewater. Control values represent the analyte in the nano-pure water without KBPs addition. Concentrations are an average of triplicate samples measured after their mentioned incubation times

3.3.4 Adsorption isotherms

Quantitative measurement of contaminant's adsorption by sorbents is an important step in developing the restitutive approach for removing the contaminants from wastewaters. Adsorption isotherms are constructed to quantify the mass distribution of dissolved solute

(heavy metals) in the liquid phase (synthetic wastewater) in equilibrium with solid phase (Keratin derived biopolymer KBPs as sorbents) at constant temperature (Donner et al., 2019). Based on their adsorption potentials, three KBPs (KBP-I for Cd^{2+} and As^{III}, KBP-IV for Cr^{VI}, and KBP-V for Ni^{2+}) were tested against different ranges of metal's concentrations. The experimental data (q measured) was plotted (Fig 3.8) along with the Ceq data fitted into Langmuir (q Langmuir) and Freundlich (q Freundlich) models.

The results indicated that KBPs exhibited adsorption behavior for (Ni^{2+}, Cd^{2+}, Cr^{VI}) best described by Langmuir model yielding higher regression coefficient (R^2) values, whereas retention of (As^{III}) is best described by Freundlich model. The Langmuir model suggests that adsorption occurs due to the formation of a monolayer of atoms (sorbate) at homogenously distributed active sites (sorbent) considering the similar adhesive forces that bind sorbate molecules to sorbent, neglecting interactions between sorbate molecules, whereas the Freundlich model demonstrates the adsorption in heterogeneous systems with the multi-layer adsorption (Donner et al., 2019; Manzoor et al., 2019).

The KBP-I had maximum adsorption capacity of 2.4 mg g^{-1} for Cd^{2+}, KBP-IV had maximum adsorption capacity of 2.8 mg g^{-1} for Cr^{VI}, and KBP-V had maximum adsorption capacity of 2.2 mg g^{-1} for Ni^{2+}. Donner et al., 2019 reported the higher maximum adsorption capacities (17 mg g^{-1} and 15 mg g^{-1}) of biopolymer (prepared from chicken feathers) for V^V and Cr^{VI}, respectively (Donner et al., 2019). Gao et al., 2014 stated the similar adsorption capacity (14.8 mg g^{-1}) of keratin sorbent for Cr^{VI} from aqueous media (having no other competing ion) at pH=6 (Gao et al., 2014). In the present, the lower maximum adsorption capacities of the developed sorbents could be assigned to the methods of preparations (chemical modifying agents: ionic liquid for KBP-IV and propyl amine for KBP-V) used to develop the sorbents from CFs.

Broad range of adsorption maxima (2-358 mg g^{-1}) observed for Cr^{VI} and V^V in aqueous media by using different sorbents with higher uptake at pH (3-5) (Rodriguez et al., 2015; Liu & Zhang, 2015; Sharififard & Soleimani, 2015; Liu et al., 2017; Wang et al., 2017; Zhang et al., 2017). Abdolali et al., 2016 reported maximum adsorption capacity of 3.3 mg g^{-1} for Cd^{2+} by using the mandarin peels as bio-based sorbent at pH=5.5 (Abdolali et al., 2016). Deshmukh et al., 2017 described the maximum adsorption capacity of 5.92 mg g^{-1} for Cd^{2+} by using the dried banana peel at pH 7-8, further suggested that the complexation interaction could take place as adsorption mechanism (Deshmukh et al., 2017). The maximum adsorption capacities of the present study sorbents (KBP-I, KBP-IV, and KVP-V) for divalent cations and oxyanion fall in the range of 2-3 mg g^{-1} as indicated by other sorbents already reported in literature (Rodriguez et al., 2015; Abdolali et al., 2016).
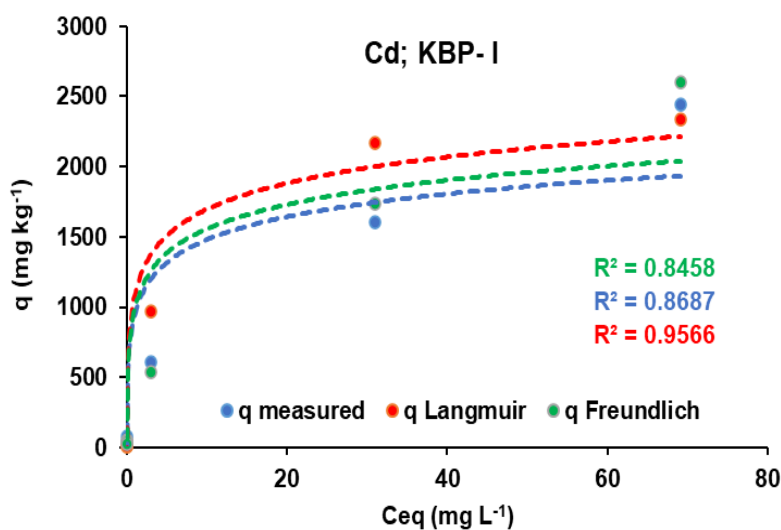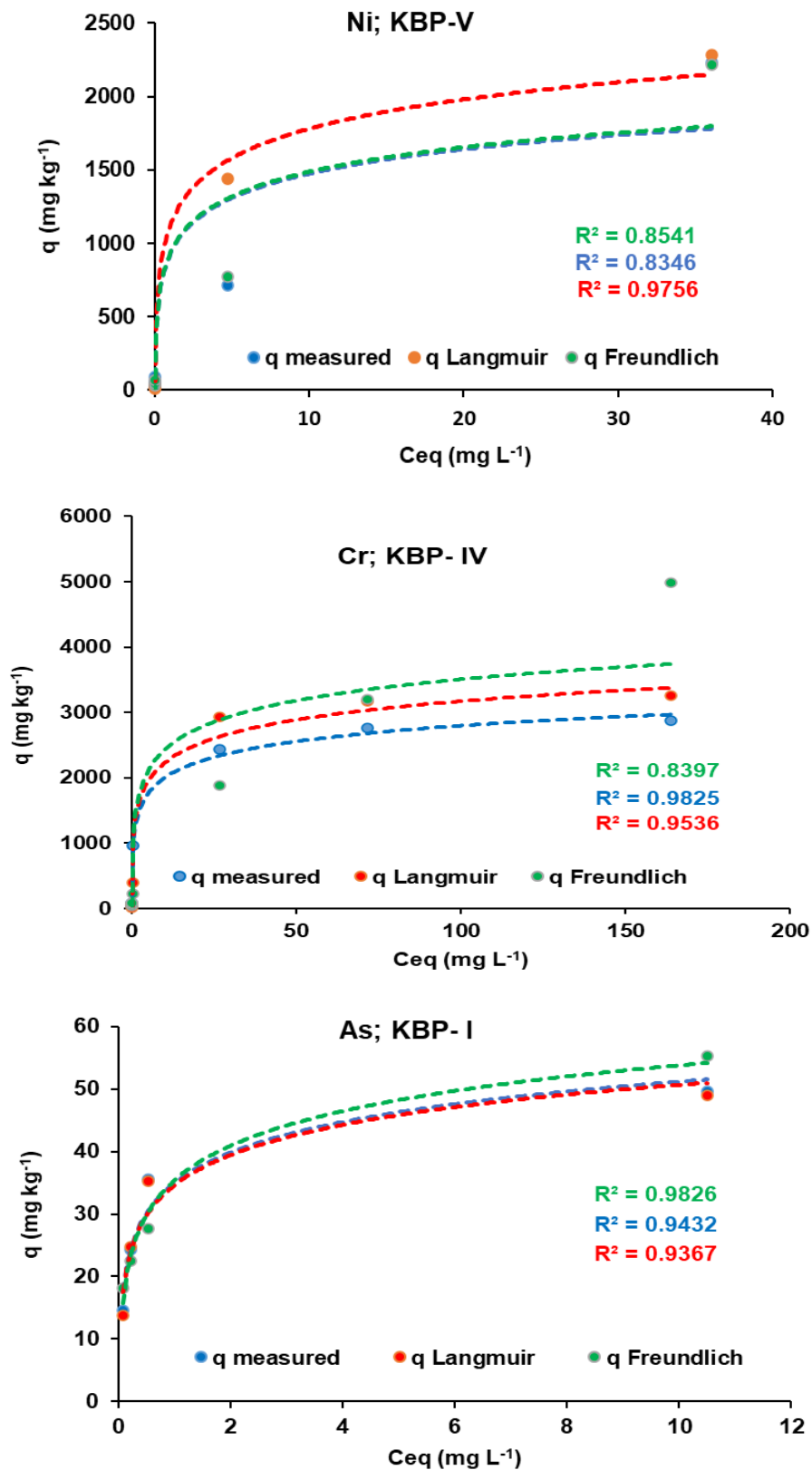
Figure 3.8. Adsorption isotherms of Cd^{2+}, Ni^{2+}, Cr^{VI} and As^{III} at 20 °C using keratin biopolymers (KBPs), KBP-I was used for Cd^{2+} and As^{III}, KBP-IV used for Cr^{VI}, whereas KBP-V was used for Ni^{2+}. The Ceq data fitted into Langmuir (q Langmuir) and Freundlich (q Freundlich) models was plotted along with the experimental data (q measured).

3.3.5 Application of keratin biopolymers towards metal ions removal from field-collected wastewater

According to the Fig 3.9, the initial level of V concentration in OSPW was 15.7 µg L^{-1} that was reduced to 11.5 µg L^{-1} by KBP-I, 5.0 µg L^{-1} by KBP-IV, 11.8 µg L^{-1} by KBP-V, and 14.7 µg L^{-1} by KBP-VII, respectively. The initial concentration of Ni^{2+} in OSPW was 7.6 µg L^{-1} that was decreased to 6.5 µg L^{-1} by KBP-I, 4.0 µg L^{-1} by KBP-IV, 4.6 µg L^{-1} by KBP-V, and 5.1 µg L^{-1} by KBP-VII. The initial concentrations of Ba and Sr in OSPW were 104 µg L^{-1} and 742 µg L^{-1}, that reduced drastically to 13.1 µg L^{-1} and 118.7 µg L^{-1} respectively by KBP-VII.

The higher adsorption affinities of divalent cations (Ba^{2+} and Sr^{2+}) towards KBP-VII could be attributed to the electrostatic attraction between anionic functional groups of mercaptopropylisobutyl-POSS modified KBP-VII and divalent metal cations. The chemical modification with mercaptopropylisobutyl-POSS provided high thiol content on the KBP surface, hence, provided the lone pairs. Anionic sulfides were generated from oxidation-coupling reactions due to the deprotonation of the thiols which led to the formation of negative charges (Atas et al., 2017). Moreover, the destruction of POSS cages that cleaved the Si-C bonds also generated the Si-OH groups. The deprotonation of the hydroxyl could also generate anionic oxide, which further increased the negative charges on the surface (Liu et al., 2019). Therefore, the KBP-VII showed higher adsorption affinities towards the removal of Ba^{2+} and Sr^{2+} from OSPW.
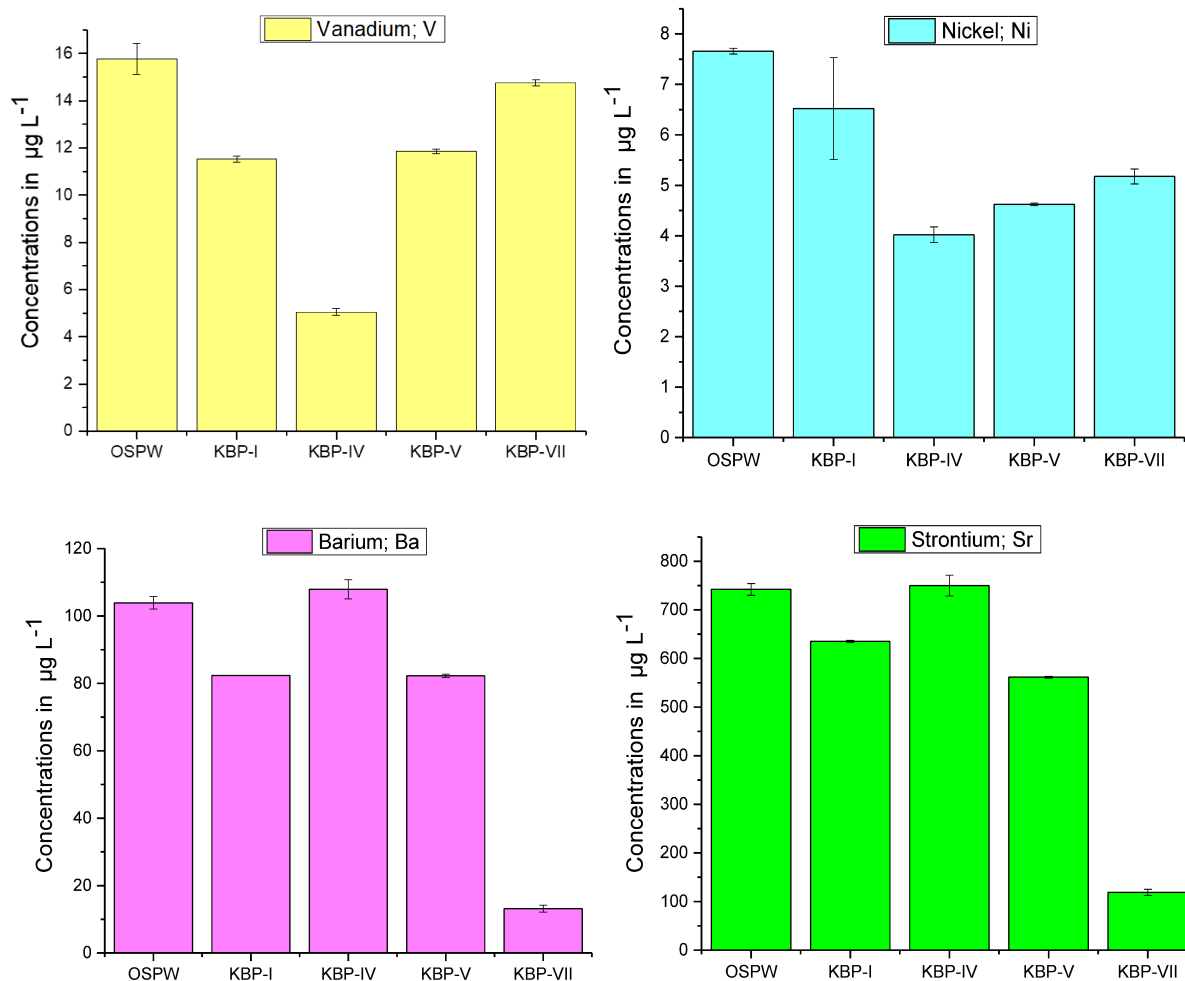
Figure 3.9. Removal of V, Ni, Ba and Sr from OSPW by KBP-I, KBP-IV, KBP-V and KBP-VII. Concentrations are average of triplicate samples measured after 24 h of incubation. OSPW values represent the analytes as controls without biopolymer addition.

3.4 Conclusion

The KBP-I, KBP-IV, and KBP-V were selected to optimize the adsorption process parameters (pH, temperature, and contact time) based on their better metal adsorption abilities owing to the larger accessibility of functional groups present on the surface. For inorganics removal from multi-metal synthetic wastewater, there are no significant differences were observed at two initial solution pH (5.5 and 8.5) ranges. However, the divalent cations and oxyanions removal from single metal synthetic wastewater at two pH (5.5 and 8.5) ranges concluded that KBP-V adsorbed divalent cations at pH 8.5 and KBP-IV removed oxyanions at pH 5.5 effectively. The results of the XPS analysis demonstrated that complexation/chelation, electrostatic attraction,

chemical reduction (represented as adsorption mechanisms) involved in the removal of divalent cations and oxyanions by KBPs from synthetic wastewater. The incubations of KBP-I, KBP-IV, and KBP-V at 30 °C and 45 °C with multi-metal synthetic wastewater, elaborated that 30 °C is the optimized temperature for the removal of divalent cations and oxyanions by using the KBP-I and KBP-IV. However, KBP-V adsorbed divalent cations effectively at 45 °C. For divalent cations and oxyanions adsorption, the fastest equilibrium was achieved within 15-60 mins by KBP-I, KBP-IV, and KBP-V. The adsorption behavior for (Cd^{2+}, Ni^{2+}, Cr^{VI}) by using KBP-I, KBP-IV, KBP-V is best described by the Langmuir model, and for As^{III} by KBP-I is best described by Freundlich model. The application of KBPs towards the inorganic removal from field-collected wastewater (OSPW) concluded that the initial concentration of Ba and Sr in OSPW was 104 µg L^{-1} and 742 µg L^{-1}, that reduced drastically to 13.1 µg L^{-1} and 118.7 µg L^{-1} by KBP-VII.

3.5 Acknowledgements

4.0 REPRODUCIBILITY OF FEATHER KERATIN DERIVED SORBENTS AND THEIR APPLICATION AS HYBRID SORBENT TOWARDS METAL IONS REMOVAL FROM SYNTHETIC WASTEWATER

4.1 Introduction

Recently, substantial efforts have been conducted to examine the reproducibility of experimental procedures/measurements in scientific fields. Scientific progress is hindered if experimental results are not reproducible (Dickey, 1955). Reproducibility in adsorption and materials chemistry has previously gained attention (Park et al., 2017). Reproducibility in adsorption involves a methodology that prepares the specific sorbents for predetermined substances (contaminants), has been repeated several times under similar conditions giving the reproducible results with more pronounced effects (Dickey, 1955). In case of bio-based sorbents, reproducible adsorption results can be achieved by crosslinking/tagging/conjugation/chemical modifications of biomolecules (proteins) with the specific bioconjugate reagents which have subsequent effects on adsorption by providing the specific affinities to more versatile adsorbing contaminants (Hermanson, 2013; Dickey, 1955). After the invention of different sorbents that preferentially adsorbed one or more sorbates, the revolutionary progress has been made that includes the development of adsorption-desorption cycle applies to sorbates (heavy metals) recovery and sorbents regeneration (Dąbrowski, 2001). The regeneration of sorbent involves the desorption of heavy metals from metal-loaded sorbents by using the desorbing eluents. Among the other desorbing eluents (NaOH, EDTA), acids have higher desorption efficiencies due to their potential to destabilize the sorbate-sorbent interactions and to regenerate/restore the sorbents with non-damaging effects (Chatterjee & Abraham, 2019). Despite being regenerated by desorption, the bio-based sorbents have limited practical applications based on their low adsorption affinities towards specific sorbates. To overcome this problem, hybrid sorbents are now being prepared (Iqbal et al., 2007). Hybrid sorbents are now being developed by combining the two sorbents for the adsorption of contaminants (Iqbal et al., 2007; Iqbal & Saeed, 2007). The hybrid sorbents present the

combined properties of each of its components and target the multi-contaminants from wastewater (Iqbal et al., 2007; Iqbal & Saeed, 2007; Samiey et al., 2014).

Based on the initial adsorption screening (second data chapter, section: *2.3.2*), the results revealed that KBP-IV had higher sorption affinities for oxyanions (V^V, Cr^{VI}) and KBP-V had better adsorption for divalent cations (Co^{2+}, Ni^{2+}, Cd^{2+}). Therefore, this study includes (i) the chemical modifications of KBP-IV and KBP-V in three replicates to examine the reproducibility of KBPs for metal ions adsorption from synthetic wastewater, (ii) regeneration of KBPs by desorbing the metal ions from metal-loaded sorbents and (iii) development of hybrid sorbent (KBP-IX) by combining the KBP-IV and KBP-V in a certain ratio to target the maximum metal ions removal with better adsorption affinities.

4.2 Materials and methods

4.2.1 Chemicals

The chemicals used for the processing and modifications of keratin feathers include: hexane (Sigma Aldrich), sodium hydroxide (Sigma Aldrich ≥97%), 1-butyl-3 methylimidazolium bromide (Sigma Aldrich ≥97%), ethanol (Fisher Brand 95%), diethyl ether (Sigma Aldrich ≥99%), sodium sulphite (Sigma Aldrich ≥98%), urea (Fischer Scientific), ethylenediaminetetraacetic acid (Sigma Aldrich ≥99%), tris base (Fischer Scientific 99.8%), 2-mercaptoethanol (Sigma Aldrich ≥99%), 3-(dimethylamino)-1-propylamine (Sigma Aldrich 99%), hydrochloric acid (Sigma Aldrich 37%) and methanol (Sigma Aldrich 99.8%).

For the adsorption experiment, individual metal stock solutions were prepared using powder reagents of the following: nickel (Ni) chloride hexahydrate (Fisher Scientific, 99.4%), cobaltous (Co) sulfate heptahydrate (Fisher Scientific, 100%), cadmium (Cd) chloride (Sigma Aldrich 99.9%), chromium (Cr^{VI}) oxide (Sigma Aldrich 99.99%), and arsenic (As^{III}) sodium meta arsenite (Sigma Aldrich ≥99%). For vanadium V^V, liquid standard solution of vanadium [CAS No: HNO_3 7697-37-2, V 7440-62-2 (SpexCertiPrep)] was used.

4.2.2 Source and processing of keratin feathers

The chicken/keratin feathers (CFs) were obtained from Sofina Foods, Edmonton, Canada, then washed, dried, and ground according to reference (Arshad et al., 2016a; Arshad et al., 2016b). Ground CFs were further Soxhlet extracted with 250 mL hexane for 5 hours to remove the fats and waxes. CFs were dried by evaporating hexane and then stored in a desiccator at room temperature (with this initial processing the product was named as KBP-I). Further modifications of KBP-1 yielded KBP-IV and KBP-V as described in Chapter: *2*, Section: *2.2.3*. To test the reproducibility, these biopolymers were developed in three separate modification reactions as given below.

4.2.3 Modification of keratin biopolymers in three replicates

4.2.3.1 Modification of keratin biopolymer (KBP-IV) with ionic liquid (IL) in three replicates

The processed CFs were modified with ionic liquid using the already reported method (Sun et al., 2009; Zahara et al., 2021). Ionic liquid (1-butyl-3 methylimidazolium bromide [BMIM]Br) was weighed (25 g) individually in three glass flasks (three replicates) and melted at 100 ℃ with continuous stirring under an inert atmosphere of N_2 gas. Then, processed CFs (5.75 g) were added to each flask and then dissolved in melted ILs under the same stirring and heating conditions. After the complete dissolution, the CFs were regenerated from solutions by adding 200-350 mL water. The suspended solutions were stirred with water for 30 mins, then filtered, and rinsed with ethanol several times to remove water. The regenerated feathers were filtered and washed with ether and then dried. The obtained end products were ground, sieved through a 40 μm sieve, and stored as [KBP-IV (a), KBP-IV (b), and KBP-IV (c)] for the adsorption of inorganic contaminants.

4.2.3.2 Modification of keratin biopolymer (KBP-V) with 3-(dimethylamino)-1- propylamine in three replicates

The KBP-V was prepared in three replicates under the same conditions by the subsequent method already reported in the literature (Zahara et al., 2021). The processed CFs (15 g) were weighed individually in three-round bottom flasks (three replicates) and mixed with 450 mL methanol. Then, the reaction mixtures were incubated with 15 g Na_2SO_3, 75 g urea, 12 g trisbase, 300 mg EDTA, and 5.4 mL of mercaptoethanol, with continuous stirring at 65 ^{o}C for 24 hours. Then, the 3-(dimethylamino)-1-propylamine was added with maintaining the same heating and stirring conditions for 168 hours. The mixtures were then filtered and washed with methanol and water respectively. The modified keratin biopolymers were dried, ground, passed through a 40 μm mesh sieve, and stored as [KBP-V (a), KBP-V (b), and KBP-V(c)].

4.2.4 Characterization studies of keratin biopolymers prepared in three replicates

The surface functional groups, structural crystallinity, thermal degradation, and thermal transition behaviors of KBP-IV (a, b, c) and KBP-V (a, b, c) were analyzed using a Fourier transform infrared spectrometer (FTIR), X-ray powder diffraction patterns (XRD), differential scanning calorimetry (DSC) and thermogravimetric analysis (TGA) (instruments specifications/details and sample analysis procedures can be seen under the section: *2.2.4* of second data chapter).

4.2.5 Batch adsorption studies by modified KBPs [KBP-IV (a, b, c) & KBP-V (a, b, c)]

The synthetic wastewater was prepared by following a method already reported in the literature (Zahara et al., 2021) with ionic strength I=0.05 and pH=7.5. The synthetic wastewater was then spiked with six metals (Ni^{2+}, Co^{2+}, Cd^{2+}, V^V, Cr^{VI}, and As^{III}) up to 100 μg L^{-1} concentrations of each. The adsorption performances of modified triplicate KBPs [KBP-IV (a, b, c) and KBP-V (a, b, c)] against synthetic wastewater were analyzed according to the protocol reported by (Zahara et al., 2021).

4.2.6 Desorption studies by KBP-1 and modified KBPs (KBP-IV & KBP-V)

Based on the initial better adsorption performances of KBPs (second data chapter, section: *2.3.2*), KBP-I, KBP-IV, and KBP-V were selected for the multi-metal desorption studies. After the adsorption experiment, metal-loaded KBPs (KBP-I, KBP-IV, and KBP-V) were filtered, dried, weighed, and shaken with 10 mL of 2 M HCl (desorbing eluent) in centrifuge tubes for 24 hours on the reciprocating shaker. Then, the centrifuge tubes (containing KBPs and desorbing eluent) were removed from shaker after 24 hours, and the samples in the tubes were filtered and analyzed by ICP-MS for desorbed metal ions.

4.2.7 Application of hybrid sorbent (KBP-IX) towards the metal ions removal from synthetic wastewater and the construction of adsorption isotherms

Based on the initial better adsorption performances of KBP-IV for oxyanions and KBP-V for cationic species these KBPs were selected and mixed in a certain ratio (hybrid sorbent) to improve the adsorption efficiencies for the removal of divalent cations and oxyanions simultaneously from synthetic wastewater. The hybrid sorbent was weighed (0.1 g of KBP-IV + 0.1 g of KBP-V) in centrifuged tubes in triplicates. Then, the 10 mL of synthetic wastewater (prepared by following the method reported by Zahara et al., 2021) containing Co^{2+}, Ni^{2+}, Cd^{2+}, V^V, Cr^{VI}, As^{III} (up to 100 $\mu g\ L^{-1}$ each) was added to each tube. The tubes were placed on reciprocating shaker for 24 hours at ambient temperature. After 24 hours, the tubes were removed form shaker, and then centrifuged at 5000 rpm for fifteen minutes. After centrifugation, 0.5 mL of supernatant was taken, diluted, and analyzed using inductively coupled plasma mass spectrometer (ICP-MS; iCapQThermo Scientific) under kinetic energy discrimination mode (KED; He gas).

The hybrid sorbent was also chosen for constructing the adsorption isotherms. The synthetic wastewater was prepared as described above (second data chapter: section *2.2.5*) and then spiked individually with either V^V (0.2, 0.4, 0.8, 10, and 50 mg L^{-1}) or Cr^{VI} (0.2, 0.4, 0.8, 10,

50, and 100 mg L^{-1}). Then the 10 mL of spiked synthetic wastewater was treated by using hybrid sorbent (0.1 g of KBP-IV + 0.1 g of KBP-V) in centrifuge tubes in triplicates as described above.

4.3 Results and discussion

4.3.1 Surface and structural characterization studies of keratin biopolymers (synthesized to examine the reproducibility)

4.3.1.1 Fourier transform infrared spectroscopy (FTIR)

The spectra of FTIR reveal the amide functionalities of triplicates of KBP-IV (a, b, c) and KBP-V (a, b, c) as shown in Fig 4.1. The three different amide vibrational transitions as amide A (N–H stretching at 3300 cm^{-1}), amide I (C$=$O, with a minor contribution from N–H bending at 1600–1700 cm^{-1}), amide II, and amide III (N–H bending and C–N stretching, at around 1540 and 1240 cm^{-1}) are identified by FTIR spectra (Sun et al., 2009). An absorption band of triplicates of KBP-IV (a, b, c) at 3352 cm^{-1} and triplicates of KBP-V (a, b, c) at 3340 cm^{-1} is designated to N–H stretching that relates to hydrogen bonding acts as a link between peptide N–H groups and C$=$O groups in the secondary structure of the protein. The band shifting at 2920 cm^{-1} and 2931 cm^{-1} in triplicates of KBP-IV (a, b, c) and KBP-V (a, b, c), respectively, is assigned to C-H stretching vibration in methylene (Arshad et al., 2016b; Zahara et al., 2021). The additional peaks observed for all triplicates of KBP-V (a, b, c) at 977 cm^{-1} can be explained in terms of unfolding and exposure of functional groups (buried inside the folded structure of keratin) by chemical modification of biomaterial (Arshad et al., 2016b). The additional peaks at 1396 cm^{-1} in all triplicates of KBP-IV and at 1156 cm^{-1} in two of the triplicates of KBP-IV (b, c) represent the asymmetric/symmetric S–O stretching vibrations of Bunte salt residues (Sun et al., 2009).
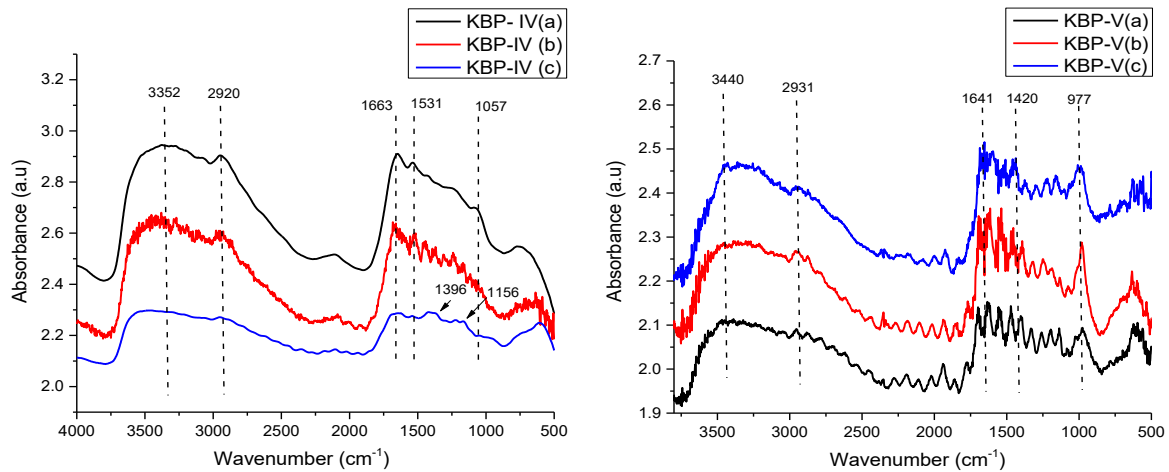
Figure 4.1. FTIR spectra of triplicates of KBP-IV (a, b, c) and KBP-V (a, b, c).

4.3.1.2 X-ray powder diffraction (XRD)

The crystalline behavior of the keratin structure was determined by XRD analysis. The typical XRD pattern of CFs includes notable 2θ degree peak at 9.9° belongs to the *α*-helix configuration, and other at 19° indicates the *β*-sheets (Arshad et al., 2016b; Zahara et al., 2021). The XRD spectra in Fig 4.2 show that all triplicates of KBP-IV (a, b, c) have characteristic crystallinity peaks at 10.8° and 22.8°. This slight shift of value from 19° to 22.8° indicates the increment of crystallinity character of biomaterial with increased d-spacing (Nuutinen, 2017). The emergence of multiple small peaks in triplicates of KBP-V (a, b, c) indicates the loss of original keratin structure with enhanced heterogeneity which is apparently responsible for new crystallinity regions and changed surface behavior, created during modifications of KBPs (Arshad et al., 2016b; Donner et al., 2019). These results suggest that the *α*-helices and *β*-sheets network in modified KBPs have been transformed, with more exposed functional groups on the surface, indicating that there is no prominent crystalline behavior variation in triplicates of KBP-IV (a, b, c) and KBP-V (a, b, c).
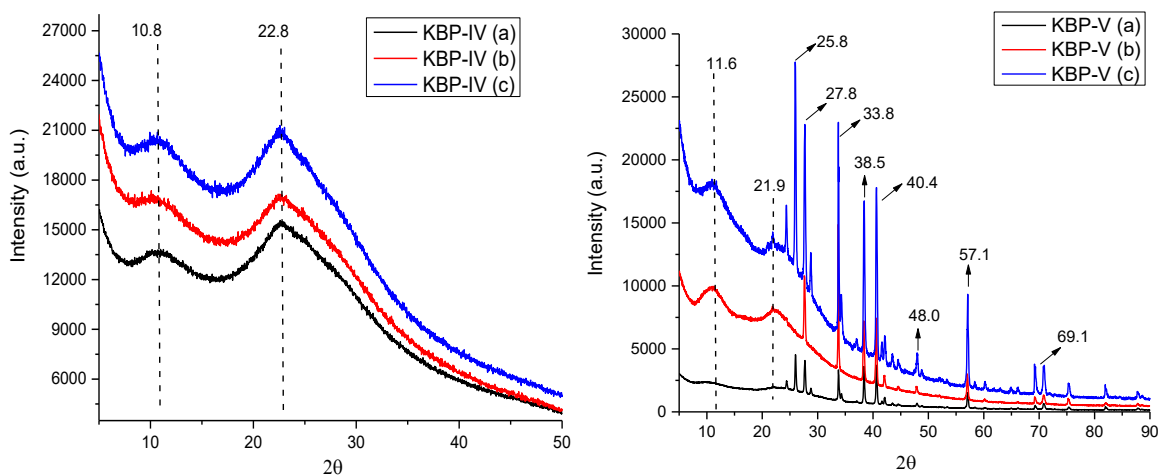
Figure 4.2. XRD patterns of triplicates of KBP-IV (a, b, c) and KBP-V (a, b, c).

4.3.1.3 Differential scanning calorimetry (DSC)

The phase transitions of developed KBPs have been determined by DSC analysis. The DSC curves in Fig 4.3 represent two phase transitions of triplicates of KBP-IV (a, b, c) and KBP-V (a, b, c) within 25–250 °C temperature range. The lower temperature phase transition around 100 °C indicates the evaporation of residual moisture/denaturation of the protein (Khosa et al., 2013). The heating curve for KBP-IV(a) drops noticeably and de-moisturizes rapidly, representing a dip in the graph along the temperature axis. The KBP-IV (b) displays smooth heat flow variation covering an increase in temperature (150 °C). The triplicates of KBP-V (a, b, c) display the broader transition with reduced peak intensities indicating heterogeneous interactions of the modifying agent with keratin molecules (Sun et al., 2009). The melting/glass transitions of triplicates of KBP-IV (a, b, c) are observed at ≥ 250 °C and KBP-V (a, b, c) observed at 200 °C which are attributed to *α*-helix disorganization and destruction (Khosa et al., 2013). The chemical interactions of modifying agents denatured the *α*-helix and *β*-sheets producing the heterogeneous KBPs surfaces, hence, responsible for the development of the DSC transitional plot (Arshad et al., 2016b).
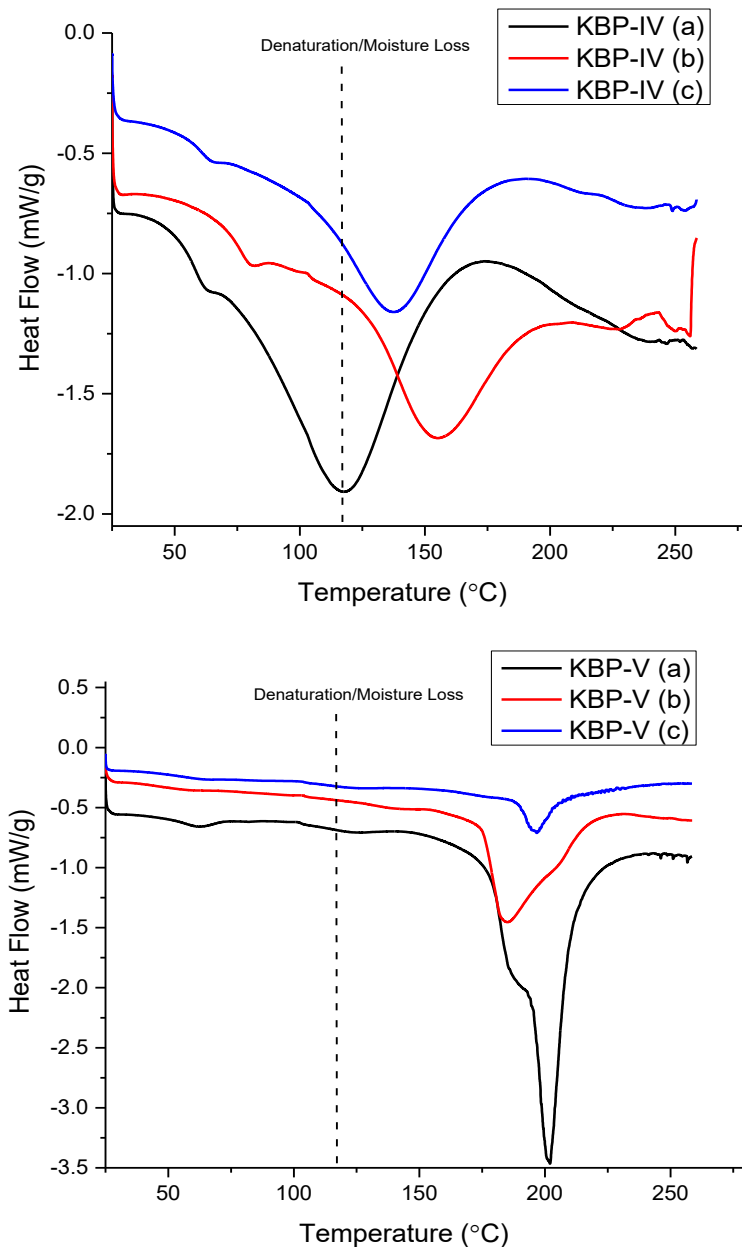
Figure 4.3. DSC heat flow signals of triplicates of KBP-IV (a, b, c) and KBP-V (a, b, c).

4.3.1.4 Thermogravimetric analysis (TGA)

The TGA analysis determines the thermal stability of triplicates of KBP-IV (a, b, c) and KBP-V (a, b, c). The keratin biopolymers usually display three steps of degradation (i) first weight loss at $\leq 100\,°C$ can be assigned to loss of entrapped moisture, (ii) second after $200\,°C$ represents that the KBPs undergo degradation and, (iii) third step indicates the KBPs decomposition from $350\,°C$ and onwards (Arshad et al., 2016a; Arshad et al., 2016b). For triplicates of KBP-IV (a, b, c) and KBP-V (a, b, c), the first slight weight loss (before $100\,°C$)

is observed (Fig 4.4). Afterwards, the KBP-IV (a, b, c) and KBP-V (a, b, c) show stability, and no weight loss is observed until at 200 °C. The second weight loss is not observed for triplicates of KBP-IV (a, b, c) but for triplicates of KBP-V (a, b, c) a steep decline in the curve is observed as a function of temperature at 200 °C. The second weight loss is dedicated to denaturation and destruction of internal hydrogen bonding/disulfide linkages and decomposition of the secondary network (positive and negative side chains) of proteins (Sun et al., 2009). The complete decomposition of triplicates of KBP-IV (a, b, c) and KBP-V (a, b, c) is observed around 300 °C. As indicated by Fig 4.4, there is no variation being observed in the thermal degradation behavior of triplicates of KBP-IV (a, b, c) and KBP-V (a, b, c).
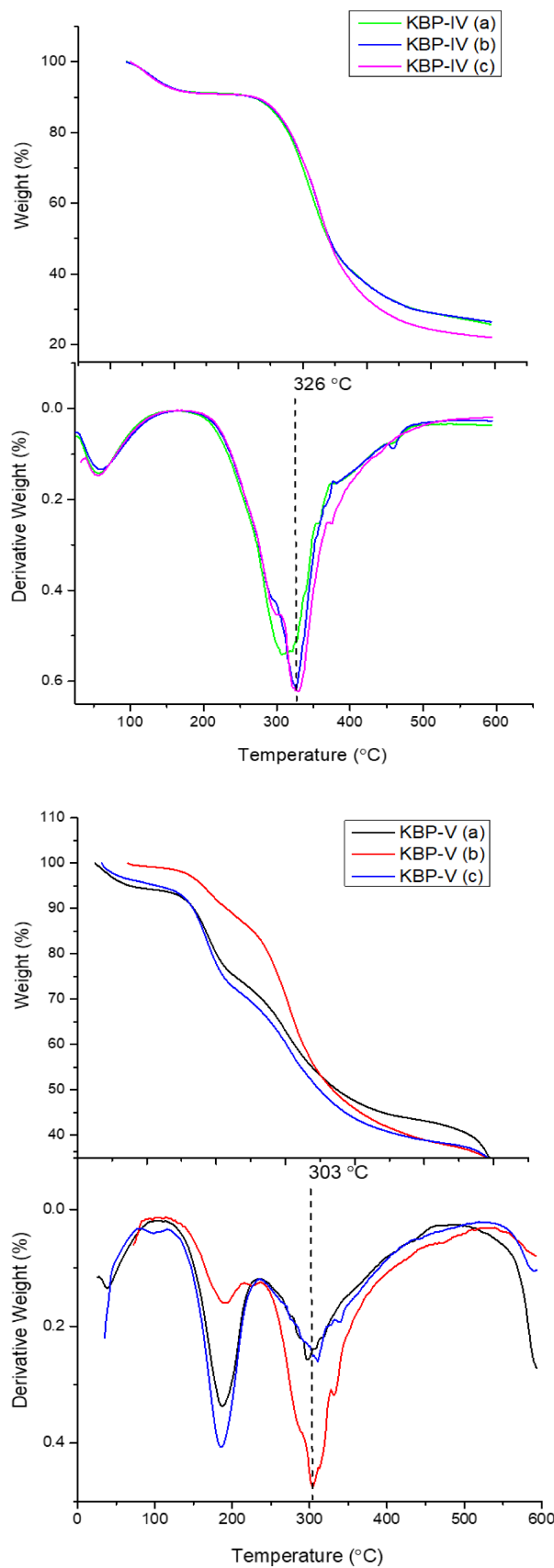
Figure 4.4. Thermogravimetric weight (%) loss and derivative curves of triplicates of KBP-IV (a, b, c) and KBP-V (a, b, c).

The results of characterization (FTIR, XRD, DSC, and TGA) analysis of modified KBPs [KBP-IV (a, b, c) and KBP-V (a, b, c)] revealed that the triplicate modifications of KBPs produced similar functional/structural properties and thermal behaviors, hence, endorsed the reproducible effects on KBPs.

4.3.2 Determining the reproducibility of KBP-IV (a, b, c) and KBP-V (a, b, c) for the removal of metals from synthetic wastewater

The developed biopolymers analyzed for morphological/structural studies were also tested for the adsorption of divalent cations and oxyanions from synthetic wastewater. With divalent cations in Fig. 4.5, KBP-IV (a) revealed very low adsorption affinities removing 21 µg L^{-1} of Ni^{2+}, and 19 µg L^{-1} of Cd^{2+}. However, KBP-IV (b) and KBP-IV (c) have not displayed adsorption for divalent cations. The KBP-V (a) and (b) adsorbed $\geq$ 70 µg L^{-1} of Co^{2+}, $\geq$ 65 µg L^{-1} of Ni^{2+}, and 60-80 µg L^{-1} of Cd^{2+}. The KBP-V (c) removed 53 µg L^{-1} of Co^{2+}, 37 µg L^{-1} of Ni^{2+}, and 69 µg L^{-1} of Cd^{2+}. For redox-sensitive oxyanions (Fig 4.5), the triplicates of KBP-IV (a, b, c) had shown higher adsorption efficiencies removing $\geq$ 80 µg L^{-1} of V^{V} and Cr^{VI}. The triplicates of KBP-V (a, b, c) had not displayed adsorption results for the removal of oxyanions from synthetic wastewater.

The consistency/repeatability of adsorption results [obtained by KBP-IV and KBP-V from previous study (chapter 2, section: *2.3.2*) and new replicates of this study] with slight variations revealed that the KBPs modifications under the same conditions have reproducible adsorption efficiencies for divalent cations and oxyanions. The adsorption mechanisms have not determined in this study, as assumed, that the KBPs exhibited same mechanisms observed in previous studies (second and third data chapters: sections: *2.7* and *3.3.1.1*).
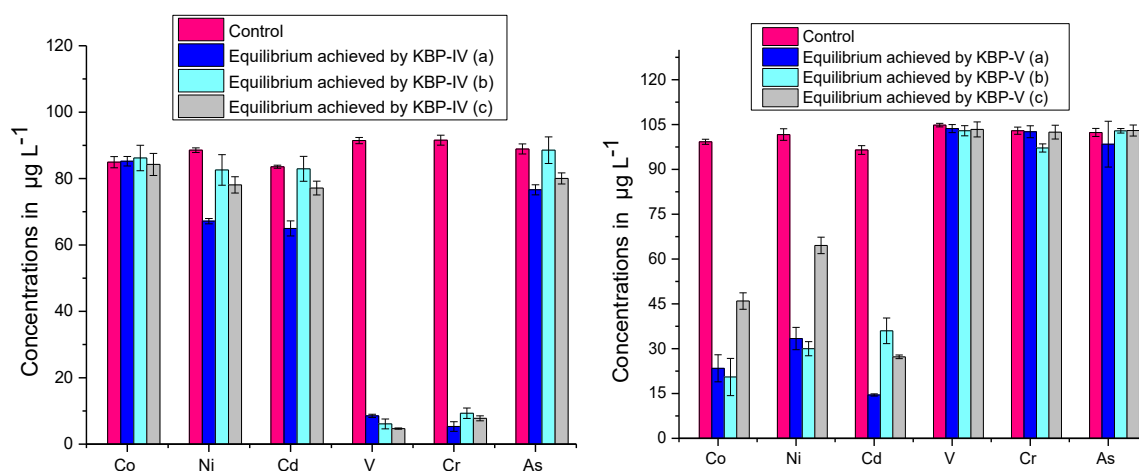
Figure 4.5. Removal of transition metals (Co^{2+}, Ni^{2+}, Cd^{2+}) and oxyanions of redox-sensitive trace metals (V^V, Cr^{VI}, As^{III}) from synthetic wastewater by triplicates of KBP-IV (a, b, c) and KBP-V (a, b, c). Concentrations of samples were measured after 24 h of incubation. Control values represent the analyte in the nano-pure water without biopolymer addition.

4.3.3 Recovery of divalent cations and oxyanions from KBPs surfaces for regeneration of KBPs

The desorption process not only recovers the metals from the sorbent's surfaces but also regenerates the sorbent materials for another cycle of adsorption application (Abdolali et al., 2015). According to the adsorption results presented in the second data chapter (section: *Fig. 2.7*), KBP-I adsorbed 19 µg L^{-1} of Co^{2+}, 55 µg L^{-1} of Ni^{2+}, 98 µg L^{-1} of Cd^{2+}, and 80 µg L^{-1} of V^V, KBP-IV adsorbed 17 µg L^{-1} of Ni^{2+}, 10 µg L^{-1} of Cd^{2+}, 102 µg L^{-1} of V^V, and 104 µg L^{-1} of Cr^{VI}. KBP-V showed adsorption results removing 100 µg L^{-1} of Ni^{2+}, 96 µg L^{-1} of Cd^{2+}, 42 µg L^{-1} of V^V, and 22 µg L^{-1} of Cr^{VI}.

The desorption results (Fig 4.6) demonstrated that 2 M HCl desorbed 16 µg L^{-1} of Co^{2+}, 47 µg L^{-1} of Ni^{2+}, 54 µg L^{-1} of Cd^{2+}, 54 µg L^{-1} of V^V from KBP-I, 19 µg L^{-1} of Ni^{2+}, 13 µg L^{-1} of Cd^{2+}, 82 µg L^{-1} of V^V, and 41 µg L^{-1} of Cr^{VI} from KBP-IV and 27 µg L^{-1} of Co^{2+}, 66 µg L^{-1} of Ni^{2+}, 56 µg L^{-1} of Cd^{2+}, and 34 µg L^{-1} of V^V from KBP-V surfaces.

For divalent cations, the 84% of Co^{2+} recovery from KBP-I, and 64-100% of Ni^{2+}, 55-100% of Cd^{2+} recoveries from KBP-I, KBP-IV, and KBP-V by HCl demonstrated that the acidic desorbing eluents protonate the sorbent surface by H_3O^+ ions, thus, resulting in the detachment of adsorbed metal cations (Chatterjee & Abraham, 2019). It has been suggested that desorption

is carried out by an ion-exchange mechanism between protons of an acid and the cations of the sorbents (Hammaini et al., 2007). The 67-82% recoveries of V^V from KBP-I, KBP-IV, and KBP-V, indicated that the reversible electrostatic attraction could take place between the protonated amine functional groups of KBPs and the oxyanions of V^V ($H_2VO_4^-$) (Padilla-Rodríguez et al., 2015). The 22-50 % recovery of Cr^{VI} from KBPs by HCl is explained by the ion exchange mechanism between the Cl^{-1} ions and Cr^{VI} oxyanionic species (Pakade & Chimuka, 2013). The ion exchange reaction is represented by the following equation:

$(2RNH^+) CrO_4^{2-} + 2Cl^- \leftrightarrow 2RNH^+Cl^- + CrO_4^{2-}$.
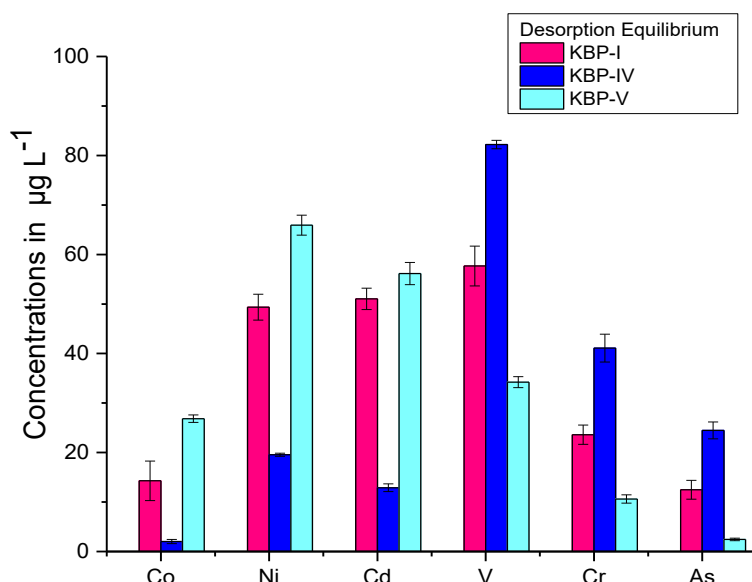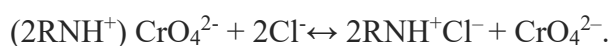
Figure 4.6. Desorbing elution results for Co^{2+}, Ni^{2+}, Cd^{2+}, V^V, $Cr^{VI,}$ and As^{III} from metal-loaded KBP-I, KBP-IV, and KBP-V.

4.3.4 Divalent cation and oxyanion's affinity towards hybrid sorbent (KBP-IX) and construction of adsorption isotherms

Selective removal of heavy metals from contaminated wastewater can be achieved by the application of hybrid sorbent (Gao et al., 1995). Furthermore, the functional variations of hybrid sorbent enhance the adsorption efficiencies of contaminants from wastewater (Samiey et al., 2014). As seen from Fig 4.7, The hybrid sorbent (KBP-IX) adsorbed 72 µg L^{-1} of Co^{2+}, 83 µg L^{-1} of Ni^{2+}, 65 µg L^{-1} of Cd^{2+}, 65 µg L^{-1} of V^V, 30 µg L^{-1} of Cr^{VI} and 10 µg L^{-1} of As^{III}.

This developed hybrid sorbent (KBP-IX) has shown the multi-metal (divalent cations and oxyanions) removal from the synthetic wastewater due to the combined effect of functional variations caused by different chemical modifying agents (KBP-IV; modified with ionic liquids and KBP-V: modified with propyl amine). The adsorption of divalent cations is characterized by the presence of amino chelating functional groups (Samiey et al., 2014), though, the adsorption of oxyanions of Cr and As has also been suggested by using the keratin amino-functionalized derivatives, elaborated that the ionic interactions between cationic amine groups and oxyanions could be involved (Yoshitake et al., 2002). The higher adsorption efficiencies were also observed for the removal of oxyanions of Cr^{VI} by using the CFs modified with ionic liquids (Sun et al., 2009; Zahara et al., 2021). However, the hybrid sorbent has displayed adsorption behavior for multi-metals (divalent cations and oxyanions), but the removal efficiencies towards single-metal removal by hybrid sorbent are lower than the adsorption efficiencies achieved by individual sorbent (KBP-IV & KBP-V) as mentioned in the previous data chapter (section: *2.3.2*).
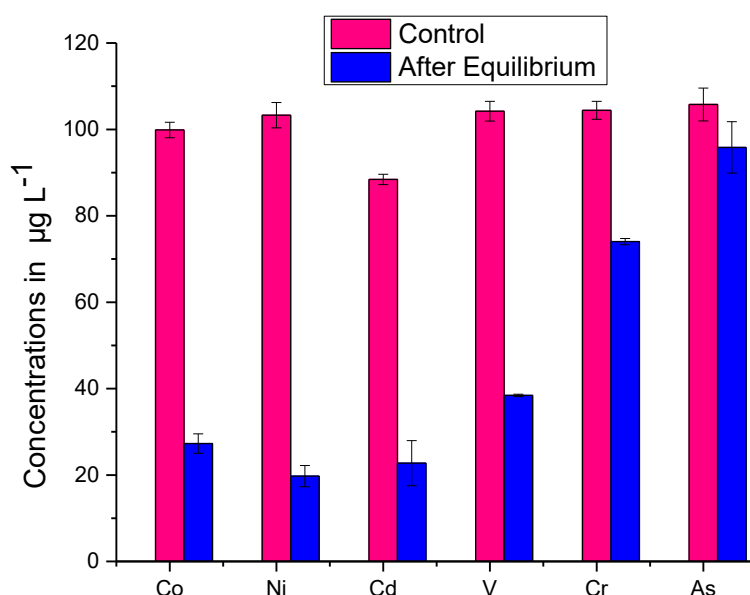
Figure 4.7. Removal of transition metals (Co^{2+}, Ni^{2+}, Cd^{2+}) and oxyanions of redox-sensitive trace metals (V^{V}, Cr^{VI}, As^{III}) from synthetic wastewater by the hybrid sorbent. Concentrations of samples were measured after 24 h of incubation. Control values represent the analyte in the nano-pure water without biopolymer addition.

Adsorption isotherms were constructed (Fig 4.8) for Cr^{VI} and V^V using the hybrid sorbent. The adsorption potential of hybrid sorbent was tested by varying the concentrations of metals in synthetic wastewater. The experimental data (q measured) was plotted against Ceq, then the data was analyzed and fitted into Langmuir and Freundlich models. The results suggested that hybrid sorbent for both metals demonstrated adsorption behavior best described by the Langmuir model yielding higher regression coefficient (R^2) values. The Langmuir model fitting analysis indicated that metals adsorbed on hybrid sorbent (KBP-IX) with monolayer formation on homogenously distributed active sites (Donner et al., 2019).
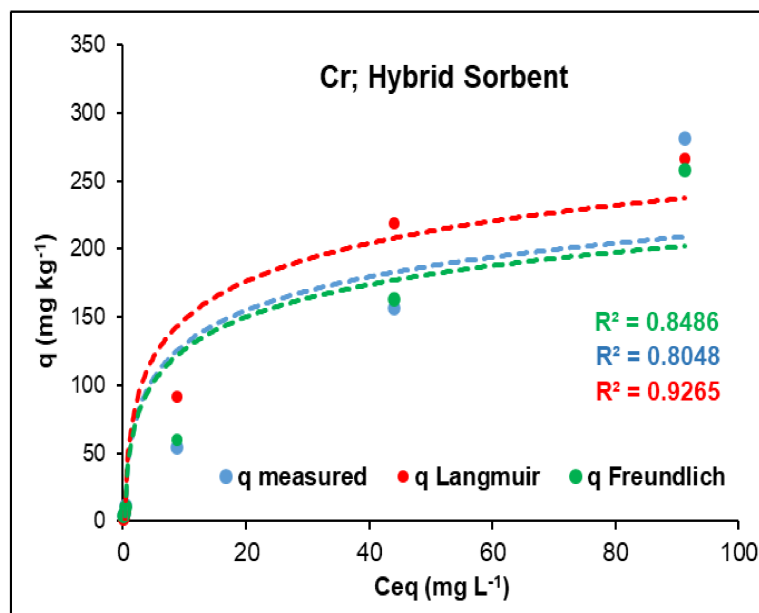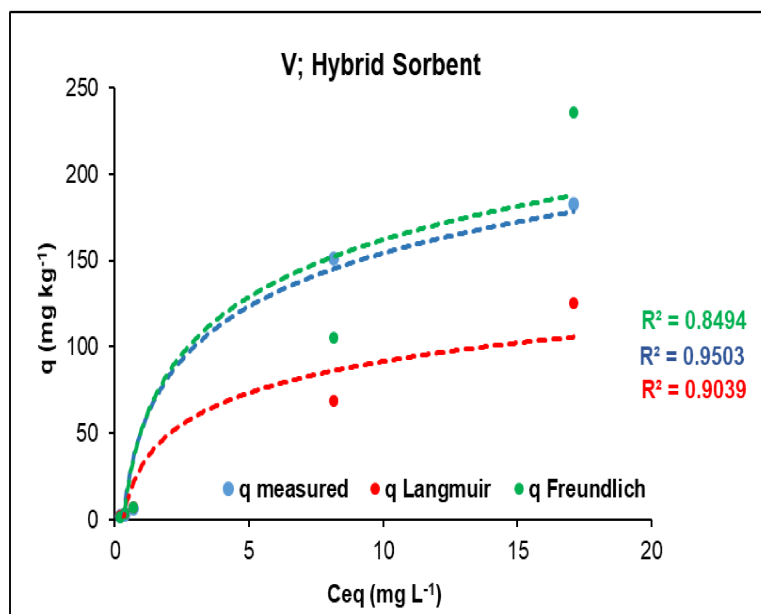
Figure 4.8. Adsorption isotherms of Cr^{VI} and V^{V} using hybrid sorbent. The experimental data (q measured) was plotted against Ceq data fitted into Langmuir (q Langmuir) and Freundlich (q Freundlich) models.

4.4 Conclusion

The influence of triplicate chemical modifications of KBPs (KBP-IV and KBP-V) on their surface physio-chemical characteristics and adsorption performances, implies that the chemical modification methods offer the reproducible specific affinities towards the removal of inorganic contaminants from synthetic wastewater. Based on the desorption results of this study, 2 M HCl was found to be an effective desorbing eluent recovering 84% of Co^{2+}, 100% of Ni^{2+}, 100% of Cd^{2+}, 82% of $V^{V,}$ and 50 % of Cr^{VI} from KBP-I, KBP-IV, and KBP-V. The hybrid sorbent (KBP-IX) prepared by mixing the (KBP-IV and KBP-V) displayed the adsorption affinities towards the divalent cations and oxyanions with the monolayer formation on homogenous sites described by higher regression (R^2) values of Langmuir model for Cr^{VI} and V^{V} removal from synthetic wastewater. Thus, maintaining reproducibility and regenerations of developed KBPs (KBP-IV and KBP-V) for many subsequent adsorption-desorption cycles as well as the hybrid application of KBPs (KBP-IX) towards inorganic contaminants removal from wastewater has both environmental and economic benefits.

4.5 Acknowledgements

5.0 CONCLUSIONS AND FUTURE DIRECTIONS

The goal of this study was to develop the sorbents from chicken/keratin feathers (CFs) for adsorbing the multi-metal contaminants with higher removal efficiencies from synthetic wastewater. The main objectives of this work were (i) to develop new sorbents by chemical modifications of CFs keratin, (ii) to evaluate the adsorption performances of developed keratin derived sorbents under the influence of process parameters (pH, contact time and temperature) with the assessment of adsorption mechanisms (iii) to reproduce and regenerate the keratin derived sorbents by triplicates modifications and desorption of contaminants and (iv) to investigate the role of mixed sorbent (as hybrid sorbent) for enhancing the adsorption affinities towards metal ions removal. Experiments were conducted to test these objectives and the obtained results ae presented in chapter 2-4. The overall conclusion is summarized here:

Chemical modifications of CFs affect their physical and chemical characteristics, consequently, influence the adsorption of contaminants from wastewaters. Hence, eight keratin derived sorbents/biopolymers (KBPs) were developed by chemical modifications, and their surface physio-chemical characterization studies were conducted. The results of FTIR and XRD analysis of the present study reveal that the chemical modifications of CFs exposed buried functional groups towards sorbent's surfaces and changed the native β-sheets, α-helices (crystalline structures) of developed KBPs. Furthermore, the prominent variations in the specific surface areas and pore size distributions of chemically modified KBPs indicates that these characteristics also depend on the modifications and ratio of precursors used to prepare the final products. As observed from adsorption results, KBP-I for As^{III} and Cd^{2+}, KBP-IV for Cu^{2+}, V^{V} and Cr^{VI}, KBP-V for Co^{2+}, Ni^{2+} and Zn^{2+}, and KBP-VI for Cr^{VI} displayed good sorption affinities having smaller surface areas. This indicates that apart from surface area, other factors such as availability of more functional groups on the KBPs surfaces aid in enhancing the metal uptake. However, the developed KBPs have not shown any adsorption results for Se^{VI}. The KBPs were also tested to remove the trace metals from OSPW, and the

adsorption results indicates that the KBP-VII removed 87% of Ba^{2+} and 84% of Sr^{2+} from OSPW.

Based on the initial better adsorption results, the adsorption performances of KBP-I, KBP-IV, KBP-V were evaluated under the influence of pH, temperature, contact time to optimize the process parameters. For multi-metal adsorption analysis at two initial (5.5 and 8.5) pH ranges of synthetic wastewater, there were no differences observed in adsorption results at both pH for the removal of divalent cations and oxyanions by KBP-I, KBP-IV, and KBP-V. The results of adsorption analysis from single-metal synthetic wastewater maintained at pH (5.5 and 8.5) by using the KBPs indicated that pH=8.5 was the suitable pH for divalent cations removal by KBP-V, whereas KBP-IV displayed high removal efficiencies for oxyanions at pH=5.5 The results for multi-metal adsorption analysis at two incubation temperatures (30 °C and 45 °C) revealed that the lower temperature (30 °C) is favorable for oxyanions (V^V, Cr^{VI} and As^{III}) removal by KBP-I, and favorable for (Co^{2+}, Ni^{2+}, Cd^{2+}, As^{III}) removal by KBP-IV, whereas higher temperature (40 °C) is favorable for the adsorption of divalent cations by KBP-V. However, KBPs (KBP-I, KBP-IV, KBP-V) tend to achieve maximum adsorption efficiencies within the 15-60 mins of incubation times for the removal of divalent cations and oxyanions from multi-metal synthetic wastewater. The adsorption mechanisms were further investigated by XPS analysis and the results of C1s, N1s and O1s high resolution spectra revealed that that metal ion adsorption by KBP-IV and KBP-V could be considered through electrostatic or chemical (chelation or complexation or reduction or ion exchange) interactions. The adsorption isotherms demonstrated that the adsorption behaviors of KBP-I for (Cd^{2+}), KBP-IV for (Cr^{VI}) and KBP-V for (Ni^{2+}) were best described by Langmuir model, whereas retention of (As^{III}) by KBP-I was best described by Freundlich model.

The results of characterization studies and adsorption analysis of triplicate modified KBPs (KBP-IV and KBP-V) revealed that the KBP-IV and KBP-V are reproducible. The results of

desorption studies showed that the 2 M HCL recovered 84-100% of divalent cations and 50-82% of oxyanions from KBPs (KBP-I, KBP-IV, and KBP-V). At last, the hybrid sorbent (KBP-IX) displayed the maximum multi-metals removal from synthetic wastewater with higher removal efficiencies.

Future studies may include (i) performing the several adsorption-desorption cycles to assess the life cycle of the spent sorbent, (ii) analyzing the role of developed sorbents towards the removal of organic contaminants from wastewater, and (ii) testing the developed sorbents on large scale application towards the removal of inorganic and organic contaminants from wastewater.

Thus, the developed KBPs possess the sustainable use and application criteria as mentioned by the 12 principles of green chemistry. Furthermore, the research gaps that were identified in the introduction chapter, tried to be fulfilled by conducting the detailed investigations on the surface physiochemical characteristics (such as functional group changes, crystallinity, thermal degradation/transitions, surface areas and pore size distributions) of the developed sorbents (modified with different modifying agents). The recent research includes the adsorption analysis for the specific sorbates (either divalent cations or oxyanions), however, the present study has tried to develop the sorbents that can target the multi-metals (divalent cations or oxyanions) from wastewater.

The developed keratin derived sorbents (KBP-IV for oxyanions and KBP-V for divalent cations) with greater adsorption performances have tremendous scope for water remediation contaminated with trace metals. At last, the cost-reduction of the developed KBPs by regeneration/recycling also opens-up the cheaper research horizons and better opportunities for water decontamination. On an optimistic approach, the keratin derived sorbents have shown prospects to be applied towards larger scale so that they can contribute as sustainable,

renewable, cost-efficient, and environmental-benign adsorption technology for water decontamination in the near future.

References

Abdolali, A., Ngo, H. H., Guo, W., Lu, S., Chen, S. S., Nguyen, N. C., Zhang, X., Wang, J., & Wu, J. (2016). A breakthrough biosorbent in removing heavy metals: equilibrium, kinetic, thermodynamic and mechanism analyses in a lab-scale study. *Science of The Total Environment, 542,* 603-611. DOI: https://doi.org/10.1016/j.scitotenv.2015.10.095.

Abdolali, A., Ngo, H. H., Guo, W., Zhou, J. L., Du, B., Wei, Q., Wang, X. C., & Nguyen, P. D. (2015). Characterization of a multi-metal binding biosorbent: chemical modification and desorption studies. *Bioresource Technology*, *193*, 477–487. DOI: https://doi.org/10.1016/j.biortech.2015.06.123.

Adaikpoh, E. O., Nwajei, G. E., & Ogala, J. E. (2006). Heavy metals concentrations in coal and sediments from river Ekulu in Enugu, coal city of Nigeria. *Journal of Applied Sciences and Environmental Management, 9*(3), 5-8. DOI: http://dx.doi.org/10.4314/jasem.v9i3.17343.

Ahalya, N., Kanamadi, R. D., & Ramachandra, T. V. (2010). Removal of hexavalent chromium using coffee husk. *International Journal of Environment and Pollution*, *43*(1–3), 106–116. DOI: https://dx.doi.org/10.1504/IJEP.2010.035917.

Aluigi, A., Zoccola, M., Vineis, C., Tonin, C., Ferrero, F., & Canetti, M. (2007). Study on the structure and properties of wool keratin regenerated from formic acid. *International Journal of Biological Macromolecules,* *41*(3), 266-273. DOI: https://doi.org/10.1016/j.ijbiomac.2007.03.002.

Anastopoulos, I., Robalds, A., Tran, H. N., Mitrogiannis, D., Giannakoudakis, D. A., Hosseini-Bandegharaei, A., & Dotto, G. L. (2019). Removal of heavy metals by leaves-derived biosorbents. *Environmental Chemistry Letters*, *17*(2), 755–766. DOI: 10.1007/s10311-018-00829-x.

Arai, K. M., Takahashi, R., Yokote, Y., & Akahane, K. (1983). Amino-Acid sequence of feather keratin from fowl. *European Journal of Biochemistry*, *132*(3), 501–507. DOI: https://doi.org/10.1111/j.1432-1033.1983.tb07389.x.

Arshad, M., Khosa, M. A., Siddique, T., & Ullah, A. (2016a). Modified biopolymers as sorbents for the removal of naphthenic acids from oil sands process affected water (OSPW). *Chemosphere, 163,* 334-341. DOI: https://doi.org/10.1016/j.chemosphere.2016.08.015.

Arshad, M., Kaur, M., & Ullah, A. (2016b). Green biocomposites from nanoengineered hybrid natural fiber and biopolymer. *ACS Sustainable Chemistry & Engineering, 4*(3), 1785-1793. DOI: https://doi.org/10.1021/acssuschemeng.5b01772.

Atas, M. S., Dursun, S., Akyildiz, H., Citir, M., Yavuz, C. T., & Yavuz, M. S. (2017). Selective removal of cationic micro-pollutants using disulfide-linked network structures. *RSC Advances*, *7*(42), 25969–25977. DOI: https://doi.org/10.1039/C7RA04775D.

Badawi, M. A., Negm, N. A., Abou Kana, M. T. H., Hefni, H. H., & Abdel Moneem, M. M. (2017). Adsorption of aluminum and lead from wastewater by chitosan-tannic acid modified biopolymers: Isotherms, kinetics, thermodynamics and process mechanism. *International Journal of Biological Macromolecules*, *99*, 465–476. DOI: https://doi.org/10.1016/j.ijbiomac.2017.03.003.

Barakat, M. A. (2011). New trends in removing heavy metals from industrial wastewater. *Arabian Journal of Chemistry*, *4*(4), 361–377. DOI: https://doi.org/10.1016/j.arabjc.2010.07.019.

Bose, P., Aparna, B. M., & Kumar, S. (2002). Critical evaluation of treatment strategies involving adsorption and chelation for wastewater containing copper, zinc and cyanide. *Advances in Environmental Research*, *7*(1), 179–195. DOI: http://dx.doi.org/10.1016/S1093-0191(01)00125-3.

Buxbaum, E. (2007). Fundamentals of protein structure and function. *Springer Science*

Business Media Inc., USA. DOI: 10.1007/978-3-319-19920-7.

Capablanca, J. S., & Watt, I. C. (1986). Factors affecting the zeta potential at wool fiber surfaces. *Textile Research Journal*, *56*(1), 49-55. DOI: 10.1177/004051758605600107.

Chakraborty, R., Asthana, A., Singh, A. K., Yadav, S., Susan, M. A. B. H., & Carabineiro, S. A. C. (2020). Intensified elimination of aqueous heavy metal ions using chicken feathers chemically modified by a batch method. *Journal of Molecular Liquids*, *312*, 113475. DOI: https://doi.org/10.1016/j.molliq.2020.113475.

Chatterjee, A., & Abraham, J. (2019). Desorption of heavy metals from metal loaded sorbents and e-wastes: A review. *Biotechnology Letters*, *41*(3), 319–333. DOI: https://doi.org/10.1007/s10529-019-02650-0.

Chen, H., Zhao, J., Dai, G., Wu, J., & Yan, H. (2010). Adsorption characteristics of Pb(II) from aqueous solution onto a natural biosorbent, fallen Cinnamomum camphora leaves. *Desalination*, *262*(1–3), 174–182. DOI: https://doi.org/10.1016/j.desal.2010.06.006.

Chojnacka, K. (2010). Biosorption and bioaccumulation - the prospects for practical applications. *Environment International*, *36*(3), 299–307. DOI: https://doi.org/10.1016/j.envint.2009.12.001.

Crini, G. (2005). Recent developments in polysaccharide-based materials used as adsorbents in wastewater treatment. *Progress in Polymer Science*, *30*(1), 38–70. DOI: https://doi.org/10.1016/J.PROGPOLYMSCI.2004.11.002.

Dabrowski, A. (2001). Adsorption - From theory to practice. *Advances in Colloid and Interface Science*, *93*(1–3), 135–224. DOI: https://doi.org/10.1016/S0001-8686(00)00082-8.

Daochalermwong, A., Chanka, N., Songsrirote, K., Dittanet, P., Niamnuy, C., & Seubsai, A. (2020). Removal of heavy metal ions using modified celluloses prepared from pineapple leaf fiber. *ACS Omega*, *5*(10), 5285–5296. DOI: https://doi.org/10.1021/acsomega.9b04326.

Davis, T. A., Volesky, B., & Mucci, A. (2003). A review of the biochemistry of heavy metal

biosorption by brown algae. *Water Research*, *37*(18), 4311–4330. DOI: https://doi.org/10.1016/s0043-1354(03)00293-8.

Deshmukh, P. D., Khadse, G. K., Shinde, V. M., & Labhasetwar, P. (2017). Cadmium removal from aqueous solutions using dried banana peels as an adsorbent: kinetics and equilibrium modeling. *Journal of Bioremediation and Biodegradation, 8,* 3. DOI: 10.4172/2155-6199.1000395.

Dhaouadi, F., Sellaoui, L., Badawi, M., Reynel-Ávila, H. E., Mendoza-Castillo, D. I., Jaime-Leal, J. E., Bonilla-Petriciolet, A., & Lamine, A. Ben. (2020). Statistical physics interpretation of the adsorption mechanism of Pb^{2+}, Cd^{2+} and Ni^{2+} on chicken feathers. *Journal of Molecular Liquids*, *319*. DOI: https://doi.org/10.1016/j.molliq.2020.114168.

Dickey, F. H. (1955). Specific adsorption. *Journal of Physical Chemistry*, *59*(8), 695–707. DOI: https://doi.org/10.1021/j150530a006.

Dincer, I. (1998). Energy and environmental impacts: present and future perspectives. *Energy Sources, 20* (4-5), 427-453. DOI: https://doi.org/10.1080/00908319808970070.

Dincer, I. (2018). Comprehensive energy systems, *Elsevier*, Amsterdam, Netherlands. https://search.ebscohost.com/login.aspx?direct=true&scope=site&db=nlebk&db=nlabk&AN=1584679.

Donner, M. W., Arshad, M., Ullah, A., & Siddique, T. (2019). Unravelled keratin-derived biopolymers as novel biosorbents for the simultaneous removal of multiple trace metals from industrial wastewater. *Science of the Total Environment*, *647*, 1539–1546. DOI: https://doi.org/10.1016/j.scitotenv.2018.08.085.

Dupont, J. (2004). On the solid, liquid and solution structural organization of imidazolium ionic liquids. *Journal of the Brazilian Chemical Society, 15* (3). DOI: https://doi.org/10.1590/S0103-50532004000300002.

Duruibe, J. O., Ogwuegbu, M. O. C., & Egwurugwu, J. N. (2007). Heavy metal pollution and human biotoxic effects. *International Journal of Physical Sciences,* 2(5), 112-118. DOI: http://www.academicjournals.org/IJPS.

Essington, M. E. (2005). Soil and water chemistry: An integrated approach. *CRC Press; 1ˢᵗ edition*, USA. DOI: https://doi.org/10.1201/b12397.

Ferraris, S., Martina, C., Veronica, P., Barbara, S., & Silvia, S. (2018). Zeta potential measurements on solid surfaces for in vitro biomaterials testing: surface charge, reactivity upon contact with fluids and protein absorption. *Frontiers in Bioengineering and Biotechnology, 6.* DOI=10.3389/fbioe.2018.00060.

Gao, P., Liu, Z., Wu, X., Cao, Z., Zhuang, Y., Sun, W., Xue, G., & Zhou, M. (2014). Biosorption of chromium(VI) ions by deposits produced from chicken feathers after soluble keratin extraction. *Clean: Soil, Air, Water, 42,* 1558–1566. DOI: 10.1002/clen.201300669.

Gao, Y. M., Sengupta, A. K., & Simpson, D. (1995). A new hybrid inorganic sorbent for heavy metals removal. *Water Research*, *29*(9), 2195–2205. DOI: https://doi.org/10.1016/0043-1354(95)00040-R.

Ghafar, H., Salem, T., Radwan, E., El-Sayed, A., Embaby, M., & Salama, M. (2017). Modification of waste wool fiber as low cost adsorbent for the removal of methylene blue from aqueous solution. *Egyptian Journal of Chemistry*, *60*(3), 395-406. DOI: 10.21608/ejchem.2017.687.1023.

Ghosh, A., & Collie, S. R. (2014). Keratinous materials as novel absorbent systems for toxic pollutants. *Defence Science Journal*, *64*(3), 209–221. DOI: https://doi.org/10.14429/dsj.64.7319.

Giri, R., Kumari, N., Behera, M., Sharma, A., Kumar, S., Kumar, N., & Singh, R. (2021). Adsorption of hexavalent chromium from aqueous solution using pomegranate peel as low-cost biosorbent. *Environmental Sustainability*, *4*(2), 401–417. DOI:

https://doi.org/10.1007/s42398-021-00192-8. https://doi.org/10.1007/s42398-021-00192-8.

Guibal, E. (2004). Interactions of metal ions with chitosan-based sorbents: A review. *Separation and Purification Technology*, *38*(1), 43–74. DOI: https://doi.org/10.1016/j.seppur.2003.10.004.

Guo, J., Yan, C., Luo, Z., Fang, H., Hu, S., & Cao, Y. (2019). Synthesis of a novel ternary HA/Fe-Mn oxides-loaded biochar composite and its application in cadmium(II) and arsenic(V) adsorption. *Journal of Environmental Sciences, 85,* 168-176, DOI: https://doi.org/10.1016/j.jes.2019.06.004.

Hammaini, A., González, F., Ballester, A., Blázquez, M. L., & Muñoz, J. A. (2007). Biosorption of heavy metals by activated sludge and their desorption characteristics. *Journal of Environmental Management*, *84*(4), 419–426. DOI: https://doi.org/10.1016/j.jenvman.2006.06.015.

Hermanson, G. T. (2013). The reactions of bioconjugation. Bioconjugate Techniques. *Academic Press,* 229–258. DOI: https://doi.org/10.1016/B978-0-12-382239-0.00003-0.

Jiang, W., Chen, X., Pan, B., Zhang, Q., Teng, L., Chen, Y., & Liu, L. (2014). Spherical polystyrene-supported chitosan thin film of fast kinetics and high capacity for copper removal. *Journal of Hazardous Materials*, *276*, 295–301. DOI: http://dx.doi.org/10.1016/j.jhazmat.2014.05.032.

Jiang, Y. J., Yu, X. Y., Luo, T., Jia, Y., Liu, J. H., & Huang, X. J. (2013). γ-Fe2O3 nanoparticles encapsulated millimeter-sized magnetic chitosan beads for removal of Cr(VI) from water: thermodynamics, kinetics, regeneration, and uptake mechanisms. *Journal of Chemical and Engineering Data*, *58*(11), 3142–3149. DOI: https://doi.org/10.1021/je400603p.

Igunnu, E. T., & Chen, G. Z. (2014). Produced water treatment technologies. *International Journal of Low Carbon Technologies, 9*(3), 157-177. DOI: https://doi.org/10.1093/ijlct/cts049.

Iqbal, M., & Saeed, A. (2007). Production of an immobilized hybrid biosorbent for the sorption

of Ni(II) from aqueous solution. *Process Biochemistry*, *42*(2), 148–157. DOI: http://dx.doi.org/10.1016/j.procbio.2006.07.022.

Iqbal, M., Saeed, A., & Zafar, S. I. (2007). Hybrid biosorbent: An innovative matrix to enhance the biosorption of Cd(II) from aqueous solution. *Journal of Hazardous Materials*, *148*(1–2), 47–55. DOI: 10.1016/j.jhazmat.2007.02.009.

Ishikawa, S. I., Sekine, S., Miura, N., Suyama, K., Arihara, K., & Itoh, M. (2004). Removal of selenium and arsenic by animal biopolymers. *Biological Trace Element Research, 102* (1-3), 113-127. DOI: https://doi.org/10.1385/BTER:102:1-3:11.

Israelachvili, J. N., McGuiggan, P. M., & Homola, A. M. (1988). Dynamic properties of molecularly thin liquid films. *Science, 240*(4849), 189–191. DOI: https://doi.org/10.1126/science.240.4849.189.

Jackson, M. M., & Mantsch, H. H. (1995). The use and misuse of FTIR spectroscopy in the determination of protein structure. *Critical Reviews in Biochemistry and Molecular Biology, 30*(2), 95-120. DOI: https://doi.org/10.3109/10409239509085140.

Johnson, D. H. (1997). Hair and hair care. *Taylor & Francis,* USA. DOI: https://doi.org/10.1201/9780203719565.

Kanamarlapudi, S. L. R. K., Chintalpudi, V. K., & Muddada, S. (2018). Application of biosorption for removal of heavy metals from wastewater; Biosorption. *Intechopen,* London. DOI: 10.5772/intechopen.77315.

Kaur, M., Arshad, M., & Ullah, A. (2018). In-situ nanoreinforced green bionanomaterials from natural keratin and montmorillonite (MMT)/cellulose nanocrystals (CNC). *ACS Sustainable Chemistry and Engineering*, *6*(2), 1977–1987. DOI: https://doi.org/10.1021/acssuschemeng.7b03380.

Khosa, M. A., & Ullah, A. (2013). A sustainable role of keratin biopolymer in green chemistry: A review. *Journal of Food Processing & Beverages, 1*(1), 8. DOI:

https://doi.org/10.7939/R3QB9VK25.

Khosa, M., Wu, J., & Ullah, A. (2013). Chemical modification, characterization, and application of chicken feathers as novel biosorbent. *RSC Advances, 3*(43), 20800-20810. DOI: https://doi.org/10.1039/C3RA43787F.

Klapiszewski, L., Wysokowski, M., Majchrzak, I., Szatkowski, T., Nowacka, M., Stefanska, K. S., Rzepka, K. S., Bartczak, P., Ehrlich, H., & Jesionowski, T. (2013). Preparation and characterization of multifunctional chitin/lignin materials. *Journal of nanomaterials, 425726.* DOI: https://doi.org/10.1155/2013/425726.

Kocaturk, S. (2008). Title of Thesis: Removal of heavy metal ions from aqueous solutions by keratin.http://acikerisim.ege.edu.tr:8081/jspui/bitstream/11454/3511/1/saniyekocaturk2008.pdf.

Kong, A., Ji, Y., Ma, H., Song, Y., He, B., & Li, J. (2018). A novel route for the removal of Cu(II) and Ni(II) ions via homogeneous adsorption by chitosan solution. *Journal of Cleaner Production*, *192*, 801–808. DOI: https://doi.org/10.1016/j.jclepro.2018.04.271.

Kumar, M. N. R. (2000). A review of chitin and chitosan applications. *Reactive and Functional Polymers, 46* (1), 1–27. DOI: https://doi.org/10.1016/S1381-5148(00)00038-9.

Kyzas, G. Z., Siafaka, P.I., Lambropoulou, D.A., Lazaridis, N.K., & Bikiaris, D. N. (2014). Poly(itaconic acid)-grafted chitosan adsorbents with different cross-linking for Pb(II) and Cd(II) uptake. *Langmuir, 30*(1), 120-31. DOI:10.1021/la402778x.

Lei, T., Li, S. J., Jiang, F., Ren, Z. X., Wang, L. L., Yang, X. J., Tang, L. H., & Wang, S. X. (2019). Adsorption of cadmium ions from an aqueous solution on a highly stable dopamine-modified magnetic nano-adsorbent. *Nanoscale Research Letters, 14*, 352. DOI: https://doi.org/10.1186/s11671-019-3154-0.

Li, T., Wang, C., Li, T., Ma, L., Sun, D., Hou, J., & Jiang, Z. (2018). Surface hydrophobicity and functional properties of citric acid cross-linked whey protein isolate: The impact of pH and

concentration of citric acid. *Molecules, 23*(9). DOI: 10.3390/molecules23092383.

Lin, Z., Yang, Y., Liang, Z., Zeng, L., & Zhang, A. (2021). Preparation of chitosan/calcium alginate/bentonite composite hydrogel and its heavy metal ions adsorption properties. *Polymers*, *13*(11). DOI: https://doi.org/10.3390/polym13111891.

Liu, X., & Zhang, L. (2015). Insight into the adsorption mechanisms of vanadium(V) on a high-efficiency biosorbent (Ti-doped chitosan bead). *International Journal of Biological Macromolecules, 79*, 110–117. DOI: 10.1016/j.ijbiomac.2015.04.065.

Liu, C., Jin, R. N., Ouyang, X. K., & Wang, Y. G. (2017). Adsorption behavior of carboxylated cellulose nanocrystal-polyethyleneimine composite for removal of Cr(VI) ions. *Applied Surface Science, 408*, 77–87. DOI: 10.1016/J.APSUSC.2017.02.265.

Liu, H., Sun, R., Feng, S., Wang, D., & Liu, H. (2019). Rapid synthesis of a silsesquioxane-based disulfide-linked polymer for selective removal of cationic dyes from aqueous solutions. *Chemical Engineering Journal, 359,* 436-445. DOI: https://doi.org/10.1016/j.cej.2018.11.148.

Luo, S., Li, X., Chen, L., Chen, J., Wan, Y., & Liu, C. (2014). Layer-by-layer strategy for adsorption capacity fattening of endophytic bacterial biomass for highly effective removal of heavy metals. *Chemical Engineering Journal, 239,* 312-321. DOI: https://doi.org/10.1016/j.cej.2013.11.029.

Lu, W. B., Shi, J. J., Wang, C. H., & Chang, J. S. (2006). Biosorption of lead, copper and cadmium by an indigenous isolate Enterobacter sp. J1 possessing high heavy-metal resistance. *Journal of Hazardous Materials, 30*(1-3). DOI: 10.1016/j.jhazmat.2005.10.036. Epub 2005 Nov 28. PMID: 16310950.

Ma, Li., Wei, Q., Chen, Y., Song, Q., Sun, C., Wang, Z., & Wu, G. (2018). Removal of cadmium from aqueous solutions using industrial coal fly ash-nZVI. *Royal Society Open Science, 5*, 171051. DOI: http://dx.doi.org/10.1098/rsos.171051.

Malaeb, L., & Ayoub, G. M. (2011). Reverse osmosis technology for water treatment: state of

the art review. *Desalination*, *267*(1), 1–8. DOI: https://doi.org/10.1016/j.desal.2010.09.001.

Manzoor, K., Ahmad, M., Ahmad, S., & Ikram, S. (2019). Removal of Pb(ii) and Cd(ii) from wastewater using arginine cross-linked chitosan-carboxymethyl cellulose beads as green adsorbent. *RSC Advances*, *9*(14), 7890–7902. DOI: https://doi.org/10.1039/C9RA00356H.

Martínez, K. O., Valentín, D. A. V., & Maldonado, A. J. H. (2018). Adsorption of contaminants of emerging concern from aqueous solutions using Cu^{2+} amino grafted SBA-15 mesoporous silica: multicomponent and metabolites adsorption. *Industrial & Engineering Chemistry Research, 57*(18), 6426-6439. DOI: https://doi.org/10.1021/acs.iecr.7b05168.

Matouq, M., Jildeh, N., Qtaishat, M., Hindiyeh, M., & Al Syouf, M. Q. (2015). The adsorption kinetics and modeling for heavy metals removal from wastewater by Moringa pods. *Journal of Environmental Chemical Engineering*, *3*(2), 775–784. DOI: http://dx.doi.org/10.1016%2Fj.jece.2015.03.027.

Melnyk, I. V., Pogorilyi, R. P., Zub, Y. L., Vaclavikova, M., Gdula, K., Dabrowski, A., Seisenbaeva, G. A., & Kessler, V. G. (2018). Protection of thiol groups on the surface of magnetic adsorbents and their application for wastewater treatment. *Scientific Reports*, *8*(1), 20–31. DOI: https://doi.org/10.1038/s41598-018-26767-w.

Meyers, M. A., Chen, P. Y., Lin, A. Y. M., & Seki, Y. (2008). Biological materials: structure and mechanical properties. *Progress in Materials Science*, *53*(1), 1–206. DOI: https://doi.org/10.1016/j.pmatsci.2007.05.002.

Mielke, E., Diaz Anadon, L., & Narayanamurti, V. (2010). Water consumption of energy resource extraction, processing, and conversion: A review of the literature for estimates of water intensity of energy-resource extraction, procesing to fuels and conversion to electricity. *Energy Technology Innovation Policy Discussion Paper*, *October*.

Morais-Coutinho, C., Chiu, M. C., Basso, R. C., Ribeiro, A. P. B., Gonçalves, L. A. G., & Viotto, L. A. (2009). State of art of the application of membrane technology to vegetable oils:

A review. *Food Research International*, *42*(5–6), 536–550. DOI: http://dx.doi.org/10.1016/j.foodres.2009.02.010.

Mrvčić, J., Stanzer, D., Šolić, E., & Stehlik-Tomas, V. (2012). Interaction of lactic acid bacteria with metal ions: opportunities for improving food safety and quality. *World Journal of Microbiology and Biotechnology*, *28*(9), 2771–2782. DOI: https://doi.org/10.1007/s11274-012-1094-2.

Ngah, W. S. W., & Fatinathan, S. (2010). Pb(II) biosorption using chitosan and chitosan derivatives beads: equilibrium, ion exchange and mechanism studies. *Journal of Environmental Sciences*, *22*(3), 338–346. DOI: https://doi.org/10.1016/s1001-0742(09)60113-3.

Nuutinen, E. M. (2017). Title of Thesis: Feather Characterization and Processing. https://pdfs.semanticscholar.org/29b4/58542c8638ad924a509af00c741bb887b7f2.pdf.

Olsson, G. (2012). Water and Energy: threats and opportunities. *IWA Publishers*, London, UK. http://aozhouiwk.com/pdf/water%26energy_sample.pdf.

Padilla-Rodríguez, A., Hernández-Viezcas, J. A., Peralta-Videa, J. R., Gardea-Torresdey, J. L., Perales-Pérez, O., & Román-Velázquez, F. R. (2015). Synthesis of protonated chitosan flakes for the removal of vanadium(III, IV and V) oxyanions from aqueous solutions. *Microchemical Journal*, *118*, 1–11. DOI: http://dx.doi.org/10.1016/j.microc.2014.07.011.

Pakade, V., & Chimuka, L. (2013). Polymeric sorbents for removal of Cr(VI) from environmental samples. *Pure and Applied Chemistry*, *85*(12), 2145–2160. DOI: https://doi.org/10.1351/pac-con-12-11-17.

Park, D., Lim, S. R., Yun, Y. S., & Park, J. M. (2007). Reliable evidences that the removal mechanism of hexavalent chromium by natural biomaterials is adsorption coupled reduction. *Chemosphere, 70*(2), 298-305. DOI: https://doi.org/10.1016/j.chemosphere.2007.06.007.

Park, D., Yun, Y. S., & Park, J. M. (2010). The past, present, and future trends of biosorption.

Biotechnology and Bioprocess Engineering, *15*(1), 86–102. DOI: https://doi.org/10.1007/s12257-009-0199-4.

Park, J., Howe, J. D., & Sholl, D. S. (2017). How reproducible are isotherm measurements in metal-organic frameworks. *Chemistry of Materials*, *29*(24), 10487–10495. DOI: https://doi.org/10.1021/acs.chemmater.7b04287.

Pivarciova, L., Rosskopfova, O., Galambos, M., & Rajec, P. (2014). Sorption of nickel on chitosan. *Journal of Radioanalytical Nuclear Chemistry, 300*, 361–366. DOI: 10.1007/s10967-014-3007-3.

Qin, R., Lillico, D., How, Z. T., Huang, R., Belosevic, M., Stafford, J., & Gamal El-Din, M. (2019). Separation of oil sands process water organics and inorganics and examination of their acute toxicity using in-vitro bioassays. *Sceince of the total Environment, 695,*133532. DOI: https://doi.org/10.1016/j.scitotenv.2019.07.338.

Rahmani-Sani, A., Singh, P., Raizada, P., Claudio Lima, E., Anastopoulos, I., Giannakoudakis, D. A., Sivamani, S., Dontsova, T. A., & Hosseini-Bandegharaei, A. (2020). Use of chicken feather and eggshell to synthesize a novel magnetized activated carbon for sorption of heavy metal ions. *Bioresource Technology*, *297*, 122452. DOI: 10.1016/j.biortech.2019.122452.

Rakesh, K. E., & Antony, R. (2017). Biosorption studies of chromium ions with modified chicken feathers. *Biomedical Journal of Scientific & Technical Research, 1*(7), 1819-1822. DOI: 10.26717/BJSTR.2017.01.000558.

Randall, J. M., Randall, V. G., McDonald, G. M., Young, R. N., & Masri, M. S. (1979). Removal of trace quantities of nickel from solution. *Journal of Applied Polymer Science*, *23*(3), 727–732. DOI: https://doi.org/10.1002/app.1979.070230307.

Raouf, M. S. A., & Raheim, A. R. M. A. (2016). Removal of heavy metals from industrial waste water by biomass-based materials: A review. *Journal of Pollution Effects & Control*, *05*(01), 1–13. DOI: http://dx.doi.org/10.4172/2375-4397.1000180.

Raouf, A., & Raheim, A. (2017). Removal of heavy metals from industrial wastewater by biomass-based materials. *Journal of Pollution Effects & Control, 5*, 1. DOI: 10.4172/2375-4397.1000180.

Rengaraj, S., Joo, C. K., Kim, Y., & Yi, J. (2003). Kinetics of removal of chromium from water and electronic process wastewater by ion exchange resins: 1200H, 1500H and IRN97H. *Journal of Hazardous Materials*, *102*(2–3), 257–275. DOI: https://doi.org/10.1016/s0304-3894(03)00209-7.

Rinaudo, M. (2006). Chitin and chitosan: properties and applications. *Progress in Polymer Science, 31*(7), 603–632. DOI: https://doi.org/10.1016/j.progpolymsci.2006.06.001.

Robert, J., Ouellette, J., & Rawn, D. (2014). Organic chemistry: structure, mechanism, and synthesis. *Elsevier,* USA. DOI: https://doi.org/10.1016/B978-0-12-800780-8.00027-9.

Rodriguez, A. P., Hernandez-Viezcas, J. A., Peralta-Videa, J. R., Gardea-Torresdey, J. L., Oscar Perales-Perez, O., & Roman-Velázquez, F. R. (2015). Synthesis of protonated chitosan flakes for the removal of vanadium (III, IV and V) oxyanions from aqueous solutions. *Microchemical Journal, 118*, 1-11. DOI: https://doi.org/10.1016/j.microc.2014.07.011.

Samiey, B., Cheng, C. H., & Wu, J. (2014). Organic-inorganic hybrid polymers as adsorbents for removal of heavy metal ions from solutions: A review. *Materials*, *7*(2), 673–726. DOI: https://dx.doi.org/10.3390%2Fma7020673.

Sapari, N., Idris, A., & Hamid, N. H. A. (1996). Total removal of heavy metal from mixed plating rinse wastewater. *Desalination*, *106*(1–3), 419–422. DOI: https://doi.org/10.1016/S0011-9164(96)00139-7.

Saravanan, A., Kumar, P. S., Yaashikaa, P. R., Karishma, S., Jeevanantham, S., & Swetha, S. (2021). Mixed biosorbent of agro waste and bacterial biomass for the separation of Pb(II) ions from water system. *Chemosphere*, *277*, 130236. DOI: https://doi.org/10.1016/j.chemosphere.2021.130236.

Sarode, S., Upadhyay, P., Khosa, M. A., Mak, T., Shakir, A., Song, S., & Ullah, A. (2019). Overview of wastewater treatment methods with special focus on biopolymer chitin-chitosan. *International Journal of Biological Macromolecules*, *121*, 1086–1100. DOI: https://doi.org/10.1016/j.ijbiomac.2018.10.089.

Sathivika, T., Soni, A., Sharma, K., Praneeth, M., Mudaliyar, M., Rajesh, V., & Rajesh, N. (2018). Potential application of saccharomyces cerevisiae and rhizobium immobilized in multi walled carbon nanotubes to adsorb hexavalent chromium. *Scientific Reports, 8*, 9862. DOI: https://doi.org/10.1038/s41598-018-28067-9.

Scheibel, T. (2005). Protein fibers as performance proteins: new technologies and applications. *Current Opinion in Biotechnology*, *16*(4), 427–433. DOI: https://doi.org/10.1016/j.copbio.2005.05.005.

Schroder, C. (2017). Proteins in ionic liquids: current status of experiments and simulations. *Topics in Current Chemistry, 375* (25). DOI: https://doi.org/10.1007/s41061-017-0110-2.

Scott, C. A., Brief, I. S., Coldwell, P. J., Klein, G., Krebs, M., Hall, V., O'Brien, T., Blevins, B. B., Williams, E. D., Simmons, J. E., Platonova, I., Programa, M. L., Clim, C., No, A. P., Duan, C., & Chen, B. (2011). Water in the energy industry. An introduction. *Energy*, *47*(12), 725–734. www.bp.com/energysustainabilitychallenge.

Sharififard, H., & Soleimani, M. (2015). Performance comparison of activated carbon andferricoxide-hydroxide–activated carbon nanocomposite as vanadium(V) ion adsorbents. *RSC Advances, 5*, 80650–80660. DOI: https://doi.org/10.1039/C5RA14493K.

Sim, S. F., Ling, T. Y., Nyanti, L., Gerunsin, N., Wong, Y. E., & Kho, L.P. (2016). Assessment of heavy metals in water, sediment, and fishes of a large tropical hydroelectric dam in Sarawak, Malaysia. *Journal of Chemistry,* 1-10. DOI: https://doi.org/10.1155/2016/8923183.

Sitko, R., Turek, E., Zawisza, B., Malicka, E., Talik, E., Heimann, J., Gagor, A., Feist, B., & Wrzalik, R. (2013). Adsorption of divalent metal ions from aqueous solutions using graphene

oxide. *Dalton Transactions*, *42*(16), 5682–5689. DOI: https://doi.org/10.1039/C3DT33097D.

Sun, P., Liu, Z. T., & Liu, Z. W. (2009). Particles from bird feather: A novel application of an ionic liquid and waste resource. *Journal of Hazardous Materials*, *170*(2–3), 786–790. DOI: https://doi.org/10.1016/j.jhazmat.2009.05.034.

Sun, G. L., Reynolds, E. E., & Belcher, A. M. (2020). Using yeast to sustainably remediate and extract heavy metals from waste waters. *Nature Sustainability*, *3*(4), 303–311. DOI: https://hdl.handle.net/1721.1/125875.

Suzelei, R., Azevedo, H., Ferrari, C. R., Roque, C. V., Ronqui, L. B., Campos, M. B., & Nascimento, M. R. R. (2012). Evaluation of surface water quality in aquatic bodies under the influence of uranium mining. *Environmental Monitoring and Assessment, 185*, 2395-2406. DOI: 10.1007/s10661-012-2719-5.

Swati, S., Arun, G., Saufi, S. M., Kee, G. Y. C., Poddar, P. K., Subramaniam, M., & Thuraisingam, J. (2017). Study of different treatment methods on chicken feather biomass. *IIUM Engineering Journal, 18* (2), 47-55. DOI: http://dx.doi.org/10.31436/iiumej.v18i2.806.

Teixeira, M. C., & Ciminelli, V. S. T. (2005). Development of a biosorbent for arsenite: structural modeling based on x-ray spectroscopy. *Environmental Science and Technology*, *39*(3), 895–900. DOI: https://doi.org/10.1021/es049513m.

Tesfaye, T., Sithole, B., Ramjugernath, D., & Chunilall, V. (2017). Valorisation of chicken feathers: characterization of physical properties and morphological structure. *Journal of Cleaner Production, 149,* 349-365. DOI: https://doi.org/10.1016/j.jclepro.2017.02.112.

Thommes, M., Kaneko, K., Neimark, A. V., Olivier, J. P., Reinoso, F. R., Rouquerol, J., & Sing, K. S. W. (2015). Physisorption of gases, with special reference to the evaluation of surface area and pore size distribution. *Pure and Applied Chemistry, 87*(9-10), 1051-1069. DOI: https://doi.org/10.1515/pac-2014-1117.

Tripathi, L., Mishra, A. K., Dubey, A. K., & Tripathi, C. B. (2013). Water pollution through energy sector. *International Journal of Technology Enhancements and Emerging Engineering Research*, *03*(03), 2347-4289. https://www.scribd.com/document/436961932/Water-Pollution-Through-Energy-Sector-pdf.

Ullah, A., Vasanthan, T., Bressler, D., Elias, A. L., & Wu, J. (2011a). Bioplastics from feather quill. *Biomacromolecules, 12*, 3826-3832. DOI: https://doi.org/10.1021/bm201112n.

Ullah, A., Alongi, J., & Russo, S. (2011b). Recent findings in (Ti) POSS-based polymer systems. *Polymer Buletin, 67*, 1169-1183. DOI: https://doi.org/10.1007/s00289-011-0445-8.

Ullah, A., & Wu, J. (2013). Feather fiber-based thermoplastics: effects of different plasticizers on material properties. *Macromolecular Materials & Engineering, 298*(2), 153-162. DOI: https://doi.org/10.1002/mame.201200010.

Vieira, R. S., Oliveira, M. L. M., Guibal, E., Rodríguez-Castellón, E., & Beppu, M. M. (2011). Copper, mercury and chromium adsorption on natural and crosslinked chitosan films: An XPS investigation of mechanism. *Colloids and Surfaces A: Physicochemical and Engineering Aspects*, *374*(1–3), 108–114. DOI: http://dx.doi.org/10.1016%2Fj.colsurfa.2010.11.022.

Wang, J., & Chen, C. (2006). Biosorption of heavy metals by Saccharomyces cerevisiae: A review. *Biotechnology Advances*, *24*(5), 427–451. DOI: https://doi.org/10.1016/j.biotechadv.2006.03.001.

Wang, H., Tian, Z., Jiang, L., Luo, W., Wei, Z., Li, S., Cui, J., & Wei, W. (2017). Highly efficient adsorption of Cr(VI) from aqueous solution by Fe 3+ impregnated biochar. *Journal of Dispersion Science and Technology*. *38,* 815–825. DOI: https://doi.org/10.1080/01932691.2016.1203333.

Weber, J., Schmidt, J., Thomas, A., & Bohlmann, W. (2010). Micropore analysis of polymer networks by gas sorption and ^{129}Xe NMR spectroscopy: toward a better understanding of intrinsic microporosity. *Langmuir, 26,* 15650-15656. DOI: https://doi.org/10.1021/la1028806.

Werber, J. R., Osuji, C. O., & Elimelech, M. (2016). Materials for next-generation desalination and water purification membranes. *Nature Reviews Materials*, *1*. DOI: https://doi.org/10.1038/natrevmats.2016.18.

Whitford, D. (2005). Proteins: structure and function, *John Wiley & Sons Ltd*, England. DOI: http://dx.doi.org/10.1373/clinchem.2005.057588.

Winfield, M., Jamison, A., & Wong, R. (2006). An Examination of Risks, Impacts and Sustainability. https://www.pembina.org/reports/Nuclear_web.pdf.

Wong, S. S., & Jameson, D. M. (2012). Chemistry of proteins and nucleic acid crosslinking and conjugation: reagents targeted to specific functional groups. *CRC Press*. DOI: https://doi.org/10.1201/b11175.

Yang, G. X., & Jiang, H. (2014). Amino modification of biochar for enhanced adsorption of copper ions from synthetic wastewater. *Water Research, 48,* 369-405. DOI: https://doi.org/10.1016/j.watres.2013.09.050.

Yoshitake, H., Yokoi, T., & Tatsumi, T. (2002). Adsorption of chromate and arsenate by amino-functionalized MCM-41 and SBA-1. *Chemistry of Materials*, *14*(11), 4603–4610. DOI: https://doi.org/10.1021/CM0202355.

Younos, T., Hill, R., & Poole, H. (2012). Water dependency of energy production and power generation systems. *Water Resources Impact*, *14*(1), 9–12. DOI: http://hdl.handle.net/10919/49493.

Yu, X. L., & He, Y. (2018). Optimal ranges of variables for an effective adsorption of lead (II) by the agricultural waste pomelo (Citrus grandis) peels using Doehlert designs. *Scientific Reports*, *8*(1), 1–9. DOI: https://doi.org/10.1038/s41598-018-19227-y.

Zahara, I., Arshad, M., Naeth, M. A., Siddique, T., & Ullah, A. (2021). Feather keratin derived sorbents for the treatment of wastewater produced during energy generation processes. *Chemosphere*, *273*, 128545. DOI: https://doi.org/10.1016/j.chemosphere.2020.128545.

Zhang, L., Zeng, Y., & Cheng, Z. (2016). Removal of heavy metal ions using chitosan and modified chitosan: A review. *Journal of Molecular Liquids*, *214*, 175–191. DOI: https://doi.org/10.1016/j.molliq.2015.12.013.

Zhang, H. (2014). Title of Thesis: Biosorption of heavy metals from aqueous solutions by using keratin biomaterials. https://www.tdx.cat/bitstream/handle/10803/284239/hz1de1.pdf.

Zhang, X., Zhang, X., & Chen, Z. (2017). Biosorption of Cr(VI) from aqueous solution by biochar derived from the leaf of Leersia hexandra Swartz. *Environmental Earth Sciences, 76*, 1–7. DOI: 10.1007/s12665-016-6336-4.

Zheng, Q., He, C., Meng, J., Fujita, T., Zheng, C., Dai, W., & Wei, Y. (2021). Behaviors of adsorption and elution on amidoxime resin for gallium, vanadium, and aluminium ions in alkaline aqueous solution. *Solvent Extraction and Ion Exchange*, *39*(4), 373–398. DOI: https://doi.org/10.1080/07366299.2020.1847783.

Zhou, Y. M., Fu, S. Y., Zheng, L. M., & Zhan, H. Y. (2012). Effect of nanocellulose isolation techniques on the formation of reinforced poly(vinyl alcohol) nanocomposite films. *Express Polymer Letter, 6*(10), 794–804. DOI: http://dx.doi.org/10.3144/expresspolymlett.2012.85.

Zubair, M., Wu, J., & Ullah, A. (2019). Hybrid bio nanocomposites from spent hen proteins. *ACS Omega, 4*(2), 3772-3781. DOI: https://doi.org/10.1021/acsomega.8b03501.

Zubair, M., Arshad, M., & Ullah, A. (2020). Chitosan-based materials for water and wastewater treatment: In handbook of chitin and chitosan. *Elsevier.* DOI: https://doi.org/10.1016/C2018-0-03014-5.

APPENDICES

Appendix-I: BET Surface Area

Surface Area	KBP-I	KBP-II	KBP-III	KBP-IV	KBP-V	KBP-VI	KBP-VII	KBP-VIII
$S_{BET\ (m^2/g)}$	0.006	6.606	0.559	2.293	0.550	1.094	0.987	0.902

Table. A.1. BET specific surface area of KBP-I and modified KBPs. The values are presented in m^2/g.

Appendix-II: Energy Dispersive X-Ray Spectroscopy (EDX): The main elements that were identified from the surface composition of KBPs by EDX analysis (Fig A.1) were carbon (C), nitrogen (N) oxygen (O) and sulphur (S) which are constituent elements of amino acids (Nuutinen, 2017). For KBP-III and KBP-IV modified with ionic liquids have additional peaks of chloride and bromide showing that the salt particles were chemically reacted with the surface of KBPs. The same trend could be seen with the KBPs modified with POSS. KBP-VI and KBP-VII have additional peaks of silicon confirming that POSS particles were entrapped onto the surface of KBPs. These EDX results can also be evident by XRD, FTIR and XPS analysis of this study.
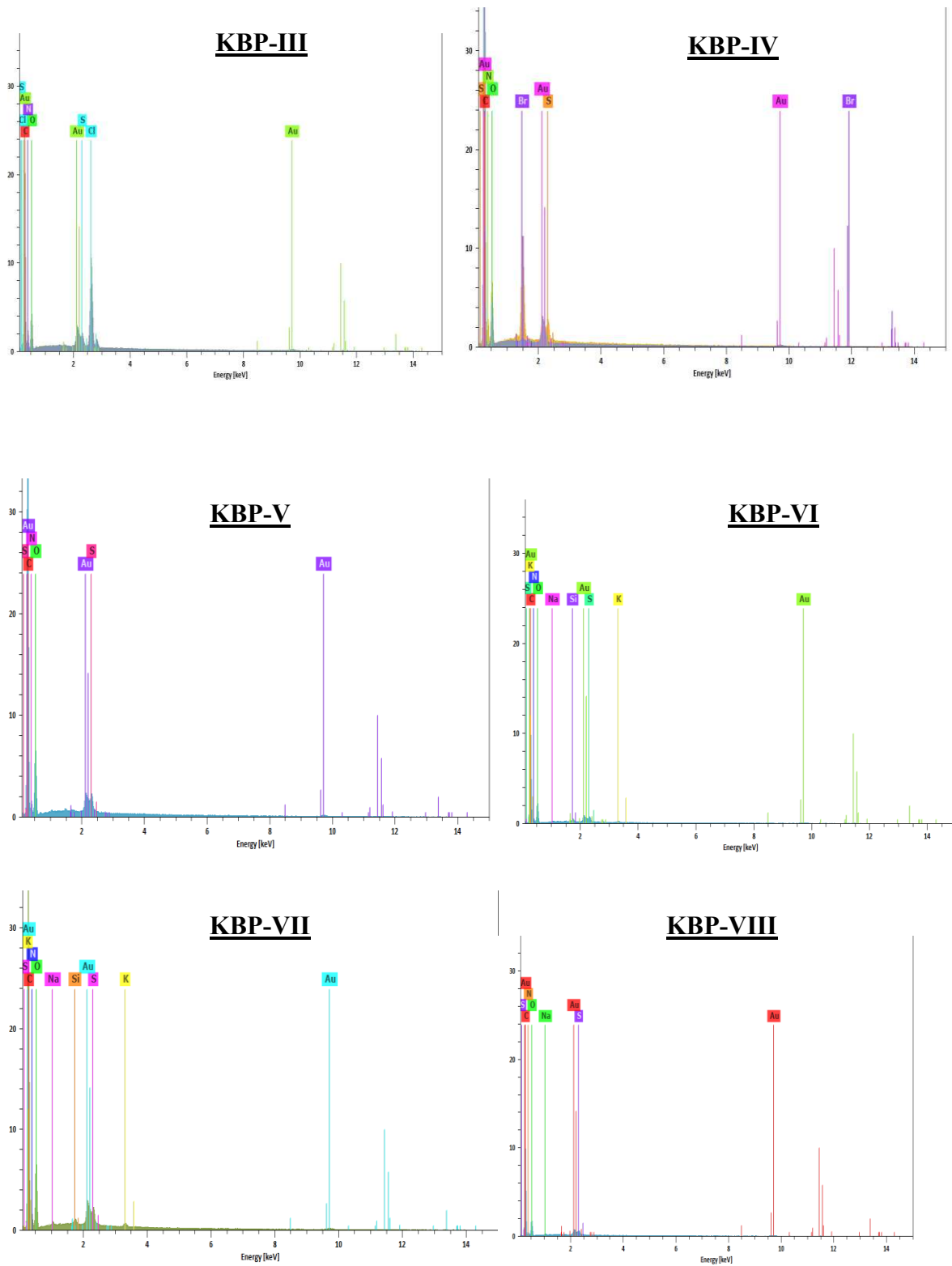

125
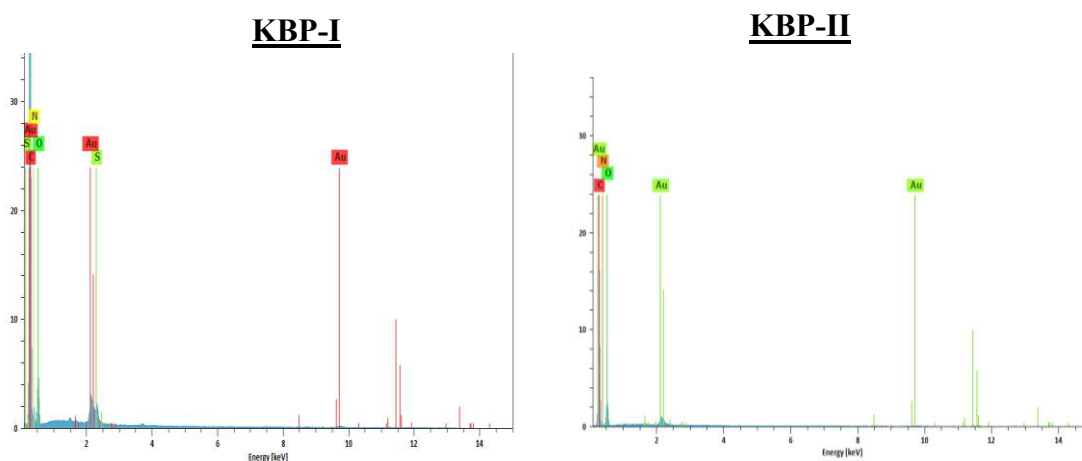
Figure. A.1. EDX data derived from KBP-I and modified KBPs.

Appendix-III: X-ray Photoelectron Spectroscopy (XPS): The elemental composition of KBP-I and modified KBPs was determined using XPS technique (Fig A.2). The peaks found in the spectrum with binding energies of about 686, 530, 398, 283, and 100 eV might correspond to F 1s, O 1s, N 1s, C 1s and Si 2p respectively. The XPS results displayed that the KBP-I, KBP-II, KBP-III, KBP-IV, KBP-V and KBP-VIII were largely composed of carbon, oxygen, and nitrogen (Arshad et al., 2016). Whereas the POSS modified biopolymers KBP-VI and KBP-VII also contains additional peaks of silicon and fluorine with carbon, nitrogen, and oxygen contents due to insertion of POSS molecules, confirming that the POSS particles were entrapped onto the surface of KBP. These results are also evident by EDX analysis of this study.
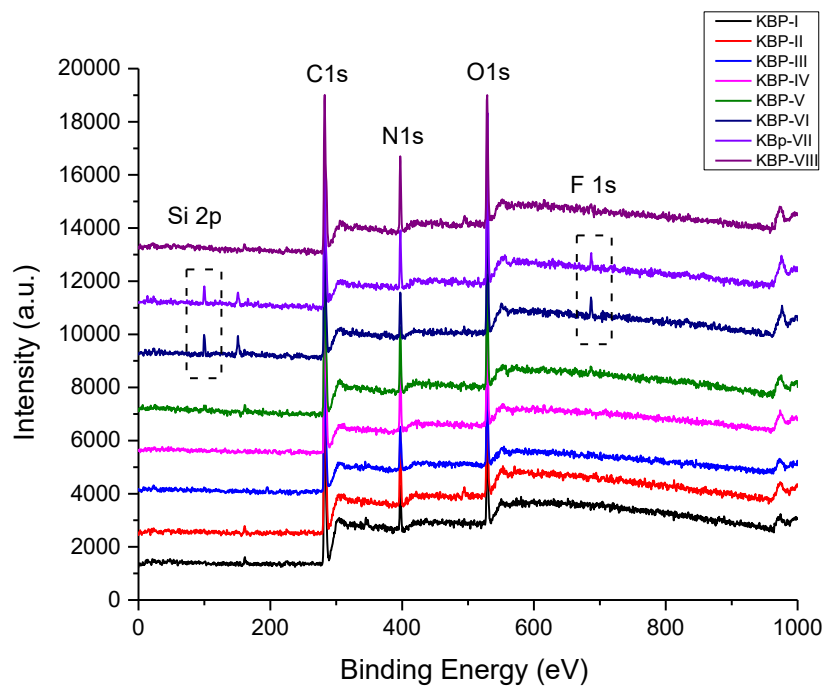

Figure. A.2. XPS survey spectra of KBP-I and modified KBPs.

**Appendix-IV: Concentrations of Transition Metal Cations and Oxyanions with Standard Deviation Values.**

Sample Type	Co	Ni	Cu	Zn	Cd
Synthetic wastewater	109.5 (5.5)	107.2 (4.9)	88.0 (9.2)	106.4 (5.4)	104.6 (4.5)
KBP-I	90.5 (4.6)	52.3 (3.3)	23.4 (7.5)	-	6.5 (2.9)
KBP-II	92 (3.4)	82.4 (6.8)	-	-	50.9 (4.8)
KBP-III	112.2 (5.4)	105.6 (4.7)	36.3 (11.0)	-	99.0 (6.0)
KBP-IV	114.9 (8.1)	89.6 (6.9)	18.1 (2.1)	-	94.9 (6.8)
KBP-V	31.9 (3.1)	5.8 (1.2)	41.3 (12.6)	40.1 (18.3)	8.1 (0.3)
KBP-VI	97.6 (7.6)	71.9 (5.3)	61.3 (11.8)	-	40.7 (3.2)
KBP-VII	165.8 (7.8)	103.2 (5.4)	70.3 (2.7)	-	58.1 (3.1)
KBP-VIII	111.1 (3.1)	32.0 (1.5)	46.5 (20.8)	-	96.6 (2.7)

Table. A.2. Concentrations of transition metal cations (Co, Ni, Cu, Zn and Cd) before adsorption (synthetic wastewater) and after adsorption (24 h incubation of synthetic wastewater with KBP-I and modified biopolymers). Values in parentheses represent the standard deviation of triplicate samples. The recovery of Cu and Zn by some biopolymers is impaired by the additional contribution of Cu and Zn from the biopolymers themselves, also indicated by the control treatment (KBPs plus ultrapure water; Fig. A3), denoting that KBPs served as a source of Cu and Zn to the equilibrating solution.

Sample Type	V	Cr	As	Se
Synthetic wastewater	118.6 (6.5)	114.4 (5.5)	111.0 (5.4)	112.8 (6.3)
KBP-I	38.6 (1.4)	10.8 (1.1)	13.8 (1.0)	108.6 (5.6)
KBP-II	79.8 (2.7)	47.7 (0.9)	106.9 (1.9)	114.7 (1.7)
KBP-III	22.9 (3.4)	21.1 (1.2)	107.1(3.4)	100.3 (8.0)
KBP-IV	16.6 (0.9)	10.1 (0.9)	106.8 (6.7)	108.1 (7.2)
KBP-V	76.9 (5.2)	92.0 (7.7)	129.7 (3.3)	132.3 (12.7)
KBP-VI	90.1 (6.6)	5.07 (0.5)	119.7 (12.3)	118.9 (9.4)
KBP-VII	65.7 (3.6)	8.5 (1.2)	111.0 (6.5)	117.9 (6.2)
KBP-VIII	76.3 (3.4)	10.0 (1.1)	97.1 (5.0)	118.5 (5.8)

Table. A.3. Concentrations of oxyanions of redox sensitive trace metals (V, Cr, As and Se) before adsorption (synthetic wastewater) and after adsorption (24 h incubation of synthetic wastewater with KBP-I and modified biopolymers). Values in parentheses represent the standard deviation of triplicate samples.

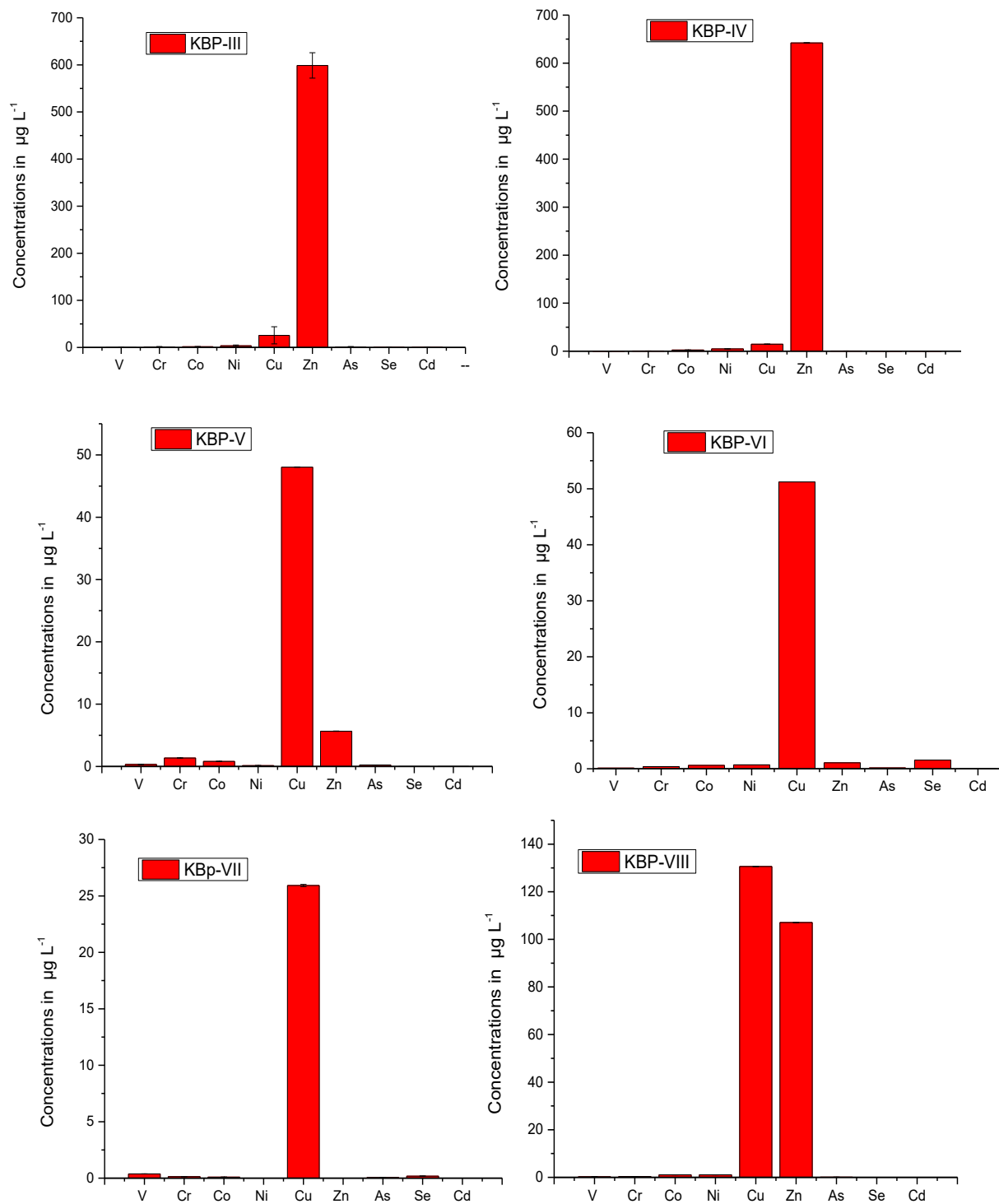**Appendix-V: Negative Control Employed in Metal Removal Study.**
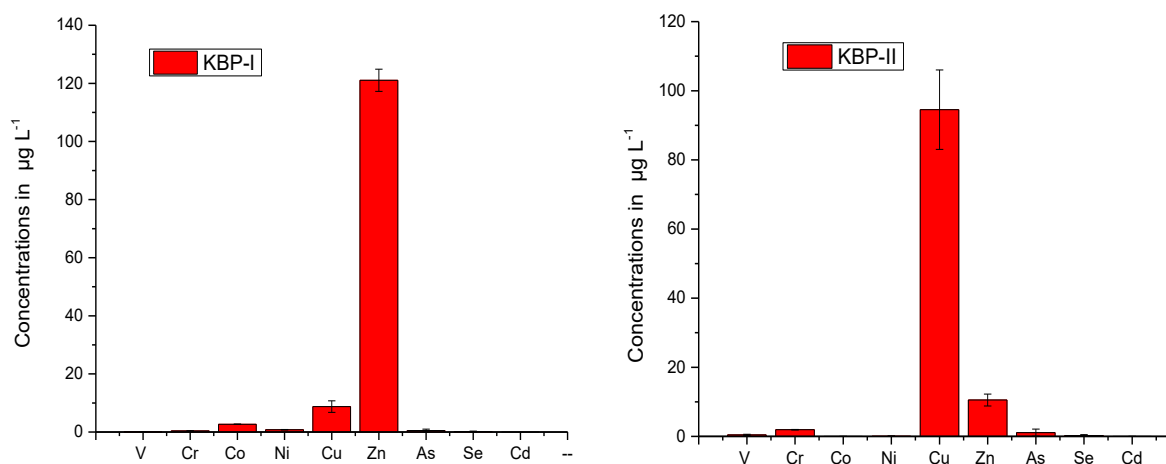
Figure A.3. Concentrations of metals in ultrapure water obtained after incubating water with keratin biopolymers (KBPs) as negative control under experimental conditions employed in metal removal study described in materials and methods section.

Appendix-VI: Buffering Capacities of KBPs neutralizing the multi-metal synthetic wastewater

KBPs	pH of synthetic wastewater after incubation of 24 hours	
	Initial pH=5.5	Initial pH=8.5
KBP-I	6.5	6.5
KBP-IV	4.2	4.5
KBP-V	7.9	8.5

Table. A.4. pH values of synthetic wastewater measured after the incubation (24 h of equilibrium with KBP-I, KBP-IV, KBP-V).

REFERENCES

Nuutinen, E. M. (2017). *Title of Thesis: Feather Characterization and Processing*. https://pdfs.semanticscholar.org/29b4/58542c8638ad924a509af00c741bb887b7f2.pdf.

Arshad, M., Kaur, M., & Ullah, A. (2016). Green biocomposites from nanoengineered hybrid natural fiber and biopolymer. *ACS Sustainable Chemistry & Engineering, 4* (3), 1785-1793.